Influence of the host cell factors CK2, hTERT, and PML, on the antiviral response to herpes simplex virus type I infection

By



Miles Christian Smith

Submitted to the graduate degree program in Molecular Biosciences and the Graduate Faculty of the University of Kansas in partial fulfillment of the requirements for the degree of Doctor of Philosophy.

_____

Chairperson David Davido

_____

Yoshiaki Azuma

_____

Steven Benedict

_____

Kristi Neufeld

_____

Thomas Yankee

Date Defended: 3 July 2013

The Dissertation Committee for Miles Christian Smith

certifies that this is the approved version of the following dissertation:

Influence of the host cell factors CK2, hTERT, and PML, on the antiviral response to herpes simplex virus type I infection

_____

Chairperson David Davido

Date approved: 26 July 2013

## Abstract

Herpes simplex virus type I (HSV-1) is a significant human pathogen that infects a large portion of the human population. As an obligate intracellular parasite, HSV-1 requires certain cellular factors for its replication; on the other hand, the cell deploys a variety of defenses to limit the extent to which the virus can replicate. This thesis is the summation of projects that examined the impact of three host cell factors – those being CK2, hTERT, and PML – on HSV-1 replication.

CK2 is a cellular kinase that, through its phosphorylation of a large number of targets, broadly functions to promote cellular growth and survival. HSV-1 encodes nine proteins that are either potential or bona fide substrates of CK2, the virus packages the kinase into progeny virions, and CK2 activity is stimulated during infection, suggesting that this kinase is important for viral replication. Two viral substrates (i.e., ICP0 and ICP27) act to counter the interferon response while a number of cellular targets function against HSV-1. I show as part of this thesis that, while the activity of CK2 is largely dispensable for viral replication, the use of CK2 pharmacological inhibitors sensitized HSV-1 to the interferon (IFN) response, an innate cellular antiviral pathway. This effect appears to function through the viral E3 ubiquitin ligase, ICP0, though it did not affect ICP0's ability to induce the loss of two of its targets. Additionally, the effect these inhibitors had on IFN sensitivity was specific to HSV-1, as there was no such result on adenovirus or vesicular stomatitis virus.

hTERT is a cellular reverse transcriptase that functions in a complex termed telomerase to regenerate the ends of human chromosomes in pluripotent cells but whose lack of expression in the major factor limiting the lifespan of terminally differentiated cells. While the reintroduction of hTERT into primary cells has been reported to extend the proliferative capacity of differentiated fibroblasts, other reports have demonstrated non-telomerase activities for hTERT and changes in the transcription profile in hTERT-restored cells. To date, however, cellular antiviral pathways have not been examined in these studies. In this thesis, I demonstrate that the IFN response is largely unchanged in fibroblasts immortalized by hTERT and that, unlike transformation by oncogenes, the requirement for HSV-1 proteins involved in overcoming cellular antiviral effectors remained high.

PML is the nucleating and central organizing factor of a nuclear suborganelle, ND10s, and coordinates the cellular efforts in response to a number of stress stimuli. Available evidence suggests that PML serves in intrinsic and innate cellular antiviral defenses against HSV-1. While the role of PML in a number of pathways is regulated through post-translational modifications, the effects of phosphorylation on its antiviral activity toward HSV-1 has been largely unexplored. As part of this thesis, a mapping of phosphorylation sites on PML was undertaken and sites of phosphorylation then examined for their effects on a number of PML's activities. I have identified a number of novel sites of phosphorylation and found that sites near a SUMO interaction motif influence the ability of PML to respond to HSV-1 infection.

## List of Figures

# Chapter 1: Introduction

## 1.1 HSV-1

Human herpesvirus 1 or, as it is more commonly known, herpes simplex virus type 1 (HSV-1), is one of eight members of *herpesviridae* for which humans are the primary host [1]. Collectively, these viruses infect most human beings. Though quite different in the cells that they infect and the symptoms they produce, these viruses are all characterized by a shared virion structure; a large coding capacity of viral factors that possess many functions (e.g., protein kinases, viral DNA polymerase); the destruction of the host cell by progeny virus production, and an ability to persist in a certain cell types in a latent state for the life of the host with the ability to reactivate and resume an active infectious cycle [1]. Owing to its relatively benign symptoms and ability to persist latently, HSV-1 is a widespread human pathogen, with upwards of 70-80% of the population, depending on socioeconomic class, being infected by the virus [2].

HSV-1 is most notable as being the etiological agent of the facial ulcerations commonly referred to as cold sores. The virus is spread by direct contact when virus-containing bodily fluid is transferred to a naïve individual and enters though cracks or abrasions in the skin or mucosal surfaces. Although most infections are asymptomatic, the initial infection can result in high fever, a painful gingivostomatitis, swollen lymph nodes, and mononucleosis-like

symptoms in adults [2]. These symptoms last for one to two weeks, during which time virus is continuously shed. As this initial infection in the epithelia resolves, progeny virus infects the surrounding sensory neurons and traffics to the trigeminal ganglia. While there, the viral genome is maintained as a quiescent episome, remaining for the most part transcriptionally silent and producing no progeny virus. Stimulation such as emotional stress, exposure to intense sunlight, fever, or forms of immunosuppression in a latently infected individual can result in a loss of immune surveillance or neuronal stimulation. As a consequence of these events, the virus exits latency, with a resumption of viral gene expression and concomitant production of progeny virus in a process known as reactivation. The virus then traffics back to primary sites of infection on the face, where it once again establishes a lytic infection, most commonly the margin around the lips. This recurrent infection can result in blisters that eventually heal over the course of several days.

While these facial ulcerations are a relatively minor concern from a health perspective, serious complications arise when the virus infects areas outside of its preferred orofacial region. When virus is introduced into the eye, repeated cycles of lytic infection in corneal epithelial cells can result in scarring of the cornea and blindness in the infected individual. Although rare, HSV-1 is capable of spreading to the brain in children or immunocompromised individuals, resulting in a frequently fatal encephalitis. Damage done during reactivation to the trigeminal ganglion or nerves extending from it may produce a painful and debilitating condition termed herpetic neuralgia. Additionally, an increasing

number of genital herpes infections are caused by HSV-1 and may be the primary agent in certain populations [3].

### 1.1.1 HSV-1 Structure

HSV-1 is a dsDNA virus with a 152 kbp genome [4] that is linear when packaged into the virion and circularized within cells. In the assembled virion, the viral DNA is surrounded by an icosahedral protein cage called the nucleocapsid, formed by the tight association of four viral proteins [1]. Surrounding this is an amorphous proteinaceous layer termed the tegument, which is comprised of 26 viral and a variety of captured cellular proteins [5] that appear to be important during the early stages of infection. The tegument in turn is enclosed by the viral envelope, a lipid bilayer derived from the host, and contains a number of viral glycoproteins necessary for attachment to the host cell and cell-to-cell spread.

### 1.1.2 HSV-1 Lifecycle

Infection begins with attachment of the viral glycoproteins to their cognate host receptors on the cell surface, the exact identity of which depends on the particular cell type that is being infected. Binding of the virion to host receptors results in rapid internalization of the viral particle through either endocytosis or fusion with the plasma membrane. In either case, the virion is ultimately de-enveloped, the contents of the tegument are released into the cytoplasm, and the viral capsid is transported along microtubules to the nucleus. Once at the nuclear pore complex, the capsid docks and injects the

viral genome into the nucleus [6], where the genome undergoes circularization and chromatinization. In the case of a lytic infection, viral gene expression occurs in a strict temporal cascade consisting of immediate-early (IE), early (E), and late (L) phases, with the expression of each phase dependent upon the preceding class [7]. Initially, the tegument member, VP16, interacts with the host proteins Oct1 and host cell factor (HCF) to transactivate the IE genes. IE gene products, generally speaking, serve to establish an environment that is conducive to the successful establishment of infection. This includes preventing silencing of the viral genome, inactivating host antiviral defenses, and initiating mechanisms that favor the production of viral proteins over those of the cell, and ultimately stimulate the transcription of the early genes. Early gene products are involved in viral genome replication, which allows for the transcription of the late genes. Late gene products serve either functional roles in the assembly and egress of progeny virus or as components used in their creation. Eventually, this nascent virus buds through the nuclear membrane into the endoplasmic reticulum, acquiring members of the inner tegument, and undergoes a de-envelopment/re-envelopment mechanism whereby it exits the ER, shedding its nuclear membrane-derived envelope. It then enters into the trans-Golgi network, acquires the final envelope and embedded glycoproteins as it picks up the outer tegument on its journey outward, and buds from the plasma membrane into the extracellular environment.

Latent infection differs from that of the lytic infection in that it occurs only within neuronal cells and most viral gene expression is ultimately repressed, with

the exception of the latency-associated transcript (LAT). Though it has been suggested that LAT may encode for proteins or miRNAs that suppress the expression of IE proteins necessary for reactivation or inhibit apoptosis of infected neurons, the exact mechanisms by which LAT functions during a latent infection are unknown. The latent viral genome persists as an episome, and, while there may be sporadic expression of certain IE or E genes, no infectious virus is produced.

### 1.1.3 ICP0

Infected cell protein 0 (ICP0) is one of five HSV-1 IE proteins that, while not strictly required for productive infection, is necessary for efficient lytic infection. ICP0 is important for viral replication when the viral particle-to-cell ratio is low, when cells are in a pre-activated antiviral state, and when the virus reactivates from latency. Its best-described activity is that of an E3 ubiquitin ligase; this activity directs the proteasome-dependent degradation of a number of cellular proteins. Known targets of ICP0-directed degradation include PML; the centromeric proteins CENP-A [8], -B [9], -C [10], -I [11], -H [11], and –N [11]; RNF8 [12]; RNF168 [12]; DNA-PKcs [13]; CD86 [14]; USP7 [15]; IkBa [16]; IFI16 [17]; and E2FBP1 [18], as well as SUMO-1- and SUMO-2/3-conjugated proteins [19].

Through its E3 ligase activity, ICP0 transactivates viral gene expression and overcomes cellular antiviral defenses by preventing, in part, the silencing of the viral genome by cellular factors.

### 1.1.4 Impairment of the host's antiviral response by ICP0

Due to the functional importance of ICP0 in the HSV-1 life cycle, a number of potential mechanisms have been proposed as to how ICP0 works on a molecular level. One established role for ICP0 during viral infection is its ability to inactivate a number of components relating to host-cell antiviral defense and stress response pathways, including factors of both intrinsic and innate defenses [20–23]. Intrinsic defense, in which many core components are also regulated as part of the innate response, consist of pre-existing host cell factors that attempt to silence viral gene expression by making the viral genome functionally inaccessible [20–23]. ICP0 has been shown to affect one component of intrinsic defense, ND10 constituent proteins, and one component of innate defense, namely the type I interferon response (which is described in more detail in section 1.2). Both topics in relation to ICP0 activities will be examined in this thesis.

ICP0's ability to activate viral gene expression is closely associated with its ability to disrupt ND10. ND10s, as will be discussed later in section 1.5, are punctate, nuclear suborganelles that contain a variety of nuclear effectors, including transcription factors, chromatin remodeling factors, DNA damage response members, which participate in proliferation, differentiation, and the antiviral response (reviewed in [24]). HSV-1 genomes were initially described as being deposited at ND10s [25]; subsequently, ND10-associated proteins have been observed to disassemble and reform around incoming viral genomes [26]. ICP0 inhibits the cumulative repressive effects of various ND10 associated

proteins by inducing the disruption of ND10 structures through the degradation or dissociation of PML, Sp100 [27,28], Daxx, and ATRX [29]. Notably, depletion of one or more ND10 constituents increases the plaque formation efficiency and gene expression of an ICP0 null mutant virus but not wild-type HSV-1 [30].

Besides disrupting or degrading preexisting cellular defenses, ICP0 is also involved in subverting innate antiviral pathways. It is required for the successful establishment of a lytic infection in cells in which the IFN response has been activated prior to infection. In cells pretreated with type I IFNs (such as IFN-β), ICP0-null mutants can be up to a thousand-fold less likely to initiate a lytic infection than wild-type virus (personal observation). Expression of ICP0 *in trans* by either an adenoviral vector or an integrated copy of ICP0 in a cell line can largely ameliorate the inhibitory effects of type I IFNs on the replication of an ICP0-null virus [31,32]. Studies performed with mouse embryo fibroblasts derived from knockout mice indicated that PML was primarily responsible for mediating the effects of the IFN response and that the loss of PML could compensate for the lack of ICP0 in IFN-treated cells [33]. However, in PML-depleted human fibroblast cells, IFN-β was still capable of inhibiting the replication of an ICP0-null mutant, although this effect was diminished [34]. This result indicates that other interferon stimulated genes (ISGs), in addition to PML, likely play a role in the repression of HSV-1 replication by IFN-β. Furthermore, a study by Halford and coworkers showed that the acute replication of an ICP0 mutant virus was equally repressed in *PML*-knockout and wild type mice, unlike what happens in mice missing the key IFN-signaling molecule, STAT1,

suggesting that the loss of PML (as an ISG) cannot complement the replication of an ICP0 mutant virus *in vivo* [35]. Although the report that used *PML*-knockout mouse embryo fibroblasts and the studies that used PML-depleted human fibroblasts and mice *in vivo* come to opposing conclusions, PML's role as a mediator of the IFN response may be dependent upon the species of the host, homology between PML orthologs, and/or the cell types used in these studies. It is still unclear how ICP0 enables HSV-1 to replicate in the presence of an established IFN response.

## 1.2 Interferon

The interferon (IFN) system provides an initial antiviral response by the innate immune system in vertebrates [22]. IFNs are cytokines that are capable of impairing or inhibiting viral replication and mark a cell as infected to the immune system. In humans, IFNs are divided into several classes – type I IFNs, as typified by the IFN-α family and IFN-β; type II IFN, consisting solely of IFN-γ; and the type III IFN family, comprised of the IFN-λ family [36]. While most cell types are capable of secreting type I and III IFNs, secretion of type II IFN is restricted to a subset of the immune system consisting of NK cells, $T_H1$ cells, and cytotoxic T-lymphocytes [37] and only select cell types express the IFN-γ receptor [36]. Detection of viral entry or intracellular viral intermediates by Toll-like receptors or other pattern recognition receptors trigger events that lead to the activation of interferon regulatory factor (IRF) 3 and nuclear factor kappa-light-chain-enhancer of activated B cells (NF-κB), which translocate to the

nucleus. Once in the nucleus, IRF3 and NF-κB coordinate to transactivate the *IFN-β* promoter and induce the production of IFN-β to initiate an IFN response. IFN is secreted from the cell, binds to its cognate receptors on the secreting cell, as well as surrounding cells, and activates the Jak-STAT (Janus kinase-signal transducers and activator of transcription) pathway by stabilizing the dimerization of the IFN-α/β receptor and initiating the cross phosphorylation of the Jaks on each opposing receptor. Activated Jaks phosphorylate their associated STATs, with the particular STATs activated depending on the species of IFN that initiated the signal – notably, in the case of IFN-β, STAT1 and STAT2 are activated [37]. Phosphorylation of STAT1 and STAT2 to their dimerization and binding to the protein interferon regulatory factor-9 (IRF-9) to form the interferon-stimulated gene factor 3 (ISGF3) complex, which translocates to the nucleus [37]. Once in the nucleus, IRF-9 and STAT1 bind to an interferon stimulated response element (ISRE) that is present in the enhancer region of interferon-stimulated genes (ISGs) and STAT2 provides the transcriptional activation activity [38]. The products of these ISGs have diverse activities that inhibit viral replication and limit the spread to surrounding cells. Examples of prototypical ISGs include 2',5'-oligoadenylate synthetases, which trigger mRNA degradation by activating an endoribonuclease, RNaseL [39]; the myxovirus-resistance proteins (Mx1 and Mx2), which interfere with viral component trafficking [40]; protein kinase RNA-dependent (PKR), which shuts down mRNA translation by phosphorylating the initiation factor eIF2α [41]; and Interferon-induced protein with tetratricopeptide repeats 1 (IFIT1), which binds

to mRNAs with a 5'triphospate and lacking 2'-O-methylation on the cap, specific properties of viral mRNAs [42].

As noted above, HSV-1 is somewhat resistant to the effects of IFN, in large part because of the activities of ICP0. However, what aspects of the IFN response function against HSV-1 and the mechanism used by ICP0 to overcome this response are poorly understood. This thesis examines the role of one host cell factor, CK2, whose activity assists in the replication of HSV-1 in cells with a preactivated IFN-response.

## 1.3 CK2

### 1.3.1 Subunits and phosphorylation activity

CK2, formerly called casein kinase II, is a highly conserved protein kinase that is expressed in all tissues [43]. It is a heterotetramer comprised of two regulatory CK2β subunits and two catalytic subunits of which, in humans, there are two isoforms – CK2α and CK2α' [43]. CK2 generally phosphorylates serines and threonines located adjacent to a patch of acidic residues, with the consensus sequence of S/T-x-x-D/E [44]. CK2, however, is also capable of phosphorylating tyrosine in a limited number of instances, including itself in an autoregulatory fashion [45]. The CK2 phosphorylation consensus sequence is found in a large number of proteins, with CK2 having over 300 putative cellular substrates, including those involved in cell cycle control, transcription, and apoptosis [43]. As such, CK2 plays a role in these pathways where its activity can be broadly described as pro-cell survival and pro-cell growth. In fact,

deletion of CK2α is embryonic lethal in mice and deletion of CK2-β causes a loss of viability in cells [46].

### 1.3.2 Cellular functions of CK2

With its wide array of targets, CK2 has a role in regulating multiple cellular pathways, including transcription, apoptosis, and the cell cycle.

CK2 functions at multiple stages of the cell cycle. For instance during G1 phosphorylation of cyclin H by CK2 is necessary for the full activity of the cyclin H/CDK7/Mat1 complex that targets CDK1, CDK2, and CDK4 and enables these kinases to phosphorylate pRb and disassociate it from E2F proteins [47]. CK2 also influences the p53 tumor suppressor pathway during G1 and S phases. In unstressed cells, phosphorylation of MDM2 by CK2 allows MDM2 to target p53 for polyubiquitination and subsequent proteasomal destruction [48]. Conversely, exposure to ultraviolet irradiation induces the FACT complex to shift CK2 phosphorylation to p53, increasing p53 transactivation activity with a subsequent block in the cell cycle [49]. CK2 activity is also required at the onset of mitosis as the use of a CK2 inhibitor slows the degradation of Wee1A and the subsequent entry into mitosis [50]. Additionally, CK2α colocalizes with the mitotic spindle and a dysregulation of CK2α activity leads to centrosomal amplification and missegregation [51].

CK2 activity is required for the transcriptional activity of all three RNA polymerases. For both RNAPI [52] and RNAPIII [53,54], CK2 phosphorylates several components, most notably TBP, and is required for reassembly of the

RNAP complex at the promoter [52]. However, the RNAPIII-related targets of CK2 are cell cycle dependent and CK2 changes from stimulatory to inhibitory during both S phase and mitosis [55]. The c-terminal domain of RNAPII is a target of CK2, as well as several other general transcription factors, with cycles of phosphorylation of the RNAPII CTD by CK2 and dephosphorylation by the phosphatase FCF being required for RNAPII recycling and reinitiation at promoters [56].

In apoptotic pathways, CK2 can be broadly described as having pro-survival activity. Overexpression of CK2 can protect cells from etoposide- or diethylstilbestrol-induced apoptosis in cancer cell lines and treatment with pharmaceutical inhibitors of CK2 can induce apoptosis in certain tumor cell lines [57,58]. The kinase activity of CK2 is capable of preventing the activation of several pro-apoptotic factors, including Bid, caspase-2, and caspase-9, as the cleavage recognition site overlaps with that of a CK2 consensus sequence and phosphorylation prevents the cleavage of these effectors [59,60]. Additionally, CK2 is able to prevent apoptosis by inducing an upregulation of the inhibitor of apoptosis family member, survivin [61].

### 1.3.3 CK2 and cellular antiviral defense

Phosphorylation of cellular factors by CK2 is implicated in the regulation of the interferon response and at least three cellular proteins that have roles in antiviral pathways: PML (which will be discussed in more detail in section 1.5.5.3), retinoic acid-inducible gene 1 (RIG-I), and interferon-induced gene 16

(IFI16). However, there does not appear to be a unified theme in the case of CK2's activities in antiviral pathways. CK2 physically associates with both JAK1 and JAK2, with the latter serving as a substrate of CK2's kinase activity [62]. CK2 activity is necessary for the proliferation of certain leukemic cells and while the use of CK2 inhibitors decreased STAT1 activation in response to Oncostatin M, it is unclear what effects CK2 has on the activation of STAT1 in response to type I IFN-signaling though CK2 has a positive effect on monocyte chemoattractant protein 1 expression in response to IFN-γ signaling. Opposite its effects in monocytes, CK2 negatively regulates RIG-I, a pattern recognition receptor that senses certain viral RNAs and functions is upstream of the IFN-response to activate IFN-β production [63]. CK2 phosphorylation of RIG-I prevents RIG-I from undergoing a multimerization necessary for its activation [63,64]. In the case of IFI16, a sensor of viral DNA that activates IFN-signaling [65], CK2 has been reported to be necessary for its nuclear accumulation, though the relevance of this phosphorylation during infection is unknown [66].

### 1.3.4 CK2 during viral infection

In addition to its plethora of cellular targets, proteins from a variety of viruses serve as substrates of CK2-mediated phosphorylation. As in the case of their cellular counterparts, the effect of CK2 on the activity of these viral proteins is varied. Viruses that express functionally relevant CK2 targets include human immunodeficiency virus type 1 [67–71], human cytomegalovirus [72–74], Epstein

Barr virus (EBV) [75–77], hepatitis C virus [78–81], human papillomaviruses [82–84], adenoviruses [85,86], and vesicular stomatitis virus [87–89].

In the case of HSV-1, proteins from all three kinetic classes contain CK2 consensus phosphorylation sites, and in several instances mutation of these sites compromises viral replication [90–93]. Perhaps owing to the potential importance of CK2 in HSV-1 replication, CK2 is the only cellular kinase, to date, that has been shown to be packaged in the tegument of the assembled virion [5].

The best described interactions between CK2 and HSV proteins include those between it and ICP0, ICP4, ICP27, VP22, and VP16. Focusing on IE proteins, potential CK2 phosphorylation sites have been implicated in controlling ICP0's E3 ubiquitin ligase activity as mutation of the sites impair the disruption of ND10s, the degradation of USP7, and increase the stability of ICP0 [94]. ICP4, the major viral transactivator during infection, contains a polyserine tract, with several sites matching a CK2 consensus sequence. While removal of the polyserine tract weakens the ability of the virus to replicate in the trigeminal ganglion, mutation of the CK2 consensus sequence alone only has a minor effect on replication in the eyes or in ganglia [95]. CK2 modulates the nuclear import of ICP27, a multifunctional mRNA/protein nuclear import/export shuttling factor and regulatory protein that promotes viral mRNA translation and inhibits cellular protein synthesis [96]. The use of the CK2 inhibitor DRB or mutation of the phosphoacceptor sites prevents nuclear export of ICP27 [97,98]. Additionally, mutants altered in the putative CK2 phosphoacceptor sites fail to

form replication compartments indicative of viral genome amplification [93] with a 2-log decrease in viral replication [98]. Lastly, ICP27 alters the intracellular localization of CK2 and stimulates its activity in *in vitro* assays [97]. Of note is that two of these viral targets, ICP0 and ICP27, are involved in counteracting the repressive effects of the IFN response.

While the above implicates CK2 playing a role in the life cycle of HSV-1, the impact of inhibiting or removal of CK2 activity on HSV-1 replication has remained largely unexplored and thus is one area of study in this thesis.

## 1.4 hTERT

In performing studies that examine cellular immune responses to viral infections, it is often necessary to work with primary cells, as the efficacy of intrinsic and innate immune pathways are frequently diminished in immortalized cells [99–102]. One disadvantage of using primary cells is their limited proliferative capacity in cell culture, which is due in part, to the progressive shortening of telomeres [103].

### 1.4.1 Telomeres

Telomeres are repetitive nucleoprotein structures that serve to cap the ends of chromosomes, facilitating their replication, and prevent their ends from appearing as DNA breaks [104]. While the exact composition of telomeres vary among species, in humans telomeres are comprised of the guanine-rich sequence TTAGGG, which may extend up to 8-12 kb long, and are coated by

what is termed the shelterin complex, a six protein complex that masks the telomeric DNA from being detected as damaged DNA by ataxia telangiectasia mutated (ATM) and ataxia telangiectasia and Rad3 related (ATR) kinases as well as suppressing non-homologous end joining and homology-directed repair at telomeres [105]. At the end of the telomere is a 3' single stranded overhang, which invades an upstream double stranded region and forms what is termed the t-loop. Due to the inability of mammalian polymerases to synthesize in the absence of a primer, in somatic cells each round of chromosomal duplication results in the loss of nearly 100 bp of telomeric sequence on the lagging strand [106,107]. In stem cells and pluripotent cells, telomeres are maintained by a complex known as telomerase, whose essential core consists of the catalytic subunit telomerase reverse transcriptase (TERT) and the telomerase RNA template component (TERC) [108,109]. TERT is loaded onto the 3' overhang of existing telomeric DNA and utilizes TERC as a template to add TTAGGG repeats; concordantly, DNA primase and DNA polymerase are recruited to the new telomeric repeats, subsequently synthesizing the complementary 5' strand [104]. In the absence of active telomerase, erosion of telomeric sequences occurs with each successive round of replication. Once telomeres are reduced from their normal 15 kb length to ~4 kb, DNA damage sensors trigger p53- and pRb-dependent mechanisms that result in cellular senescence, inducing a $G_1$ cell cycle arrest [110].

### 1.4.2 Senescence and immortalization

Replicative senescence is thought to be a mechanism of cellular lifespan regulation, preventing diseases such as cancer, and is intrinsic to the health of an organism [111–114]. However, for technical reasons it can be desirable to extend the proliferative capacity and prevent the senescence of a primary cell culture or strain. One way to avoid or reverse replicative senescence is transformation with viral oncogenes, such as the simian virus 40 (SV40) large T antigen (TAg) or the human papillomavirus (HPV) E6 and E7 proteins [115–117]. In both cases, these viral proteins reverse senescence through the inactivation of p53 and/or pRb. While this allows cells to resume progression through the cell cycle and replicate, these cells still undergo telomeric erosion and ultimately undergo a phenomenon termed crisis [115], where massive cell death occurs due to gross genomic rearrangements and instability in the absence of telomeres. While the estimated 1 in $10^7$ cells (for human cells) that survive crisis exit immortalized [118,119], this transformation results in the dysregulation of several cellular pathways, including the antiviral type I interferon (IFN) response [99].

As part of their differentiation program, human cells cease expressing hTERT, while continuing to produce other essential telomerase subunits such as TERC [120]. It has been shown by a number of labs that the lifespan of fibroblasts is efficiently extended by the reintroduction of hTERT into these cells [121,122]. Exogenous expression of hTERT presumably allows terminally differentiated fibroblasts to resume the extension of their telomeres, delaying or

avoiding the production of signals that trigger replicative senescence and in turn prevents the chromosomal damage encountered by replication through crisis [123]. Unlike transformation with viral oncogenes, fibroblasts that exogenously express hTERT do not, for the most part, exhibit an oncogenic phenotype [124]. Notably, the effect that life-extension by exogenous expression of hTERT on innate antiviral pathways, and in particular the IFN response, has not been examined.

## 1.5 PML

### 1.5.1 Introduction

As mentioned above, host cells initially attempt to limit the activities of HSV-1 through intrinsic defense mechanisms. One mediator of the intrinsic antiviral defense is the promyelocytic leukemia protein (PML).

PML is a nuclear regulatory protein present in a majority of cell types. It is constitutively expressed but as the *PML* promoter contains both type I and type II interferon response elements as well as binding sites for p53-family members, it is upregulated in response to IFN-stimulation or activated p53 [125,126]. The *PML* gene contains nine exons, giving rise to seven major isoforms that all share a common N-terminal set of domains but differ greatly in their C-terminus [127]. PML is capable of extensive interactions with itself and other proteins, especially those that are SUMO-modified, allowing it to serve as the nucleating constituent of the nuclear suborganelle, nuclear domain 10

(ND10). Current evidence suggests that PML is itself an E3 SUMO ligase [128,129], though its physiological targets are currently unknown. Through its ability to interact with a wide variety of partners, PML plays a role in numerous cellular pathways, such as apoptosis, the DNA damage response, telomere maintenance, stem cell maintenance, transcription, translation, cellular proliferation, differentiation, and antiviral defense; in most cases, PML responds to stress conditions to slow or limit growth [130].

### 1.5.2 ND10

ND10s (also called PML oncogenic domains and PML nuclear bodies) are matrix associated protein aggregates with which numerous proteins associate but to which no definite function has been ascribed. It has been suggested that ND10s serve as modification platforms where effector proteins and their substrates are brought together to facilitate post-translational modification or as storage depots that regulate the availability of transcription factors or other effectors [131]. While the list is ever growing, over 160 cellular proteins have been described as localizing to ND10s [132]; however, as ND10s appear to serve a role in protection from aggregated and misfolded proteins [133,134], it is unclear whether the localization of some of these proteins is due to artifacts of overexpression. Notable ND10 members include p53, MDM2, CBP/p300, myc, pRB, Daxx, Nbs1, HIPK2, Mre11, and CHK2 [135].

Not surprisingly, ND10s are dynamic structures, with their number and size varying depending on cell type, position in the cell cycle, and exposure to

stress conditions. These bodies are generally spherical shells with an exterior formed of PML and another ND10 resident, Sp100, and the interior consisting of proteins temporarily localized to ND10s [136]. Typically there are 2-30 ND10s per cell, which range in size between 0.2-1 μM in diameter [20]; however, a variety of stimuli can alter these attributes due to changes in the composition or modification of resident proteins or through changes in chromatin structure that results in torsional effects on ND10s, where increased condensation strains ND10s and causes their fragmentation [137].

### 1.5.3 PML Structure

PML is a member of the TRIM family of proteins, so named because they all share a triplet set of characteristic domains, those being a Really Interesting New Gene (RING) finger, one or two B-boxes, and a coiled-coil domain (Figure 1.1) [127]. The RING finger is a $Zn^{2+}$-coordinating cross-brace structure that is commonly found in the E3-ligase proteins of the ubiquitin and ubiquitin-like modification systems. Indeed, a number of TRIM family proteins, including PML, have been shown to possess E3 activity in one or more of these pathways, with the RING finger forming a site with which the E2 conjugation enzyme binds [129,138,139]. B-boxes comprise another $Zn^{2+}$-binding motif, one found only in TRIM proteins; while their purpose is, as of yet, poorly understood, it has been suggested that they serve as an intramolecular E4 site that binds a substrate protein and enhances the activity of the RING finger in a manner similar to that of BARD1 in the BRCA1:BARD1 complex [140]. The coiled-coil is an alpha-

helical structure involved in both PML dimerization and interaction with partner proteins [127,141,142].

While most TRIM proteins contain the above-described domains, they differ in those that are found in the C-terminus. Specific to PML is a nuclear localization signal and a SUMO-interaction motif (SIM) [143]. The SIM, present in five of the seven major isoforms of PML, is a hydrophobic patch of amino acids that allows for the non-covalent interaction with a partner protein that is SUMO conjugated. Additionally, the various isoforms of PML may contain different functional domains in the variable C-terminus. For instance, PML-I encodes a nuclear export signal and an exonuclease III domain [144], whereas a region of PML-V is capable of recruiting other ND10-associated protein independently of any other PML-isoforms or regions [145].

### 1.5.4 Antiviral activities of PML

Likely due to its effect on the various partner proteins found at ND10s, PML has a role in regulating a wide variety of cellular processes as previously mentioned. As these pathways overlap with intrinsic antiviral defenses, it is of little surprise that PML serves to restrict the replication of a number of viruses. Currently, PML and ND10s have been shown to impair the growth of vesicular stomatitis virus (VSV), rabies virus, Lassa virus, lymphocytic choriomeningitis virus, influenza A virus, poliovirus, encephalomyocarditisvirus, murine leukemia virus, human foamy virus (HFV), adenovirus, human papilloma virus (HPV), herpes simplex viruses type 1 and 2 (HSV-1 and -2), varicella zoster virus (VZV),

human cytomegalovirus (HCMV), and Epstein-Barr virus (EBV) [20]. Elimination of PML in cells or animals can result in an increase in replication for many of these viruses, whereas its overexpression can in turn diminish replication. As yet, it is unclear how PML functions to restrict the replication of many of these viruses, especially for RNA viruses whose lifecycles take place in the cytoplasm. However, in the case of poliovirus, it has been shown that infection induces a phosphorylation- and SUMOylation-dependent increased recruitment of p53 to ND10s, potentiating p53's activation of apoptotic programs [146]. For encephalomyocarditisvirus, PML sequesters the viral polymerase, 3Dpol, in ND10s, decreasing its ability to function in replication [147].

The antiviral functions of PML have been better defined for viruses that replicate in the nucleus. In general, the presence of PML appears to decrease or delay viral gene expression and promote the apoptosis of infected cells. In many cases, ND10s will break down and individual components will form around viral DNA as it enters the nucleus. For infection by HSV-1 ICP0-null mutants at low multiplicities of infection, this can result in encapsidation of the viral genome, silencing it by precluding its accessibility to transcription factors [148]. Additionally, PML colocalizes with latent viral genomes, suggesting that PML plays a role in maintaining latency in neurons [149]. In the instance of human foamy virus, PML physically binds to the major viral transactivator, tas, impairing its ability to activate LTR-driven gene expression [150]. As well as preventing VZV gene expression, PML can also form large cages around assembled

capsids and prevent them from leaving the nucleus and forming infectious particles [151].

While PML functions as part of the intrinsic antiviral response against some viruses, in some cases basal levels of PML do not provide adequate protection. For HFV, only increased levels of PML caused by overexpression or upregulation by IFNs result in a PML-dependent decrease in viral replication [152].

As the viruses have evolved in the presence of PML, many have developed mechanisms mediated by viral proteins, allowing them to inactivate the antiviral effect of PML and ND10s. Encephalomyocarditisvirus 3Cpro [153], HSV-1 [154] and HSV-2 ICP0 [155], EBV EBNA1 [77], and HPV-18 E6 [156] induce proteasome-dependent degradation of PML. HCMV IE1 and EBV BZLF inactivate PML by causing a loss of SUMOylated PML [157–159], while KSHV LANA2 does so by inducing SUMOylation of PML, which results in its loss through a proteasomal-dependent mechanism [160]. In some cases, viruses overcome PML's activity by causing its redistribution, such as Rabies virus P protein, LCMV Z protein, and Lassa Z protein, all of which causes a cytoplasm sequestration of PML [161], or adenovirus E4orf3, which reorganizes ND10s into long tracts [162], though in the latter case it is not known how this reorganization inactivates PML.

### 1.5.5 Post-Translational Modifications

As PML is constitutively expressed yet responds to a variety of cellular stimuli and changing conditions, the activity of PML must be dynamically controlled. As such, PML is extensively post-translationally modified by SUMOylation, acetylation, ubiquitination, and phosphorylation [163] (Figure 1.1). These modifications are essential for the activity of PML, and its ability to form ND10s and respond to cellular signals. This introduction will focus on SUMOylation, ubiquitination, and phosphorylation.

#### 1.5.5.1 SUMO

SUMO-1 was first discovered as a PML interacting protein and was soon found to be covalently bound to PML [164]. PML is SUMOylated on at least three lysine residues [165], with several large-scale mass spectrometry screen suggesting additional minor SUMOylation sites, especially upon arsenic trioxide treatment [166,167]. The physiological relevance of these minor sites is unknown, as the effect that mutation of these sites has on PML SUMOylation has not been examined. PML is modified by SUMO-1, -2 and -3, though the precise role of each paralogue in controlling PML activity and mechanisms determining the usage of a particular paralogue at a specific site are poorly understood. Beside itself, PML interacts with at least three other E3 SUMO ligases, PIAS1, PIAS2α, and RanBP2, that result in conjugation of SUMO to PML [141,168,169]. Additionally, the histone deacetylases HDAC7 [170] and

Sirt1 [171] stimulate PML SUMOylation in a manner that is independent of their deacetylase activity.

SUMOylation of PML at its major sites, including K65, K160, and K490, is necessary for proper ND10 formation, with mutation of the SUMOylation acceptor sites resulting in ND10s that are much larger and fewer in number [143]. Exchange of PML between ND10s and the nucleoplasm is regulated by SUMO modification, with lysine to arginine mutations at K160 and K490 resulting in a form of PML that is poorly retained at ND10s, while additionally mutating K65 nearly eliminates diffusion into the nucleoplasm [172]. In some cases, SUMOylation of PML is required for partner protein recruitment, such as the ND10 protein, Daxx [173].

Modification by SUMO also controls PML stability. SUMOylation by PIAS1 on K160 results in increased interaction with CK2, leading to phosphorylation of PML and subsequent polyubiquitination [141]. Likewise, in response to arsenic trioxide treatment, PML is polySUMOylated by PIAS1 [141], resulting in increased interactions with either of two SUMO-targeted ubiquitin ligases (STUbL), RNF4 [174] and Arkadia [175], which ubiquitinate the polySUMO chains on PML and induces PML's proteasomal-dependent degradation. On the other hand, SUMOylation of PML at K490 can inhibit interaction with the peptidyl-prolyl *cis-trans* isomerase, Pin1, preventing a conformational change that results in degradation of PML [176].

PML SUMOylation changes in response to cellular conditions and stresses. Perhaps the best studied is the effect of arsenic trioxide, where

arsenic directly binds to cysteines present in the RING finger, causing a conformational change that results in a phosphorylation-dependent polySUMOylation and subsequent degradation of PML as detailed above [177]. Other factors that change PML SUMOylation include TNF-α [170], IFN [152], and DNA damage [178], all of which increase PML SUMOylation while stress such as heat-shock and heavy metal exposure leads to deSUMOylation [179].

#### 1.5.5.2 Ubiquitination

PML interacts with the cellular E3 ubiquitin ligases RNF4 [174], Arkadia [175], Siah1/2 [180], Cul3-KLHL20 [181] and UHRF1 [182], as well a number of viral E3s as detailed above. In all known cases, ubiquitination of PML results in its proteasome-mediated destruction. Inhibiting PML ubiquitination results in a strengthening of its effects on proliferation and as such can slow cell cycling, diminish tumor growth in xenografts [183], and decrease cellular migration [182].

#### 1.5.5.3 Phosphorylation

PML is extensively phosphorylated, being modified on a number of serines and threonines. While one early report showed that PML was labeled by a phosphotyrosine-specific antibody [184], no phosphotyrosine have been found in subsequent mass spectrometric screens [176,185].

Activation of three of the four MAP kinase groups, that is ERK1/2 [186], p38 [183], and BMK1 [187], in response to mitogens or cellular stress results in PML phosphorylation. Treatment of cells with arsenic trioxide stimulates ERK1/2 to phosphorylate PML at T28, S36, S38, S40, S527, S530, with

phosphorylation of one or more of these sites in turn stimulating SUMOylation of PML [186]. Phosphorylation of PML at S403, S505, S518, and S527 by ERK2 influence the ability of Pin1 to bind to PML in response to extracellular growth factor (EGF) [188] or insulin-like growth factor-1 [189] signaling. The subsequent interaction with Pin1 induces a conformational change in PML that results in its polyubiquitination by the E3 ubiquitin ligase Cul3-KLHL20 [181]. EGF also regulates PML through its stimulation of BMK1, which phosphorylates PML on S403 and T409 [187]. Phosphorylation of PML by BMK1 disrupts interactions between PML and MDM2, promoting p53 degradation [190]. Mutation of the S403 and T409 phosphoacceptor sites in PML or the use of BMK1 inhibitors increase p21 levels, and pharmacological inhibition of BMK1 shrinks tumor formation in mice in a PML-dependent manner [187]. Osmotic stress, irradiation by ultraviolet light [183], or arsenic trioxide treatment [141] induce a p38-dependent activation of CK2, which then phosphorylates PML on S560, S561, S562, and S565 [183]. These sites are adjacent to both the SIM and to an amino acid sequence that promotes PML degradation. On the one hand, phosphorylation at these sites increases the ability of the SIM to bind to SUMOylated proteins [191,192]; on the other hand, phosphorylation at S565 leads to polyubiquitination and proteasomal degradation of PML [183]. The use of CK2 inhibitors can prevent tumor growth in mice in a PML-dependent manner [183]. In contrast, heat shock and heavy metal exposure induce p38 and ERK1/2 dependent deSUMOylation of PML, ND10 fission, and the loss of the ND10 members [179].

DNA damage result in changes to PML phosphorylation as well. Upon γ-irradiation, CHK2 phosphorylates PML at S117 [193]. Blocking this phosphorylation prevents apoptosis while exogenous expression of an S117E PML-IV mutant induced apoptosis in U937 cells. DNA double strand breaks induced by doxorubicin treatment result in phosphorylation of PML by ATR [194], causing PML to relocate to the nucleolus, bringing MDM2 with it and sequestering Mdm2 away from p53. DSBs also induce phosphorylation of PML at S8 and S38 by HIPK2 [178]. Again, phosphorylation of PML on the N-terminus results in increased amounts of PML, though in this instance SUMOylation leads to increased stability.

In addition to being phosphorylated in response to EGF stimulation, S518 is phosphorylated under hypoxic conditions, although in this case it is by CDK1 and CDK2 [181]. Again, this promotes interaction with Pin1 and, in turn, ubiquitination of PML by the Cul3-KLHL20 E3 ubiquitin ligase and allows for full upregulation of HIF1α target genes.

Phosphorylation plays a part in the control of PML's activity in granulocyte differentiation. In this process, the ability of PML to cooperate with C/EBPε to transactivate G-CSF-responsive genes is dependent on phosphorylation of PML at S505, S518, S527, and S530 [195].

Finally, while the sites involved are currently unknown, PML undergoes a mitosis-regulated phosphorylation that is involved in the deSUMOylation and dismantling of ND10s as cells enter mitosis [196]. Additionally, this phosphorylated form of PML is also seen in heat-shocked cells.

Altogether, the large number of post-translational modifications and the amount of cross-talk between different modifications demonstrate the importance of these modifications in the activity of PML. However, most attention, particularly in the context of HSV-1 infection, has focused on the role that SUMOylation plays in PML's antiviral activity while the function of phosphorylation has been relatively unexamined and as such is one focus of this thesis.

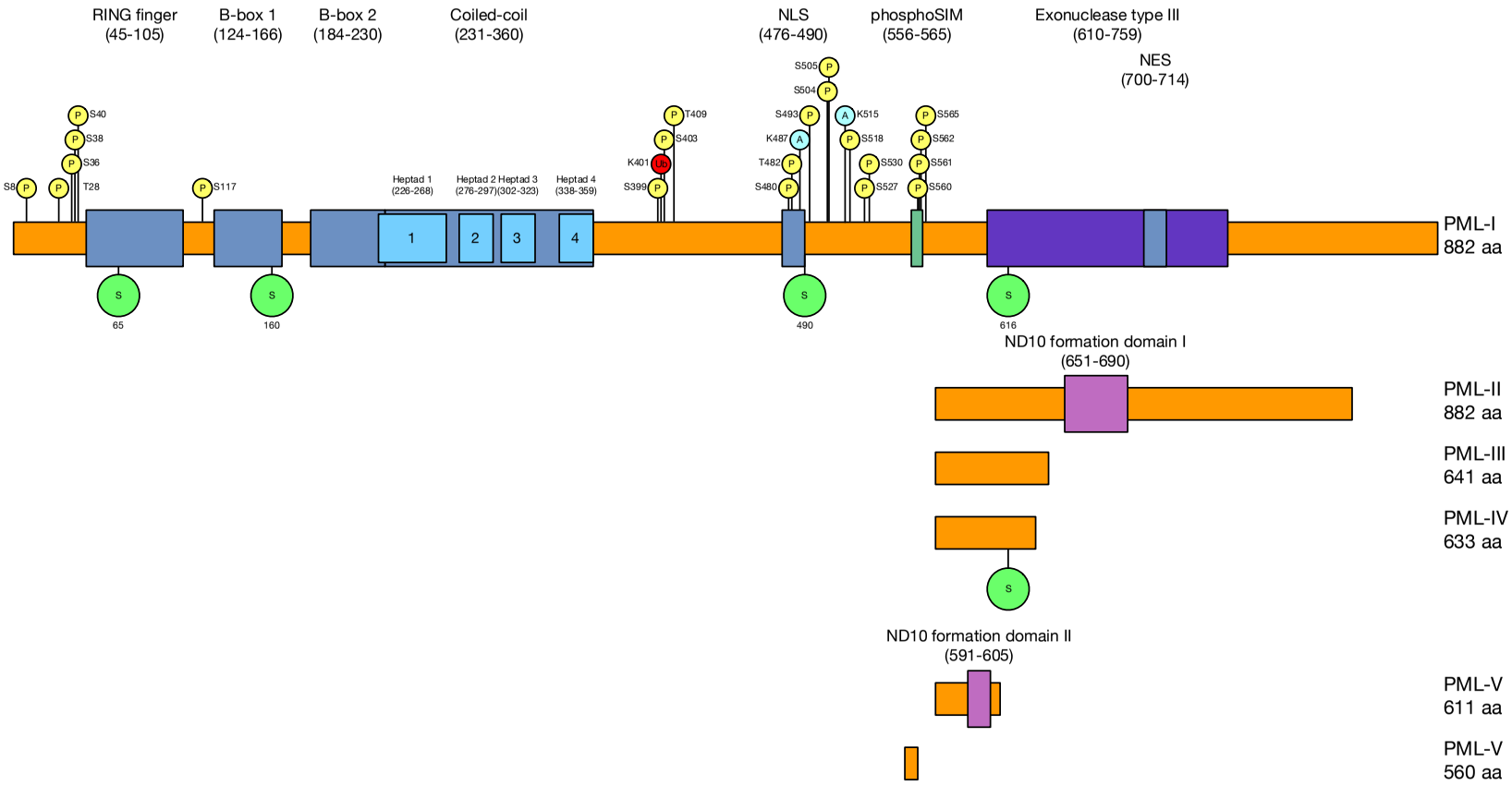
RING finger
(45-105)
B-box 1
(124-166)
B-box 2
(184-230)
Coiled-coil
(231-360)
NLS
(476-490)
phosphoSIM
(556-565)
Exonuclease type III
(610-759)
NES
(700-714)
Heptad 1
(226-268)
Heptad 2 Heptad 3
(276-297)(302-323)
Heptad 4
(338-359)
S8
T28
S40
S38
S36
S117
T409
S403
K401
S399
S505
S504
S493
K487
T482
S480
K515
S518
S530
S527
S565
S562
S561
S560
1
2
3
4
S
65
160
490
616
PML-I
882 aa
ND10 formation domain I
(651-690)
PML-II
882 aa
PML-III
641 aa
PML-IV
633 aa
ND10 formation domain II
(591-605)
PML-V
611 aa
PML-V
560 aa

**Figure 1.1. Location of functional domains and sites of post-translational modification on PML.**

Location of the Really interesting New Gene (RING) finger, B-box 1, B-box 2, coiled-coil, Nuclear Localization Signal (NLS), and Nuclear Exclusion Signal (NES) are shown in as dark blue boxes (with the heptad repeats that create the coiled-coil in light blue boxes), the endonuclease type III domain of PML-I as a purple box, and the ND10 formation domains of PML-II and PML-V as mauve boxes. Sites of phosphorylation (P), SUMOylation (S), acetylation (Ac), and ubiquitination (Ub) are indicated by the spheres above and below with the modified residue listed.

# Chapter 2: CK2 Inhibitors Increase the Sensitivity of HSV-1 to Interferon-β

## 2.1 Introduction

For HSV-1, the successful establishment of infection and progression through the lytic phase of replication requires the coordinated effort of many viral and cellular factors to stimulate viral gene expression to ultimately produce infectious progeny virus [7]. A common theme in the regulation of these proteins is their post-translational modification by phosphorylation. Although HSV-1 encodes at least two of its own protein-directed kinases – UL13 and US3 – efficient replication appears to require several cellular kinases, most notably certain cyclin-dependent kinases [197] and stress activated protein kinases [198]. HSV-1's requirement for cellular kinases makes the use of pharmacological inhibitors against these kinases a potential avenue for anti-herpetic treatments.

The host kinase, CK2, has been shown or is predicted to modify a number of HSV-1 proteins and has been hypothesized to affect many aspects of the viral lifecycle. Previous studies examining the role of CK2 during HSV-1 infection were unable to assess the effect of CK2 on replication due to limitations of the inhibitors available at the time. For example, at the concentrations necessary to inhibit CK2 with a commonly used CK2 inhibitor,

5,6-Dichloro-1-β-D-ribofuranosylbenzimidazole (DRB), the drug also blocks the activity of CDK9 [97,199]. In this study, we have taken advantage of recently developed compounds that are more selective in their inhibitory properties. Our results indicate that CK2 inhibitors have a minor impact on HSV-1 replication in cultured human fibroblasts; however, the use of CK2 inhibitors compromises the ability of the virus to replicate in cells pretreated with the type I interferon, IFN-β, in a manner that was only observed with HSV-1.

## 2.2 Methods and Materials

### 2.2.1 Cell and viruses

Human embryonic lung (HEL) cells were obtained from the American Type Culture Collection (CCL-137) and grown in Minimum Essential Medium Eagle Alpha Modification (αMEM) supplemented with 10% fetal bovine serum (FBS), 2 mM L-glutamine, 10 U/mL penicillin, and 10 U/mL streptomycin. Vero cells and L7 cells, which are Vero cells that contain the *ICP0* gene [200], were grown in Dulbecco's modified Eagle's medium supplemented with 5% FBS, 2 mM L-glutamine, 10 U/mL penicillin, and 10 U/mL streptomycin. KOS [201] is the wild type HSV-1 strain used in these studies. 7134 is an ICP0-null mutant in which the *ICP0* open reading frame is replaced by the *E. coli lac*Z gene [202]. KOS and 7134 viral stocks were prepared in Vero cells and titered on either Vero (for KOS) or L7 cells (for 7134) as previously described [91,203]. Adenovirus 5 (Ad5) was purchased from the American Type Culture Collection (VR-5) and

propagated and titered on HEK-293 cells [204]. The vesicular stomatitis virus recombinant, VSV-eGFP [205], which encodes the enhanced green fluorescent protein gene inserted between the G and L genes, was a gift from Dr. Asit Pattnaik and was propagated and titered on Vero cells.

### 2.2.2 Reagents

The CK2 inhibitors 4,5,6,7-tetrabromo-1H-benzotriazole (TBB) and 2-dimethylamino-4,5,6,7-tetrabromo-1*H*-benzimidazole (DMAT) were purchased from EMD Chemicals and 2-(4,5,6,7-tetrabromo-2-(dimethylamino)-1H-benzo[d]imidazol-1-yl)acetic acid (TMCB) from Ascent Scientific. All CK2 inhibitors were constituted in DMSO (Fisher Scientific). Recombinant human IFN-β was purchased from R&D Systems.

### 2.2.3 Viral plaque reduction assays

For HSV-1 plaque reduction assays, HEL cells were plated in 24-well plates. Upon reaching 70% confluency, cells were either mock treated or treated with a given concentration of IFN-β. After 16 h of IFN-treatment, cells were prewashed with either medium; medium plus IFN-β; medium plus DMSO (as vehicle control), TBB, or TMCB; or medium plus IFN-β and either vehicle or CK2 inhibitor. Cells were then infected with 10-fold serial dilutions of HSV-1 in the aforementioned media. At 1 h post infection (hpi), the cells were overlaid with cell culture medium containing 0.5% methylcellulose and the appropriate compounds. At 3 days post infection (dpi), monolayers were fixed with 3.7% formaldehyde, probed with a horseradish peroxidase (HRP)-conjugated anti-

HSV antibody (Dako), and the resulting plaques were visualized with Vector Red substrate (Vector Labs). Plaque areas were determined by capturing images of immunohistochemically stained plates with a flatbed scanner (Canon), measuring the number of pixels that corresponded to an individual plaque in Adobe Photoshop. Pixel values were converted to $mm^2$ by dividing by the number of pixels per inch for the image. Four to twenty plaques were measured per treatment from two experiments.

For Ad5 plaque reduction assays, HEL cells were treated and infected as described for the HSV-1 plaque assays. At 5 dpi, cells were washed once with PBS, fixed for 5 minutes with 5% formaldehyde in PBS, washed three times with PBS, permeabilized at 4°C for 15 minutes with 0.5% NP-40 in PBS, and washed an additional three times with PBS. Ad5 infected cells were detected by probing the cells with a FITC-conjugated anti-adenovirus antibody (B65140F, Meridian Life Science) diluted in PBS and the resulting plaques and cells were visualized and counted by fluorescence microscopy (Nikon).

For VSV-eGFP reduction assays, HEL cells were again treated and infected as described for HSV-1 plaque assays with the exceptions that the cells were treated with 10 U/mL of IFN-β, and the monolayers were overlaid with 2% methylcellulose. At 1 dpi, the cells were washed three times with PBS and fixed with 3.7% formaldehyde in PBS for 5 minutes at room temperature. Plaques were detected and counted by fluorescence microscopy (Nikon).

### 2.2.4 Viral yield assays

HEL cells were plated at $1 \times 10^5$ cells per well in 12-well plates and one day later were either mock treated or treated with IFN-β. 16 hs later, cells were prewashed as described above and subsequently infected for 1 h in the presence of the appropriate compounds with either KOS or 7134 at a multiplicity of infection of 1. After 1 h, the cells were overlaid with cell medium containing the previously described compounds. At 24 hpi, cells were harvested, and viral titers were determined on Vero or L7 cells for KOS or 7134, respectively.

### 2.2.5 Western blots

HEL cells were plated, treated, and infected as described for HSV-1 yield assays. 12 and 24 hpi, cells were washed once with PBS and then scraped into boiling Laemmli loading buffer [206] containing 1 μg/mL leupeptin, 1 μg/mL aprotinin, 1 mM phenylmethanesulfonylfluoride, 10 mM sodium vanadate, 50 mM sodium fluoride, and 20 mM N-ethylmaleimide. 10% of each sample was resolved on a 4-12% Bis-tris polyacrylamide gel, transferred to nitrocellulose, blocked at room temperature for 1 h with 2% nonfat dry milk in Tris-buffered saline with 0.1% Tween 20 (TBS-T), and probed overnight at 4°C with antibodies directed against either ICP4 (H1A021, EastCoast), UL42 (mAB3678, Millipore), PML (A301-167A, Bethyl Laboratories), or β-actin ((I-19)-R, Santa Cruz Biotechnology). Membranes were then washed three times with TBS-T and probed at room temperature with either goat-anti-mouse IgG or goat-anti-rabbit IgG conjugated to HRP (Jackson Immunoresearch). Membranes were again

washed with TBS-T and developed with chemiluminescent substrate (Femto ECL, Pierce Laboratories). Some membranes were stripped by incubation in 2% SDS, 100 mM β-mercaptoethanol, 62.5 mM Tris-HCl (pH 6.7) at 55°C for 30 minutes. These membranes were thoroughly washed with TBS-T, blocked at room temperature for 1 h with 2% milk/TBS-T, and probed overnight at 4°C with antibodies directed against either ICP0 (sc-53070, Santa Cruz Biotechnology) or VP5 (ab6508, Abcam). The membranes were then washed, probed with a secondary HRP-conjugated antibody, and developed as before. Chemiluminescence was detected using an Image Station 4000R (Kodak) and Carestream Molecular Imaging software. Images were assembled using Photoshop and Illustrator (Adobe Systems) and band intensities were measured by densitometry analyses using ImageJ.

### 2.2.6 Immunofluorescence

HEL cells were plated at $1 \times 10^5$ cells per well in collagen-coated glass bottom 24-well plates, treated, and infected as described above for the HSV-1 yield assays. At 12 hpi, the cells were fixed and permeabilized as described above in the Ad5 plaque reduction assays. Samples were blocked with 1% BSA, 5% FCS, 1% goat serum in PBS for 1 h at room temperature. Cells were then probed with antibodies against ICP0 (sc-53070), PML (A301-167A), and DNA-PKcs (sc-5282, Santa Cruz Biotechnology) for 1 h in blocking solution at 37°C. Monolayers were washed with PBS and probed with goat-anti-mouse immunoglobulin (IgG) 2b Dylight 488 (Jackson Immunology), goat-anti-rabbit

IgG Alexa 405 (Molecular Probes), and goat-anti-mouse IgG1a Dylight 594 (Jackson Immunoresearch) to detect ICP0, PML, and DNA-PKcs, respectively. Proteins were viewed by confocal fluorescent microscopy (Olympus) and captured with a digital camera (Hamamatsu). Images were assembled using Photoshop and Illustrator (Adobe Systems).

## 2.3 Results

### 2.3.1 CK2 inhibitors reduce the plating efficiency and plaquing of HSV-1 in IFN-β-treated cells

We initially sought to determine the requirement for CK2 activity during HSV-1 replication. To this end, we employed plaque reduction assays to test the effect that two specific CK2 inhibitors, TBB ($IC_{50}$ = 0.15 μM) and TMCB ($IC_{50}$ = 0.50 μM) [207], which block the active site of CK2, have on the plating efficiency and spread of HSV-1 in HEL cells. Additionally, because cellular factors responsible for the innate antiviral response (e.g., IFN) and the viral factors that counteract this response are either known to be or are potential CK2 substrates, we also examined how these inhibitors affected the ability of HSV-1 to plaque in the presence of a type 1 interferon, IFN-β. HEL cells were untreated or pretreated with 1000 U/mL of IFN-β for 16 hs and then infected with serially diluted HSV- 1 in the presence of the compounds as listed in Table 2.1. In these and subsequent assays, TBB was used at 50 μM as previously described [183], while a preliminary dose response curve suggested that the same concentration

was appropriate for TMCB (data not shown); DMSO was used at 0.5% v/v as a vehicle control. As seen in Table 2.1, the use of each CK2 inhibitor alone resulted in only a modest reduction in plaque size (3.9- and 1.4-fold decrease for TBB and TMCB, respectively) and plating efficiency of HSV-1 (0 and 2-fold decrease for TBB and TMCB, respectively) compared to the untreated samples. As expected, IFN-β reduced plaque size and plating efficiency 26- and 25-fold, respectively. When DMSO was added to IFN-β, it had a slight effect on plaque size (1.8-fold decrease versus IFN-β alone), and a negligible impact on plating efficiency. However, the combination of IFN-β and either CK2 inhibitor further reduced viral plaque size and plating efficiency (3.5- and 2.8-fold for TBB, and 2.6- and 2.1-fold for TMCB, respectively), compared to IFN-β-treated cells. These results were further confirmed when we used a third CK2 inhibitor, DMAT (data not shown). We then tested whether these inhibitors would also enhance the IFN-sensitivity in cells treated with a suboptimal concentration (50 U/mL) of IFN-β. This reduced amount of IFN, in either media alone or with DMSO, indeed proved to be less effective at reducing either plaque size (~5-fold) or plating efficiency (4-fold). Again, we found that both inhibitors, in combination with IFN-β, reduced the plating efficiency of HSV-1 (9- and 7-fold) and both decreased viral plaque size (42.1- and 10.3-fold for TBB and TMCB, respectively) beyond that of IFN alone. These decreases in viral replication were not due to a loss of cell viability, as treatment with IFN, CK2 inhibitor, or a combination of IFN and inhibitor did not increase cell death as measured by trypan blue exclusion assays. Specifically, by three days post treatment, there was a 15% loss in cell

viability with mock-treated HEL, where all other treatment groups had a similar (9-23%) loss in cell viability.

### 2.3.2 CK2 inhibitors reduce viral replication in IFN-β-treated cells in an ICP0-dependent manner

We then examined whether the decreases in the plating efficiencies and plaque sizes observed in Table 2.1 correlated with reductions in productive infection. In addition, we included an ICP0-null mutant virus in these experiments because ICP0 has been shown to assist HSV-1 in counteracting the IFN response [31,208,209] and is a potential target of CK2 phosphorylation [91]. Cells were pretreated with IFN-β and infected with 1 PFU per cell of either HSV-1 or an ICP0-null mutant virus in the presence of the reagents. As shown in Figure 2.1, IFN-β treatment alone reduced the replication of HSV-1 by 28-fold and the ICP0-null mutant by 212-fold, while treatment with DMSO or either CK2 inhibitor resulted in a minor (~2 fold) reduction in replication. However, when the inhibitors were used in conjunction with IFN-β, the replication of HSV-1 was decreased by a factor of 145-fold with TBB and 69-fold with TMCB whereas the ICP0-null mutant was reduced by a factor of 182-fold with TBB and 141-fold with TMCB. These results demonstrate that CK2 inhibitors increase the antiviral effects of IFN-β on HSV-1 productive infection and suggest the enhancement by the CK2 inhibitors may be related to the anti-IFN-mediated activity of ICP0.

### 2.3.3 CK2 inhibitors in conjunction with IFN-β decrease the levels of early and late proteins

To identify the point(s) in the viral life cycle impaired by the combination of CK2 inhibitor and IFN-β, we analyzed the accumulation of specific viral proteins by western blot analysis. HEL cells were again pretreated with IFN-β and infected with HSV-1 at 1 PFU per cell in the presence of the reagents. At 12 and 24 hpi, western blots were used to assess the levels of the viral proteins ICP4, UL42, and VP5 as representative examples of IE, E, and L proteins, respectively. The results in Figure 2.2 show that, as expected, the CK2 inhibitors alone had little effect on the accumulation of the viral proteins examined. IFN treatment delayed viral protein expression, with an overall reduction for all three kinetic classes tested. While the combination of IFN-β and CK2 inhibitor did not decrease ICP4 levels more than for IFN-β alone, there was a decline in UL42 (>100-fold for TBB and TMCB) and VP5 (>9-fold for TBB and TMCB) levels at 24 hpi. These results indicate that the use of the CK2 inhibitors impairs the function of at least one IE protein to activate the synthesis of E and L proteins.

### 2.3.4 CK2 inhibitors do not affect the stability of ICP0-directed targets of degradation

Since the viral replication assays indicated that the CK2 inhibitors did not increase the IFN sensitivity of an ICP0-null mutant, we assayed the impact that the CK2 inhibitors had on the E3 ubiquitin ligase activity of ICP0. ICP0, through

its E3 ubiquitin ligase activity, induces the proteasomal-dependent degradation of a number of cellular targets in order to assist HSV-1 in overcoming cellular antiviral responses. As a result, we examined whether the CK2 inhibitors impaired ICP0's ability to induce the loss of two cellular targets, PML and DNA-PKcs. HEL cells were pretreated with IFN-β and infected with HSV-1 in the presence of CK2 inhibitors as described above. At 12 hpi, the cells were assayed for the presence of ICP0, PML, and DNA-PKcs by immunofluorescence; at 12 and 24 hpi, cell lysates were analyzed for PML and ICP0 levels by western blot. As shown in Figure 2.3, while the use of either CK2 inhibitor, IFN-β, or the combination of CK2 inhibitor and IFN-β decreased the number of ICP0-positive cells, a majority of cells that were positive for ICP0 either showed a decrease or loss of DNA-PKcs and PML, irrespective of treatment. When we examined PML levels by western blot (Figure 2.4), however, it appeared that treatment with TBB alone resulted in a slight stabilization of PML at 12 hpi, and at 24 hpi when TBB was used with IFN-β in HSV-1 infected cells. While this might indicate that CK2 is involved in ICP0-induced PML degradation, it is also likely that PML levels were higher due to a smaller proportion of cells expressing ICP0 (Figure 2.3) resulting in the decreased levels of ICP0 produced in cells treated with CK2-inhibitor (Figure 2.4). These results suggest that the CK2 inhibitors do not compromise the E3 ubiquitin ligase activity of ICP0, or at least the ability of ICP0 to induce the degradation of two of its targets.

### 2.3.5 The enhanced effect of CK2 inhibitors on IFN is observed with HSV-1 but not VSV and Ad5

Our results suggest two possibilities to explain how the use of CK2 inhibitors increase the sensitivity of HSV-1 to an IFN-β-induced antiviral response: CK2 negatively regulates one or more cellular components of the IFN response that repress HSV-1 replication and thus the inhibitors increase the overall potency of IFN-β or CK2 alters the activities of one or more viral components that impairs the ability of IFN to restrict HSV-1 replication. It is also conceivable that both possibilities are true. To test these possibilities, we examined the effect that the CK2 inhibitors had on the plating efficiency of two other viruses, VSV and Ad5. VSV and Ad5 were chosen for these studies as they represent viruses that are genetically distinct from HSV-1 and are either very sensitive to the effects of IFN (for VSV) or show high levels of IFN resistance (for Ad5) [210]. HEL cells were pretreated with IFN-β for 16 hs and infected with 10-fold serial dilutions of either Ad5 or the VSV recombinant, VSV-eGFP, as described for HSV-1. At 1 dpi, VSV-eGFP-infected monolayers were fixed and GFP-positive plaques counted; Ad5-infected monolayers were fixed at 5 dpi, stained with an antibody directed against adenovirus, and plaques visualized by immunofluorescence. As shown in Table 2.2, VSV replication was highly impaired by pretreatment with IFN, whereas Ad5 was highly resistant, as expected. Similar to HSV-1, both of the CK2-inhibitors had little to no effect on either VSV or Ad5 replication; however, unlike HSV-1, neither inhibitor increased the IFN-sensitivity of VSV or Ad5. These data suggest that the activity of CK2 is

necessary for the ability of HSV-1 to diminish the effects of IFN on replication, that this mechanism is specific to HSV-1, and that, at least in HEL cells, CK2 activity is not required for the plaquing of either VSV or Ad5 regardless of the IFN response.

## 2.4 Discussion

HSV-1 requires the activities of a number of both viral and cellular kinases for efficient viral replication. Because several of the potential viral CK2 substrates are involved in overcoming cellular intrinsic and innate antiviral defenses and a number of those defenses are themselves CK2 phosphorylation substrates [63,66,91,183,211], we investigated the effect that CK2 inhibitors have on HSV-1 replication in cells treated with the type I interferon, IFN-β. Surprisingly, while the inhibitors alone had little impact on replication, they functioned synergistically with IFN-β. When we investigated the point in the viral life cycle affected, we found that the levels of the IE proteins ICP0 and ICP4 were relatively unaltered while there was large decrease in both the E protein, UL42, and L protein, VP5. This result suggests that the CK2 inhibitors impair the activity of an IE protein that functions to overcome the IFN response. Of the HSV-1 IE proteins, both ICP0 and ICP27 have been identified as antagonists of the IFN response. This study focused on whether inhibition of CK2 activity influenced ICP0's ability to counteract the IFN response. We were unable to examine the role of ICP27 in this study as the loss of ICP27 is deleterious [212]

and, as is discussed below, mutations that either block or mimic phosphorylation at the CK2 phosphoacceptor sites of ICP27 significantly impair HSV-1 replication [93]. Our results demonstrate that the CK2 inhibitors were unable to increase the IFN sensitivity of an ICP0-null mutant, indicating a requirement for CK2 in ICP0's anti-IFN activity. To determine if the combination of CK2 inhibitor and IFN-β impede a key function of ICP0, we examined the ability of ICP0 to direct the degradation of two of its targets, PML and DNA-PKcs, in cells treated with the CK2 inhibitors. In these assays, we did not observe the inhibitors inducing a stabilization of either target. While ICP0 may be a CK2 substrate, it appears that phosphorylation of ICP0 by CK2 is not necessary for its E3 ubiquitin ligase activity in our assays. It is possible that phosphorylation of ICP0 by CK2 may affect an activity of ICP0 not linked to its E3 ligase activity in order to promote efficient viral replication in the presence of IFN-β, or that ICP0 activates the expression of an E and/or L gene and that the protein product of this viral gene is phosphorylated by CK2 to inactivate components in the IFN response. Indeed, previously work using transient transfection assays showed that ICP0 mutated in two regions containing potential CK2 phosphorylation sites exhibit defects in its transactivation activity [91]; however, initial tests of a virus encoding one of these mutants, Phos1, behaved like a wild type virus in plaque assays (data not shown).

We also noted in this study that the CK2 inhibitors alone do not appear to greatly impede the replication of HSV-1, thus making CK2 activity likely dispensable for the growth of HSV-1. This is unexpected given the number of

HSV-1 proteins that have been identified as potential CK2 substrates and that mutation of these CK2 phosphorylation sites is detrimental to viral replication [92,93,213–215]. As one example, mutation of CK2 phosphorylation sites in the IE protein, ICP27, impairs viral replication [93]. This mutation, however, may prevent a large conformational shift in the N-terminus of ICP27 that appears to be necessary for its functions [98] and do so in a CK2 phosphorylation-independent manner. It is also probable that residual CK2 kinase activity may remain after TBB or TMCB treatment or that the stimulation of CK2 activity by ICP27 [97] is able to overcome the effect of the CK2 inhibitors; however, these possibilities seem unlikely as a further reduction in plaque size or plating efficiency was not observed when higher levels of either inhibitor were used (data not shown).

While the enhanced sensitivity of IFN induced by CK2 inhibitors requires at least one HSV-1 protein, it is also plausible that this effect could be mediated by one or more cellular factors. To explore this possibility, we examined whether the CK2 inhibitors influenced the IFN-sensitivity of two other viruses, VSV and Ad5. We found that the CK2 inhibitors used alone affected neither virus. While IFN-β impaired the replication of VSV, neither inhibitor increased this impairment beyond that of IFN-β alone. Ad5, on the other hand, was largely impervious to the effect of IFN-β and the use of the CK2 inhibitors failed to change this. Although the CK2 inhibitors alone did not alter VSV replication, it was recently reported that use of the CK2 inhibitor, DMAT, or siRNA-mediated silencing of CK2 increased VSV replication [63]. Likewise, the CR2 region of the

Ad5 E1A protein contains a consensus CK2 phosphorylation motif [216]. In the case of VSV, the discrepancy may lie in the cell lines used, as those studies were carried out in the highly transformed HEK-293s while we used primary-like HEL-299s. As for Ad5, while the CK2 site was implicated in binding to the retinoblastoma protein and resistance to Ad-induced cell death, the role of phosphorylation at this site in Ad5 replication is likely to be minimal as mutation of this site failed to affect E1A transactivation activity [216]. In either case, the fact that the CK2 inhibitors did not increase the IFN-β sensitivity of VSV or Ad5 suggests that the CK2 inhibitors compromise an anti-IFN mechanism that is specific to HSV-1.

While we did not note either CK2 inhibitor having a large impact on the replication of either VSV or Ad5, a number of other viruses have shown a dependence on CK2 activity for efficient replication. For example, CK2 phosphorylation is involved in multiple steps of the human immunodeficiency virus 1 (HIV-1) life cycle, including reverse transcription and gene expression [69,217], and treatment with a CK2 inhibitor has been reported to inhibit HIV-1 replication [217]. Additionally, a CK2 inhibitor was recently shown to have antiviral activity towards varicella-zoster virus [218]. It remains to be seen, however, if the enhancement by CK2 inhibitors on the potency of IFN is restricted to HSV-1 or if this extends to other members of the herpesvirus family or more broadly to other viral families. Nevertheless, CK2 inhibitors show promise as anti-HSV-1 therapeutic agents when used in combination with other

antiviral treatments. Notably, the CK2 inhibitor, TBB, has been shown to be efficacious in limiting retinal pathologies in mice [219].

## 2.5 Tables

**Table 2.1 Plaque size and plating efficiency of HSV-1 in CK2 inhibitor-, IFN-β-, or IFN-β plus CK2 inhibitor-treated cells.**

| Treatment | Area ($mm^2$)[a] | Area (fold change)[b] | Area (fold decrease vs IFN-β)[c] | Plating efficiency (fold decrease)[d] |
|---|---|---|---|---|
| None | 5.470 (± 0.564) | – | – | – |
| DMSO | 4.670 (± 0.644) | ↓1.2 | – | 1 |
| TBB | 1.410 (± 0.193) | ↓3.9 | – | 1 |
| TMCB | 3.830 (± 0.414) | ↓1.4 | – | ↓2 |
| 50 U/mL IFN-β | 1.160 (± 0.126) | ↓4.7 | – | ↓4 |
| 50 U/mL IFN-β + DMSO | 0.970 (± 0.106) | ↓5.6 | ↓1.2 | ↓4 |
| 50 U/mL IFN-β + TBB | 0.130 (± 0.011) | ↓42.1 | ↓8.9* | ↓9 |
| 50 U/mL IFN-β + TMCB | 0.530 (± 0.065) | ↓10.3 | ↓2.2* | ↓7 |
| 1000 U/mL IFN-β | 0.210 (± 0.025) | ↓26.0 | – | ↓25 |
| 1000 U/mL IFN-β + DMSO | 0.120 (± 0.011) | ↓45.6 | ↓1.8 | ↓27 |
| 1000 U/mL IFN-β + TBB | 0.060 (± 0.005) | ↓91.2 | ↓3.5* | ↓71 |
| 1000 U/mL IFN-β + TMCB | 0.080 (± 0.007) | ↓68.4 | ↓2.6* | ↓52 |

[a] Plaque areas were determined by capturing images of immunohistochemically stained plates with a flatbed scanner and measuring the number of pixels that corresponded to an individual plaque in Adobe Photoshop. The pixel values were converted to $mm^2$ by dividing that value by the number of pixels per inch for the image. Four to twenty plaques were measured per treatment for two experiments, and the results for one experiment are shown above. Data are shown as the means (± SEM).

[b] Fold change relative to untreated cells (“None”).

[c] One-Way ANOVA ($P < 0.05$), Bonferroni’s multiple comparison post-test (*, $P < 0.05$) compared to the IFN-treated group

[d] Plating efficiency decrease was calculated by dividing the number of plaques in the untreated sample by the number of plaques for a given treatment. The data shown are the means of two experiments.

**Table 2.2. Plating efficiency of VSV and Ad5 in CK2 inhibitor-, IFN-β-, or IFN-β plus CK2 inhibitor-treated cells.**

| Virus | Treatment | Plating efficiency (fold decrease)[a] |
|---|---|---|
| VSV | None | – |
| | DMSO | 1 |
| | TBB | 1 |
| | TMCB | 1 |
| | IFN-β | ↓100 |
| | IFN-β + DMSO | ↓74 |
| | IFN-β + TBB | ↓66 |
| | IFN-β + TMCB | ↓65 |
| Ad5 | None | – |
| | DMSO | 1 |
| | TBB | 1 |
| | TMCB | 1 |
| | IFN-β | ↓2 |
| | IFN-β + DMSO | ↓3 |
| | IFN-β + TBB | ↓5 |
| | IFN-β + TMCB | ↓4 |

[a]Plating efficiency decrease was calculated by dividing the number of plaques in the untreated sample by the number of plaques for a given treatment. The data shown are the means of two experiments

## 2.6 Figures

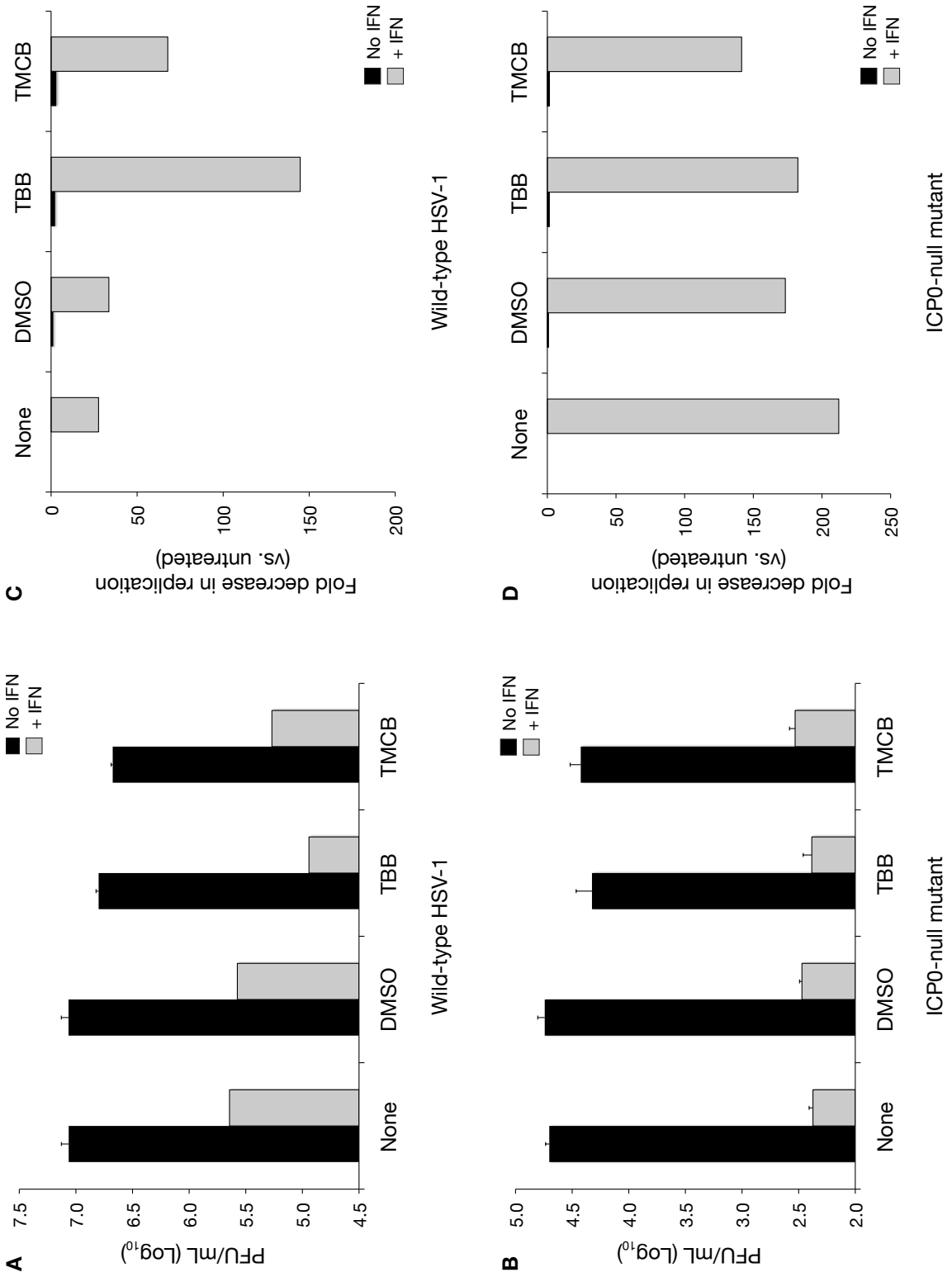


**Figure 2.1. The effect of IFN-β and CK2 inhibitors on viral replication.**

HEL cells were pretreated with or without IFN-β for 16 hs and subsequently infected with wild-type HSV-1, strain KOS, (A and C) or an ICP0 null mutant, 7134, (B and D) at 1 PFU per cell in the presence of IFN-β, DMSO (vehicle), TBB, or TMCB or a combination of IFN and DMSO, TBB, or TMCB. At 24 hpi, infected cells were harvested, and wild-type HSV-1 was titered on Vero cells and the ICP0 null mutant on L7 cells. The data shown in A and B are the mean titers (± SEM) of two experiments performed in duplicate; C and D are the titers expressed as fold decrease relative to untreated cells.

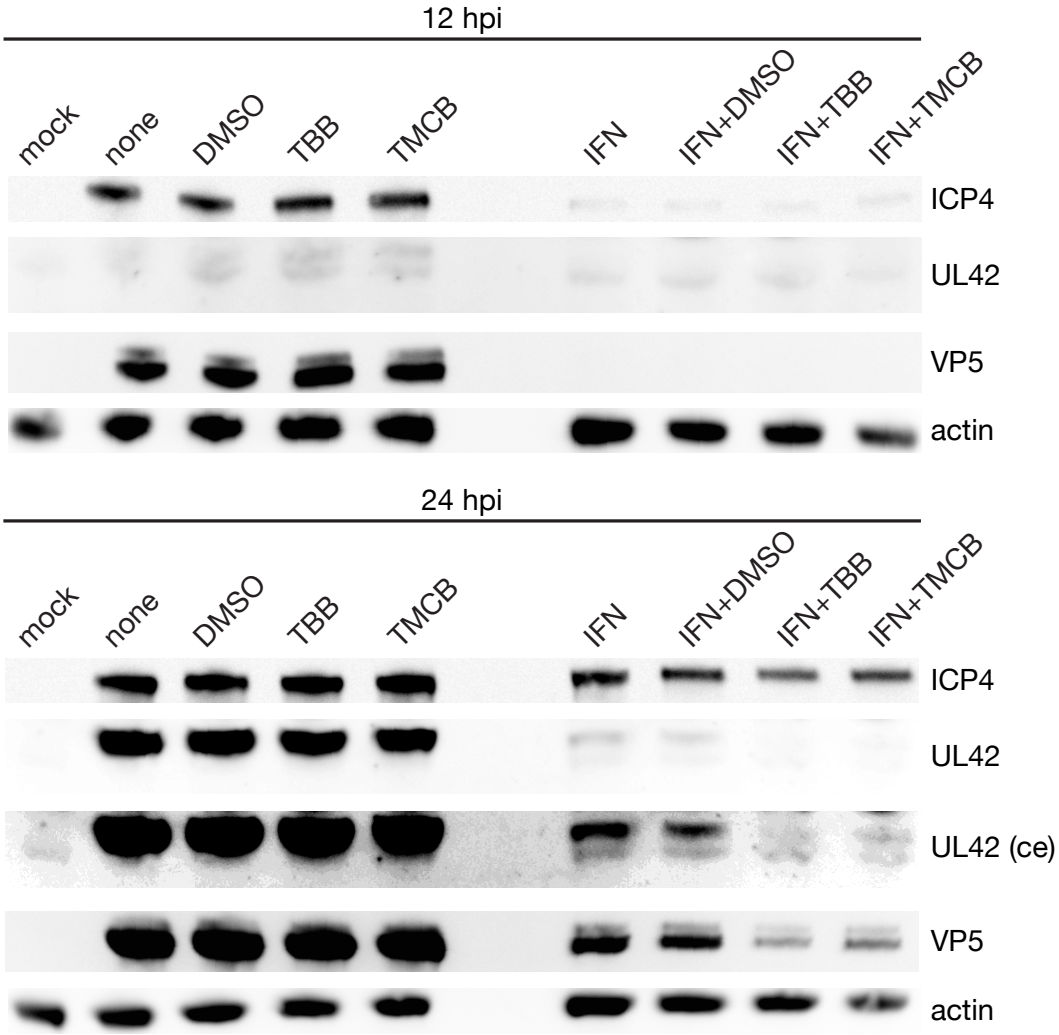


**Figure 2.2. The combination of CK2 inhibitor and IFN-β decreases early and late protein levels.**

HEL cells were treated and infected as described in Figure 2.1. At 12 and 24 hpi, cells were washed with PBS before being resuspended into loading buffer. Lysates were resolved by SDS-PAGE and analyzed by western blot for ICP4, UL42, VP5, or β-actin expression. Band intensities were measured by densitometry analyses using ImageJ. UL42 (ce): the UL42 24 hpi lanes contrast enhanced (ce) using Adobe Photoshop.

**2.3A**

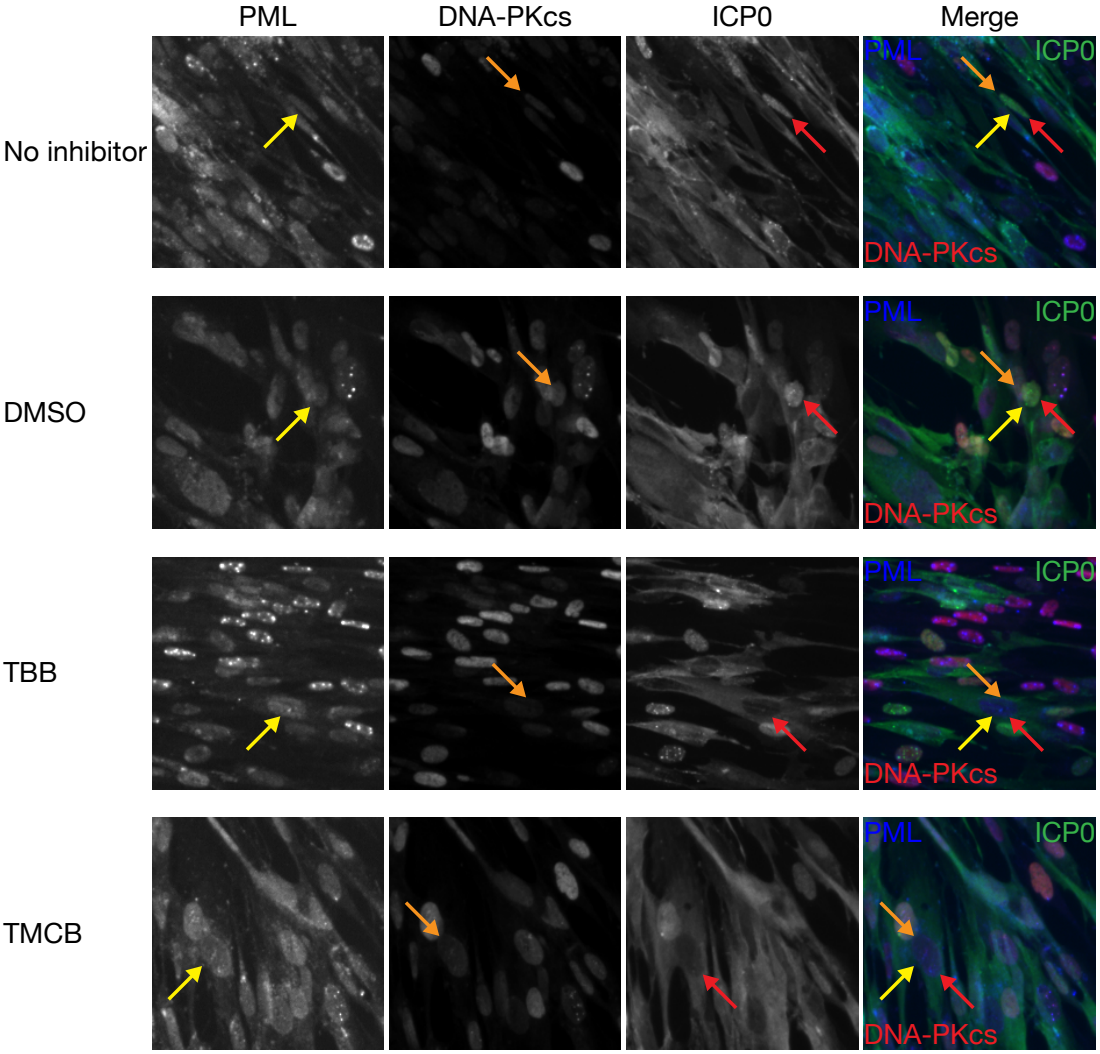
PML
DNA-PKcs
ICP0
Merge
No inhibitor
DMSO
TBB
TMCB
PML
ICP0
DNA-PKcs

**2.3B**

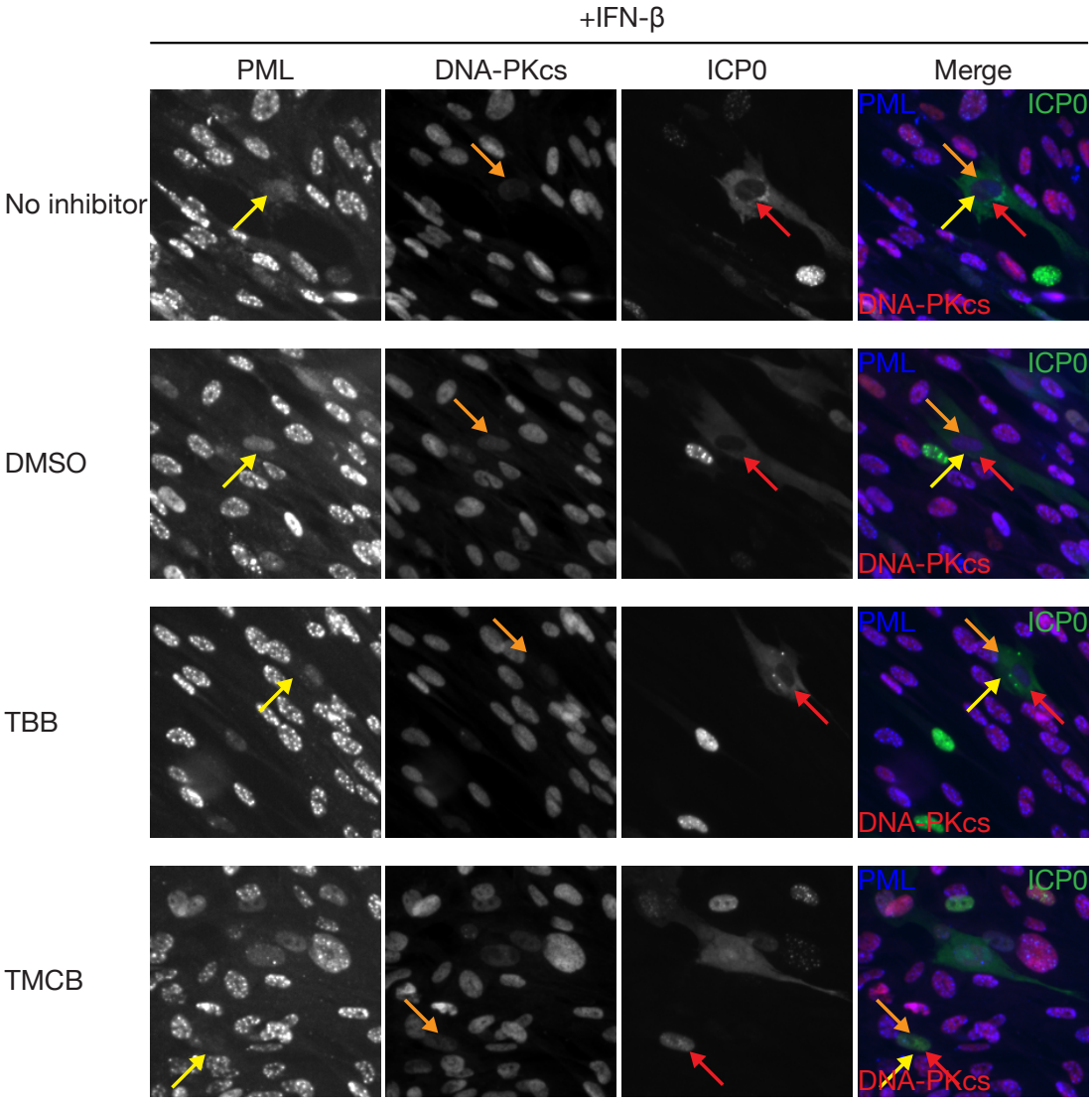


**Figure 2.3. CK2 inhibitors do not prevent the loss of PML and DNA-PKcs staining mediated by ICP0.**

HEL cells were treated and infected as described in Figure 2.1. At 12 hpi, cells were fixed and stained with antibodies against DNA-PKcs, PML, and ICP0. PML is shown as blue, DNA-PKcs as red, and ICP0 as green in the merged image. The yellow, orange, and red arrows indicate a cell that stains positive for ICP0 (red arrow) but has reduced or no apparent staining for PML (yellow arrow) and DNA-PKcs (orange arrow).

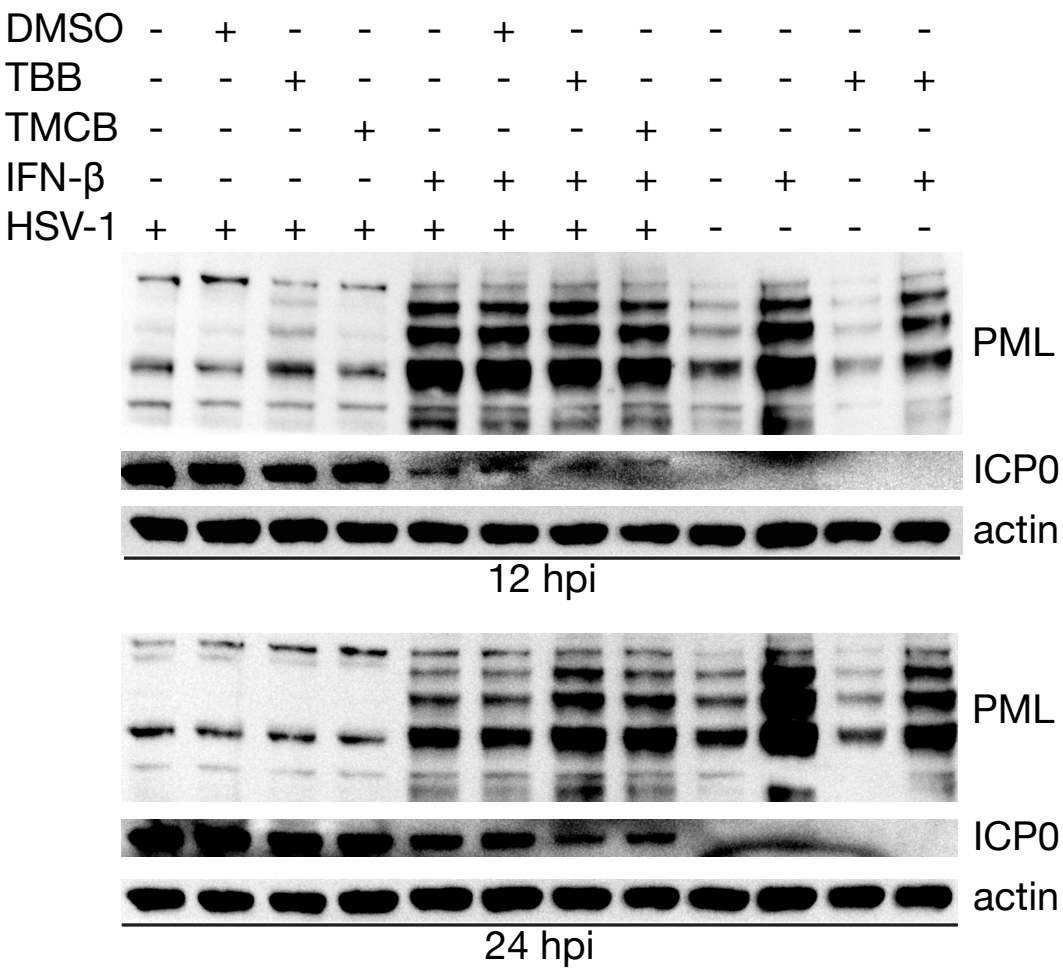


**Figure 2.4. CK2 inhibitors do not stabilize PML levels during infection.**

HEL cells were treated, as described in Figure 2.1, infected with wild-type HSV-1, and harvested at 12 and 24 hpi. Cell lysates were analyzed for PML, ICP0, or β-actin expression by western blot analyses.

# Chapter 3: hTERT extends the life of human fibroblasts without compromising type I interferon signaling.

## 3.1 Introduction

In performing studies that examine cellular defenses to viral infections, it is often necessary to work with primary cells, as the efficacy of intrinsic and innate immune pathways are frequently diminished in immortalized cells [99–102]. One disadvantage of using primary cells is their limited proliferative capacity in cell culture, which is due in part, to the progressive shortening of telomeres [103].

Telomeres are repetitive nucleoprotein structures that serve to cap the ends of chromosomes, facilitating their replication, and prevent their ends from appearing as DNA breaks [104]. Telomeres are maintained by a complex known as telomerase, whose essential core consists of the catalytic subunit telomerase reverse transcriptase (TERT) and the telomerase RNA template component (TERC) [108,109]. Along with a number of other factors, TERT is loaded onto the 3' overhang of existing telomeric DNA and utilizes TERC as a template to add repeats of a guanine-rich sequence, 5'TTAGGG3', in all vertebrates; concordantly, DNA primase and DNA polymerase are recruited to the new telomeric repeats, subsequently synthesizing the complementary 5' strand [104]. In the absence of active telomerase, erosion of the telomeres occurs with each

successive round of replication, resulting in the loss of telomeric (~100 bps) sequence [106,107]. Once telomeres are reduced from their normal 15 kb length to ~4 kb, DNA damage sensors trigger p53- and pRb-dependent mechanisms that result in cellular senescence, inducing a $G_1$ cell cycle arrest [110].

Replicative senescence is thought to be a mechanism of cellular lifespan regulation, preventing diseases such as cancer, and is intrinsic to the health of an organism [111–114]. However, for technical reasons it can be desirable to extend the proliferative capacity and prevent the senescence of a primary cell culture or strain. One way to avoid or reverse replicative senescence is transformation with viral oncogenes, such as the simian virus 40 (SV40) large T antigen (TAg) or the human papillomavirus (HPV) E6 and E7 proteins [115–117]. In both cases, these viral proteins reverse senescence through the inactivation of p53 and/or pRb. While this allows cells to resume progression through the cell cycle and replicate, these cells still undergo telomeric erosion and ultimately undergo a phenomenon termed crisis [115], where massive cell death occurs due to gross genomic rearrangements and instability in the absence of telomeres. While the estimated 1 in $10^7$ cells (for human cells) that survive crisis exit immortalized [118,119], this transformation results in the dysregulation of several cellular pathways, including the antiviral type I interferon (IFN) response [99].

The IFN response is an innate antiviral pathway that, upon detection of viral molecular patterns, results in the production and release of the cytokine

and type 1 IFN, IFN-β [37,220,221]. The IFN response serves as a major restriction point for many viruses as evidenced by the increased pathogenesis of these viruses in animal models in which either the type I IFN receptor, IFNAR, or a key signaling molecule, STAT1, are deleted [222–228]. One virus that interacts with the IFN response is HSV-1 [1]. Notably, HSV-1 encodes for viral proteins that inactivate or delay this IFN response [229,230]. Studies examining how HSV-1 counteracts the IFN response are often performed in primary cultures or cell strains, such as human embryonic lung (HEL) cells, because these cells possess a robust IFN response and phenotypes that are apparent in HEL cells are often greatly diminished in transformed lines [99,231]. A potential drawback with using HEL cells is their rapid progression into senescence.

As part of their differentiation program, human cells cease expressing hTERT, while continuing to produce other essential telomerase subunits such as TERC [120]. It has been shown by a number of labs that the lifespan of fibroblasts is efficiently extended by the reintroduction of hTERT into these cells [121,122]. Exogenous expression of hTERT presumably allows terminally differentiated fibroblasts to resume the extension of their telomeres, delaying or avoiding the production of signals that trigger replicative senescence and in turn prevents the chromosomal damage encountered by replication through crisis [123]. Unlike transformation with viral oncogenes, fibroblasts that exogenously express hTERT do not, for the most part, exhibit an oncogenic phenotype [124]. Notably, the effect that life-extension by exogenous expression of hTERT on

innate antiviral pathways, and in particular the IFN response, has not been examined.

Here we report the creation of a life-extended HEL cell line via transduction of a human diploid primary-like cell strain, HEL-299, with a retrovirus encoding *hTERT*. HEL-299s were chosen as a parental cell line since they are both capable of supporting high levels of HSV-1 and VSV replication and retain a strong innate immune restriction of viral replication (Chapter 2 and [232]). Our results show that the derivative cell line, HEL-TERT, unlike the parental cells, replicated to at least 100 population doublings, exhibited telomerase activity, and failed to undergo either replicative senescence or crisis. Morphologically, HEL-TERT cells appeared indistinguishable from HEL-299 cells. HEL-TERTs responded to IFN-β by upregulating representative ISGs and supported the replication of HSV-1 and VSV to similar levels as HEL-299 cells. Additionally, the introduction of the SV40 large TAg counteracted the IFN-β-directed restriction of HSV-1 and VSV replication. In summary, our data indicate that hTERT extends the replicative potential of human fibroblasts while not perturbing the type 1 IFN response, making these cells a valuable tool in virological and virus-cell interaction studies.

## 3.2 Methods

### 3.2.1 Cells and Viruses

HEL-299 cells from the American Type Culture Collection (CCL-137), HEL telomerase life-extended (HEL-TERT), and HEL-TERT SV40 large TAg transformed (HEL-TERT-T) cells (the latter two of which were created as part of this work, as detailed below) were maintained in Minimum Essential Medium Eagle Alpha Modification ($\alpha$MEM) containing 10% fetal bovine serum (FBS), 2 mM L-glutamine, 10 U/mL penicillin, and 10 U/mL streptomycin. In addition, HEL-TERT cells were kept under drug selection using hygromycin-B (Sigma) at 50 µg/mL while HEL-TERT-T cells were maintained under selection with hygromycin-B at 50 µg/mL and phleomycin at 10 µg/mL. HeLa, GP2-293, Vero, and L7 (Vero cells that contain the *ICP0* gene [200]) cells were maintained in Dulbecco's modified Eagle's medium (DMEM) containing 5% FBS, 2 mM L-glutamine, 10 U/mL penicillin, and 10 U/mL streptomycin.

HEL-299 (passage 4) cells were transduced with the retroviral vector, pMX-hTERT-hygro vector. pMX-hTERT-hygro was created by subcloning the *hTERT* (catalytic subunit of human telomerase) and hygromycin resistance genes from the vector, pBABE-hygro-hTERT [233] (Addgene plasmid 1773), into the retroviral vector, pMX-GFP [234]. A control vector, pMX-dTERT-hygro, was created by excising a BamHII fragment, which removes the N-terminal 849 residues of hTERT (Uniprot: O14746) [235] (including the TERC-interaction and most of the reverse-transcriptase domains), from pMX-hTERT-hygro. Retroviral

stocks were generated using the Pantropic Retroviral Expression System (Clontech) as recommended by the manufacturer. HEL-299 cells were transduced with filtered retroviral stocks and two days later placed under selection with hygromycin B at 100 μg/mL, which was lowered to 50 μg/mL 7 days later for subsequent culturing. HEL-TERT SV40 large TAg-expressing cells were created by transduction with the vector, pLVX-LgT-zeo. pLVX-LgT-zeo was created by subcloning the CMV promoter, SV40 TAg ORF, SV40 early promoter, and zeomycin resistance genes from pBABE-zeo largeTcDNA [236] (Addgene plasmid 1779) into the lentiviral vector, pLVX-AcGFP-N1 (Clontech), replacing the region containing the CMV promoter, AcGFP ORF, phosphoglycerate kinase promoter, and puromycin resistance genes. Lentiviral stocks were prepared essentially as described above for pMX-hTERT-hygro with the inclusion of the lentiviral packaging vector, psPAX2 (Addgene plasmid 12260) during lentiviral stock preparation. HEL-TERT cells were transduced with filtered lentiviral stocks and two days later placed under selection with phleomycin (Invivogen) at 20 μg/mL for 42 days, which was lowered to 10 μg/mL for long term culturing.

KOS was the wild type strain of HSV-1 used in our viral experiments [201]. 7134 is an ICP0-null mutant HSV-1 strain in which the *E. coli lacZ* gene has replaced the *ICP0* open reading frame [202]. KOS and 7134 were grown on Vero cells and titered on Vero or L7 cells, respectively [91,203]. The vesicular stomatitis virus recombinant, VSV-eGFP, contains the enhanced green fluorescent protein gene between the G and L genes [205] and was a gift from

Dr. Asit Pattnaik. VSV-eGFP stocks were grown and titered on Vero cells. Sendai virus (SeV, Cantrell strain) was purchased from Charles River Laboratories.

### 3.2.2 β-galactosidase Staining

To detect senescence, HEL-299, and moderate and high passage HEL-TERT cells were plated at 1 x $10^5$ cells per well in 12 well plates and grown to confluence. The cells were fixed in 3.7% formaldehyde, washed twice with 1x phosphate buffered saline (PBS), and stained for β-galactosidase activity as previously described [237]. Cells were viewed with a Nikon Eclipse TE2000-U microscope and photographed with a digital camera (Canon).

### 3.2.3 Life-Extension Characterization

Low passage HEL-299 and HEL-TERT cells were plated in 60 mm dishes at 1-2 x $10^5$ cells per dish. Prior to reaching confluence, the cells were trypsinized, counted with a hemocytometer, and replated at the above-mentioned amount. This was repeated until cells reached senescence and died. Using cell counts and days in culture, the population doublings were determined for each cell line.

### 3.2.4 Telomeric Repeat Amplification Protocol (TRAP) Assay

TRAP assays were performed essentially as described [238]. 2 x $10^5$ HEL-299, HEL-TERT, and HeLa cells were collected, pelleted, and frozen at -80°C. The cell pellets were resuspended in 200 μL of CHAPS lysis buffer (0.5%

CHAPS, 10 mM Tris-HCl pH 7.5, 1 mM $MgCl_2$, 1 mM EGTA, 3.5% 2-mercaptoethanol, 10% glycerol, 1 mM phenylmethylsulfonyl fluoride, 1 μg/mL aprotinin, and 1 μg/mL leupeptin) and incubated on ice for 30 minutes before cell pellets were collected by centrifugation. Telomeric repeats were amplified in a solution of 10 ng of cell extract, 1x Taq buffer (NEB), 0.2 mM dNTPs, 0.04 μg/μL of T4 Gene 32 Protein (NEB), and 2 U of the Taq polymerase (NEB) containing 0.5 ng/μL of the primers: TS (5'-AATCCGTCGAGCAGAGTT-3') and ACX (5'-GCGCGG$(CTTACC)_3$CTAACC-3') by polymerase chain reaction (PCR) in an MJ Mini Personal Thermal Cycler (Bio-Rad). Final PCR products were gel electrophoresed on 20% polyacrylamide gel, visualized with ethidium bromide staining, and photographed with a VisiDoc-It Imaging System (UVP).

### 3.2.5 Quantitative Reverse Transcriptase Real Time PCR

HEL-299, HEL-TERT, and HEL-TERT-T cells were plated at 1 x $10^5$ cells per well. Twenty-four hs post-plating, cells were mock treated or treated with human IFN-β at 1000 U/mL (AbD Serotec). At 9 hs post treatment, cells were washed twice with PBS and harvested in Trizol (Invitrogen) to isolate total RNA. RNA was converted into cDNA using iScript cDNA synthesis kit (Bio-Rad) according to manufacturers recommendations. For each sample, real time PCR was performed using FastStart SYBR green master (Rox) (Roche) in a StepOnePlus Real-Time PCR System (Applied Biosystems). Transcripts were amplified using the following primer sets: *hTBP* (5'-TGCACAGGAGCCAAGAGTGAA-3' and 5'-CACATCACAGCTCCCCACCA-3'),

*ISG15* (5'-GGTGGACAAATGCGACGAAC-3' and 5'-ATGCTGGTGGAGGCCCTTAG-3'), *IFIT1* (5'-TAGCCAACATGTCCTCACAGAC-3' and 5'-GTGCCTTGTAGCAAAGCCCTAT-3'), *IFIT2* (5'-ACGCATTTGAGGTCATCAGGGTG-3' and 5'-CCAGTCGAGGTTATTTGGATTTGGTT-3') [239], and *Mx1* (5'-AGAAGGAGCTGGAAGAAG-3' and 5'-CTGGAGCATGAAGAACTG-3') [240]. All transcript levels were normalized to hTBP.

### 3.2.6 Western Blot

HEL-299, HEL-TERT, and HEL-TERT-T cells were plated at 1.5 x$10^5$ of cells per well in a 12-well plate. 24 hs later, cells were either mock treated or treated with IFN-β at 1000 U/mL for 16 hs before being washed with PBS and then lysed into Red Loading Buffer (62.5 mM Tris-HCl (pH 6.8), 2% SDS, 10% glycerol, 0.01% phenol red, 42 mM DTT) plus with protease inhibitors (1 µg/mL aprotinin, 1 µg/mL leupeptin, 1 mM phenylmethylsulfonyl fluoride). Samples were resolved on a 4-12% Bis-Tris gradient polyacrylamide gel, transferred to nitrocellulose, blocked with 5% BSA in Tris-buffered saline with 0.1% Tween-20 (TBS-T) for 1 h at room temperature. Membranes were probed with an antibody against IFIT1 (PA3-848, Thermo Scientific) diluted in 5% BSA/TBS-T overnight at 4°C. Membranes were washed three times with TBS-T, probed with HRP-conjugated goat-anti-rabbit IgG diluted in 5% BSA/TBS-T for 1 h at room temperature, washed three times with TBS-T, developed with chemiluminescent substrate (Femto ECL, Pierce Laboratories), and detected using an Image

Station 4000R (Kodak) and Carestream Molecular Imaging software. The membranes were then striped and probed with β-actin ((I-19)-R, Santa Cruz Biotechnology) as described section 2.2.5. Images were assembled using Adobe Photoshop and Adobe Illustrator (Adobe Systems).

### 3.2.7 Plaque Reduction Assays

Plaque assays for KOS and 7134 on HEL-299, HEL-TERT, and HEL-TERT-T cells (-/+ IFN-β) were carried out as described in section 2.2.3. Images of viral plaques were captured by scanning the immunohistochemically stained plates with a flatbed scanner (Canon).

### 3.2.8 HSV-1 Viral Yield Assays

To examine HSV-1 productive infection, HEL-299, HEL-TERT, and HEL-TERT-T cells were plated at 1 x $10^5$ cells per well in 12 well plates. One day post-plating, cells were mock-treated or treated with 1000 U/mL of human IFN-β. Sixteen hs post-treatment, cells were infected with either KOS or 7134 at 5 plaque forming units (PFU)/cell, washed with PBS (-/+ IFN-β) after 1 h to remove unabsorbed virus, and placed back in growth medium (-/+ IFN-β). At 24 hs post-infection, cells were harvested and frozen at -80°C. Virally infected samples were thawed and sonicated, and standard plaque assays were performed on either Vero cells (for KOS) or L7 cells (for 7134) to determine viral titers

### 3.2.9 VSV Viral Yield Assays

To measure VSV replication, HEL-299, HEL-TERT, and HEL-TERT-T cells were plated, mock-treated or treated with IFN, and infected as for the HSV-1 yield assays except that cells were infected with VSV-eGFP at 0.1 PFU/cell. At 24 hs post-infection, cells were harvested and frozen at -80°C. Virally infected samples were thawed and sonicated, and standard plaque assays were performed on Vero cells to determine viral titers.

### 3.2.10 Antiviral cytokine-production assay

To assess the ability of various cell lines to produce antiviral cytokines, HEL-299, HEL-TERT, or HEL-TERT-T cells were plated at 1 x $10^5$ in 12-well plates. The next day, the cells were either mock infected with serum-free αMEM or infected with SeV at 100 hemagglutination units (HAU) per $10^6$ cells in serum-free medium for 1 h, after which the virus was removed from the cells and fresh αMEM containing 10% FCS was added to the cells. At 24 hpi, SeV-infected HEL cells were irradiated with ultraviolet light to inactive the virus. To test for the production of antiviral cytokines secreted from these cells, duplicate Vero cell monolayers (2 x $10^5$ cells per well in 12-well plates) were exposed to HEL supernanes. In addition, one set of Vero cells were treated with either fresh αMEM or αMEM containing IFN-β at 1, 10, 100, or 1000 U/mL as positive controls. Six hs later, untreated and treated Vero cells were infected with VSV-eGFP at ~200 PFU/well. At 1 hpi, the Vero cells were overlaid with αMEM containing 10% FCS and 1% methylcellulose. Twenty-four hs post-VSV

infection, the methylcellulose was removed, Vero cells were washed with PBS and fixed with 3.7% formaldehyde, and fluorescent plaques were counted.

## 3.3 Results

### 3.3.1 HEL-TERT cells exhibit an expanded proliferative capacity

HEL-299 cells are a primary strain that have been used to study viral replication and the type 1 IFN response [209,241]. This cell strain, nonetheless, can only be passaged in culture a limited number of times before undergoing senescence [242]. We wanted to determine whether ectopic expression of hTERT in HEL-299 cells would allow for a longer period of culturing. HEL-299s were transduced with a retrovirus encoding both hTERT and hygromycin resistance. The resulting antibiotic resistant mass population, hereafter called HEL-TERT, were then used in subsequent experiments. To first examine whether hTERT conferred an extended ability to replicate, HEL-299 and HEL-TERT cells were maintained in culture for an extended period of time, comparing the number of population doublings to days in culture. As expected, HEL-299s proliferated just under 60 days in culture and underwent a total of 23.5 population doublings (from two experiments); at which point the cells ceased to divide and underwent widespread cell death two weeks later (Figure 3.1). It should be noted that in a couple of instances, HEL-299 cells were able to undergo approximately 35 population doublings (data not shown). In contrast, the HEL-TERT cells were maintained in culture for 185 days and went through

114 population doublings (Figure 3.1), at which point the experiment was terminated. Transduction of HEL-299 cells with a retroviral vector that either expresses the green fluorescent protein or contains a deletion of *hTERT* failed to extend the life span of the HEL-299s (data not shown). These results demonstrate that expression of hTERT significantly extends the life span of HEL-299 cells.

### 3.3.2 HEL-TERT cells contain active telomerase

To establish that transduced hTERT resulted in telomerase activity in HEL-TERT cells, we performed TRAP assays. In this assay, telomerase activity is monitored by examining the laddering or amplification of 6 base-pair 5'TTAGGG3' telomeric repeats [243]. HeLa cells, which express hTERT [244], exhibited the characteristic 6 bp laddering, while the non-immortalized HEL-299 failed to do so (Figure 3.2). Unlike the parental cell line, the HEL-TERT cells showed a clear laddering effect, indicating that exogenous hTERT is active and capable of extending telomeres. To ensure that the inability to detect telomerase activity in HEL-299 cellular extracts was not due to the presence of a PCR inhibitor [245], we amplified the cellular promyelocytic leukemia (*PML*) gene (data not shown). Thus, HEL-TERT cells contain active telomerase, suggesting that the extended proliferative capacity of this cell line can be attributed to the maintenance of telomeres.

### 3.3.3 Prolonged culture of HEL-TERTs does not result in senescence

As fibroblasts reach senescence, they exhibit characteristic changes in cellular morphology, such as an increase in area, due to dysregulation of cytoskeleton elements [103,246]. Additionally, senescent cells can be detected by their upregulation of a lysosomal β-galactosidase [247]. When we compared low (6 population doublings) and high (20 population doublings) passage HEL-299 cells, we noted that many of the higher passage cells exhibited a clear enlargement of the cytoplasm, with a change from their typical narrow, drawn-out morphology to one that was shortened and/or broader (Figure 3.3A). When we compared the HEL-TERT cells to low passage HEL-299 cells, we were able to detect little if any morphological changes either shortly after transduction with hTERT or at 100 population doublings later (Figure 3.3A). As part of these studies, we also examined another HEL-TERT derivative cell line that expresses SV40 large Tag (hereafter named HEL-TERT-T). SV40 large Tag is known to alter the IFN-response [248]. From this experiment, HEL-TERT-T cells appeared to have an altered cellular morphology, with the cells decreasing in length and broadening in width. When we examined all the cell types for senescence-associated β-galactosidase activity, β-galactosidase activity was clearly detected in older HEL-299 cells, whereas we failed to detect β-galactosidase activity in either low passage HEL-299 or low or high passage HEL-TERT, or high passage HEL-TERT-T cells (Figure 3.3B). These results indicate that not

only do HEL-TERT cells retain their ability to proliferate but also fail to exhibit signs of senescence.

### 3.3.4 Treatment of HEL-TERT cells with human IFN-β induces strong ISG expression

Because the IFN response has been reported to be altered in immortalized cells [100–102], we decided to examine the effect that exogenous hTERT expression had on ISG levels upon IFN-β-treatment. HEL-299, HEL-TERT, and HEL-TERT-T cells were stimulated with IFN-β for 9 hs and the transcript levels of four prototypic ISGs (*IFIT1*, *IFIT2*, *ISG15,* and *Mx1*) were monitored by qRT-PCR. Both HEL-299 and HEL-TERT cells showed robust upregulation in the transcript levels of all four genes after the addition of IFN-β (Figure 3.4). Three of the ISGs induced to similar levels between the two cell lines while *ISG15* was induced to slightly higher levels in the HEL-TERTs. On the other hand, the overall upregulation of these genes upon IFN-β treatment was greatly diminished in HEL-TERT-T cells. When we examined IFIT1 protein levels, we found that, as expected [42], unstimulated HEL-299 and HEL-TERT cells contained little to no detectable IFIT1; however, IFIT1 was readily detected 9 hs after IFN-β treatment (Figure 3.5). Notably, IFN-treated HEL-299 and HEL-TERT cells showed comparable levels of IFIT1 protein. HEL-TERT-T cells, on the other hand, showed persistent production of IFIT1 and a greatly reduced difference between the unstimulated and IFN-treated states (as compared to that found in the other two cell lines), in agreement with a previous report [249].

Thus, the ectopic expression of hTERT in HEL-299 cells via retroviral transduction does not largely affect the ability of HEL cells to induce the expression of these four ISGs by IFN-β nor does it lead to a dysregulation of ISG protein production (i.e., IFIT1) as does the expression of TAg.

### 3.3.5 HSV-1 and VSV replicate to comparable levels, +/- IFN-β, in HEL-299 and HEL-TERT cells

As another measure to assess whether the IFN response is active and functional in HEL-TERT cells, we examined the replication of three viruses in the presence of IFN-β. For these studies, we chose HSV-1 (strain KOS), which is largely resistant to type I IFNs, as well as both an ICP0-null mutant of HSV-1 (7134) and VSV, as these latter two viruses are sensitive to type I IFNs [208,250,251]. Initially, we examined the ability of wildtype (WT) and ICP0-null HSV-1 to form plaques on untreated and IFN-β-treated HEL-299, HEL-TERT, and HEL-TERT-T cells. Both viruses had visually comparable plaque sizes on both HEL-299 and HEL-TERT cell types (Figure 3.6), even on higher passage HEL-TERT cells (data not shown). Plaques for both wild type and ICP0-null viruses appeared to be smaller on HEL-TERT-T cells, which is most likely due a decrease in the size of the cells that occurred upon transduction of TAg (Figure 3.3A). When the cells were pretreated with IFN-β, there was a large decrease in plaque size for both WT HSV-1 and the ICP0-null mutant on HEL-299 and HEL-TERT cells, while plaque size on the HEL-TERT-T cells remained largely the same. The ability of WT virus to form plaques was similar on the three cell lines

in untreated cells (Figure 3.7A), though the ICP0-null virus showed slight increases of 2-fold and 4.5-fold on HEL-TERT and HEL-TERT-T cells, respectively. Upon the addition of IFN-β, the plaquing efficiencies of the WT and ICP0-null viruses were decreased ~10 fold and ~50-100-fold, respectively, on both HEL-299 and HEL-TERT cells (Figure 3.7C). In contrast to the introduction of hTERT into HEL-299 cells, expression of large TAg greatly diminished the ability of IFN-β to restrict the plaquing of either WT or the ICP0-null virus (3-fold for either) (Figure 7C), resulting in a nearly 80-fold increase in the plating efficiency of the ICP0-null virus on IFN-treated HEL-TERT-T cells as compared to IFN-treated HEL-299 cells (Figure 3.7B). To further examine the effect of hTERT on HSV-1 replication, we also performed viral yield assays in the three cell types. (Figure 3.7D). WT HSV-1 replicated to comparable levels in all three cell lines, with IFN-pretreatment producing a slight reduction in yields from both HEL-299 and HEL-TERT but not from HEL-TERT-T cells. Like WT HSV-1, the ICP0-null mutant replicated nearly as well among the three cell types in untreated cells; however, IFN-pretreatment resulted in a 100-fold decrease of viral yields in HEL-299 and HEL-TERT cells while producing little to no effect in HEL-TERT-T cells.

To monitor reductions in VSV production, we again performed viral yield assays in the presence and absence of IFN-β. Just as for HSV-1, VSV grew equally well among the three cell lines in untreated cells. In IFN-β-treated cells, however, VSV growth in both HEL-299 and HEL-TERT cells was reduced by $>10^6$-fold while it was reduced by only 200-fold in pretreated HEL-TERT-T cells

(Figure 3.8). Thus, HEL-TERT cells are similar to HEL-299s in their ability to support the replication of two genetically distinct viruses, and they retain an IFN response that is as functional as the parental cell line. Overall, ectopically expressed hTERT does not appear to adversely affect viral replication or the type I IFN response in a human lung fibroblast cell strain.

### 3.3.6 Effect of hTERT on antiviral cytokine production

In addition to determining its effect on ISG upregulation and on the efficacy of an IFN-induced antiviral state, we decided to assess whether ectopic hTERT expression altered the ability of cells to produce IFN and other antiviral cytokines in response to infection. We used infection by SeV, which is known to be a strong inducer of IFNs and other antiviral cytokines in human cells [252]. For this assay, media from uninfected and infected HEL cells are placed onto naïve Vero cells, which respond to but cannot produce IFN, and restrictions on VSV plaquing are monitored [253,254]. Media from mock-infected HEL cells had no effect on the ability of VSV to plaque on Vero cells while IFN-β pretreatment, at the highest concentration tested (1000U/mL), was able to reduce the number of plaques formed by approximately 35-fold (Table 1). When we tested the ability of media from SeV-infected HEL cells, we found that media from all three cell types were capable of lowering the number of plaques that formed by 5-7 fold. These reductions were similar to the antiviral activity of 100U/mL of IFN-β. Although we are unable to distinguish between IFN-β or among the IFN-α subtypes with this assay, the protective effect produced by

media from HEL-299 and HEL-TERT cells was identical and suggests that hTERT does not affect the activation of IFN-production in response to viral infection.

## 3.4 Discussion

Due to their unperturbed DNA damage, senescence, and antiviral pathways, primary cells are considered biologically relevant cells when studying how these cellular processes affect viral replication. However, their limited ability to proliferate makes their use in examining these pathways technically challenging. For example, the establishment of a cell line depleted for a particular cellular protein is generally difficult because of the rapid and inevitable onset of senescence. Thus, in studying cell-virus interactions, there is a need for life-extended cell lines that retain many of the characteristics of a primary cell (e.g., antiviral responses) while allowing for the analysis of specific cellular genes or proteins (e.g., depletion, gene knockout). It is possible to immortalize primary cells with viral and cellular oncoproteins, but immortalization can result in alterations of cellular processes and inhibit antiviral pathways, affecting the replication of wild-type and mutant viruses [255–258]. Another approach is to use the *TERT* gene, which has been reported to extend the life of human fibroblasts [121], and avoids many of the problems associated with cellular or viral oncogene immortalization or transformation [124]. Prior to this study, the

effect of hTERT expression on the IFN response had not, to the best of our knowledge, been examined.

The traditional approach used to immortalize primary cells has been the introduction of cellular or viral oncogenes. The most commonly used of these include E1A and E1B from adenovirus [259], E6 and E7 from human papillomavirus [116], and large TAg from SV40 [119,260]. In general, these proteins bypass senescence by the inactivation of one or both of the tumor suppressor proteins, p53 and pRb [261–263]. Unfortunately, in addition to perturbing the cell cycle, many of these viral proteins also serve to antagonize or inactivate antiviral pathways in order to promote viral replication. E1A, E6, E7, and large TAg are capable of disrupting the activity of, among others, cellular histone deacetylases [264] and CBP/p300 [265–267] resulting in widespread transcriptional and epigenetic changes [268–272]. In the case of E1A, this interaction prevents the major type I IFN transcription factor, STAT1, from binding to CBP/p300 and upregulating ISGs [273]. Likewise, E6 is capable of preventing activation of the IFN response by blocking the transcriptional activity of IRF3 [274]. E1B proteins inhibit apoptosis and are capable of inactivating the cellular DNA damage response [275–277] . Large TAg, on the other hand, has recently been reported to activate STAT1 and induce ISGs upregulation in the absence of IFN-exposure [249]. In agreement with this, we saw persistent production of IFIT1 protein in TAg-transduced cells. However, the expression of large TAg, independent of SV40 infection, has also been shown to decrease the phosphorylation of the cellular translation factor eIF2α by an IFN effector,

double-stranded RNA protein kinase (PKR) [278]. This decrease in phosphorylation increases the translation capability of viral mRNAs. Similarly, our results show that while large TAg may lead to high levels of ISG protein production, it functionally inactivates the IFN response. Furthermore, immortalization by mechanisms not involving viral oncogenes may inactivate antiviral pathways, as observed with the loss of induction of ISGs in immortalized cells derived from Li-Fraumeni patients [99].

Our approach in this study was to extend the life of human fibroblasts with hTERT. Cells transformed with hTERT arrest in response to serum starvation, maintain anchorage dependence, double at a rate similar to untransformed cells, and do not exhibit genomic instability [124]. While it has been reported that expression of hTERT can alter the expression of a limited number of genes, none of these have an apparent role in antiviral pathways [279]. We found that hTERT expression does not impair the upregulation of four representative ISGs (*IFIT1*, *IFIT2*, *ISG15*, and *Mx1*) does not lead to aberrant ISG protein production, nor does its expression affect the replication of two genetically distinct viruses, HSV-1 and VSV. This is in agreement with previous work demonstrating that exogenous expression of hTERT in fibroblasts does not affect the replication of human cytomegalovirus [280,281] nor does it affect the upregulation of the IFN-induced senescence mediator, IFI16, upon IFN-stimulation [282]. Furthermore, unlike SV40 large TAg, exogenous hTERT did not impair the ability of IFN to restrict the replication of VSV or an ICP0-null mutant of HSV-1, both viruses being quite sensitive to the effects of IFN-β, nor

did it hinder the ability of HEL cells to produce antiviral cytokines in response to viral infection. While we did observe slight differences in the levels of induction for the four ISGs between HEL-299 and HEL-TERT cells, these differences failed to translate into an appreciable effect on the ability of IFN-β to suppress replication of VSV or the ICP0-null HSV-1 mutant. hTERT overexpression has been reported to enhance the formation of apoptotic markers during HSV-1 infection in HeLa cells, which express the human papillomavirus E6 and E7 oncoproteins, and sensitizes them to apoptosis [283]. Our results, however, suggest that exogenous expression of hTERT in a primary cell strain has little impact on viral replication.

In conclusion, HEL-TERTs are permissive for HSV-1 and VSV growth, have a robust antiviral response, and a significantly enhanced lifespan. They recapitulate the phenotype of an HSV-1 ICP0-mutant, which is known to be complemented by the loss of proteins involved in the DNA damage response [284], antiviral pathways [35], or overexpression of certain cyclins [285], suggesting that these pathways are unperturbed. Because the phenotypes of certain HSV-1 mutants are only apparent in primary cells, we believe the HEL-TERT cell line to be an ideal choice due to their longevity and robust antiviral response. Additionally, they will allow for the establishment of derivative cell lines that are depleted or overexpress targets of interest, facilitating a better understanding of cellular pathways (including the IFN response) and the viruses that alter these pathways.

## 3.5 Figures

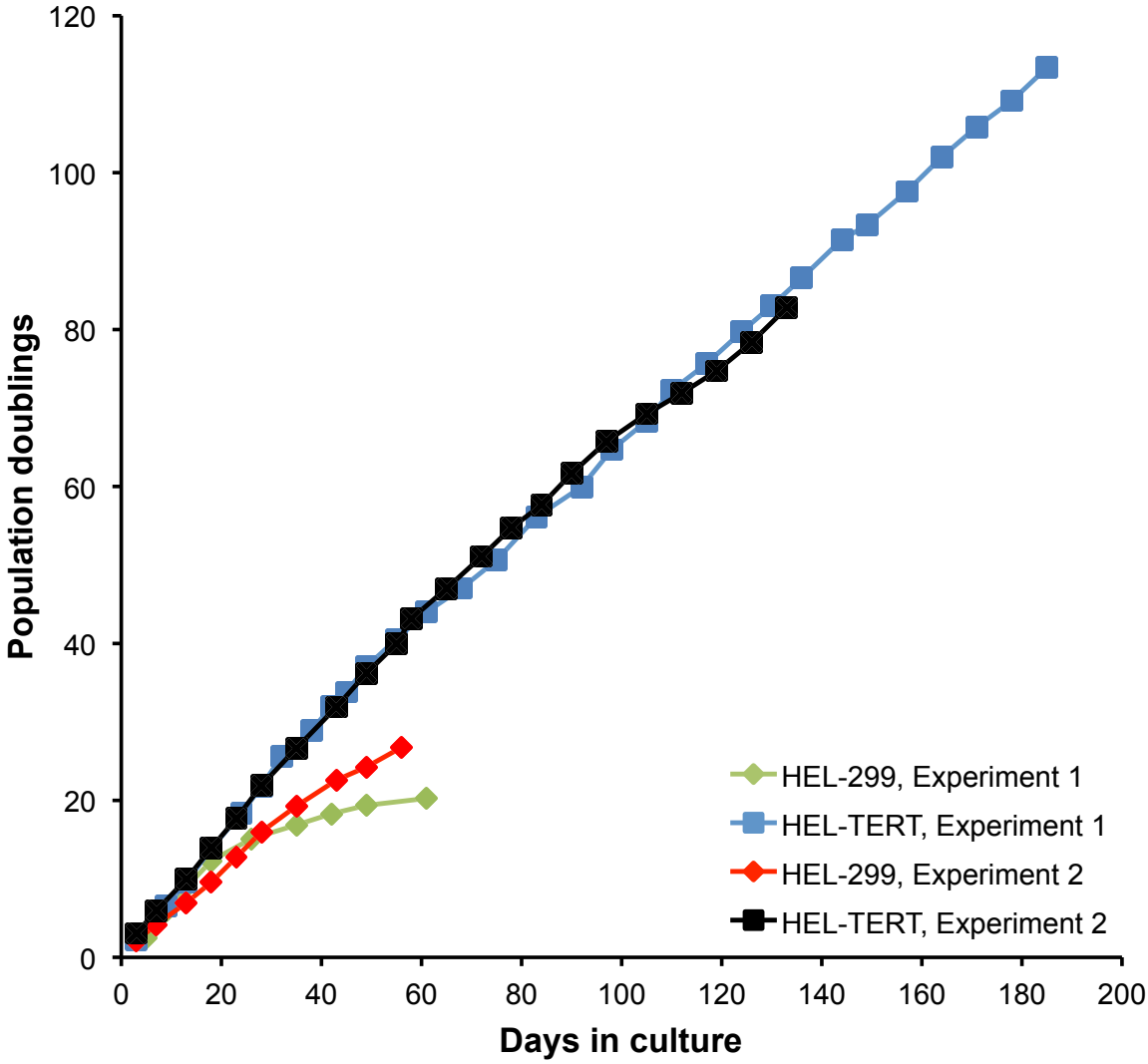


**Figure 3.1. HEL-TERT cells are life-extended compared to HEL-299 cells.**

HEL-TERT and HEL-299 cells were plated as duplicate cultures in 60 mm dishes at $1x10^5$ and $2x10^5$ cells per plate, respectively. For each passaging, cells were counted and re-plated. Population doublings were determined by using cell counts and days in culture.

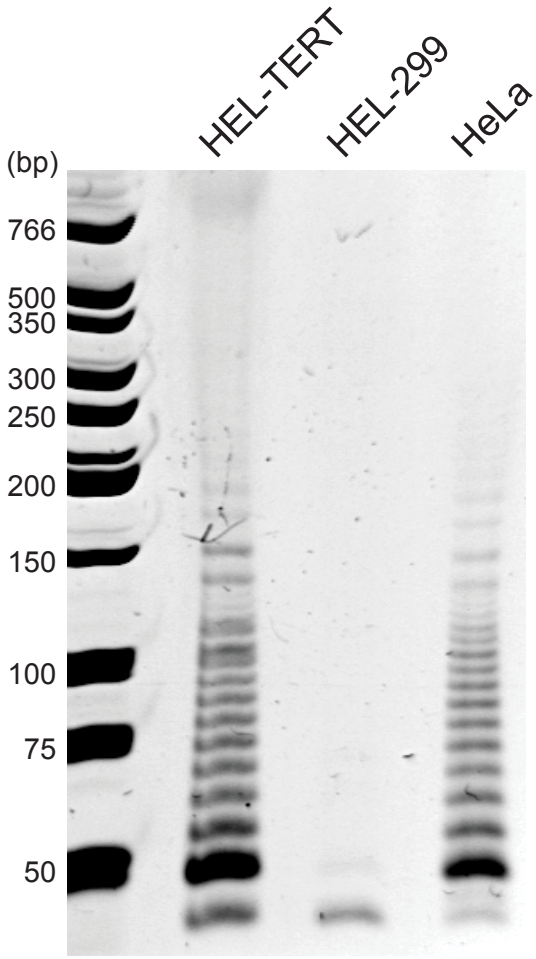


**Figure 3.2. Telomerase activity is detectable in HEL-TERT and HeLa cells but not HEL-299 cells.**

HEL-299 (3 population doublings), HEL-TERT (3 population doublings), and HeLa cells were examined for telomerase activity using the TRAP assay. HeLa cells were used as a positive control for telomerase activity. The numbers at the left side of the figure are DNA size markers (bp: base pair).

**A**

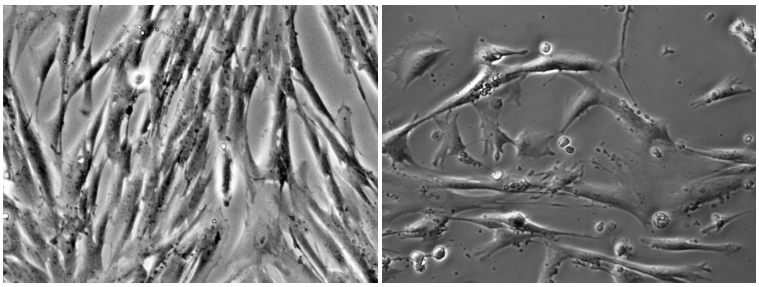

HEL-299
3 population doublings

HEL-299
22 population doublings

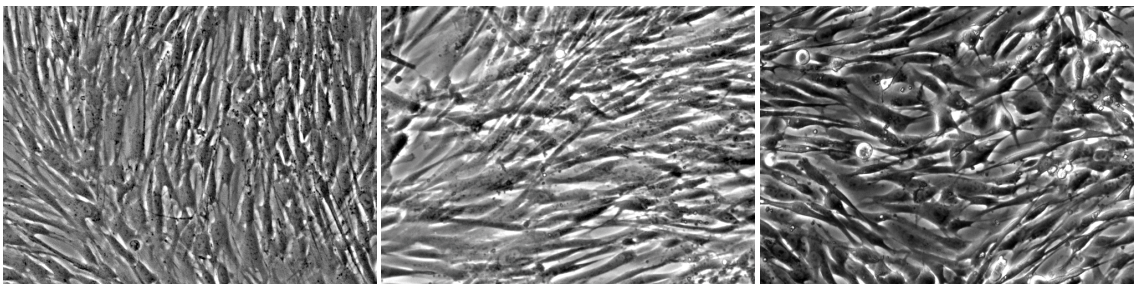

HEL-TERT
6 population doublings
post transduction

HEL-TERT
100 population doublings
post transduction

HEL-TERT-T
~30 population doublings
post transduction

**B**

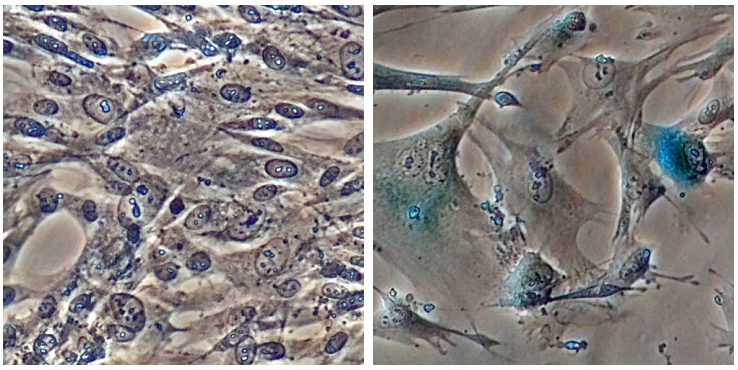

HEL-299
6 population doublings

HEL-299
33 population doublings

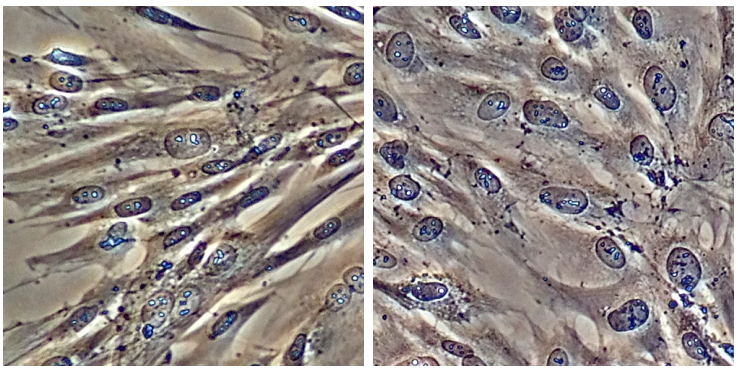

HEL-TERT
42 population doublings

HEL-TERT-T
>70 population doublings

**Figure 3.3. HEL-299, HEL-TERT, and HEL-TERT-T cell morphology and senescence.**

(A) Transduction of HEL-299 cells with hTERT does not alter morphology. Light microscopy of live HEL-299 cells at 3 (left panel) and 22 population doublings (left middle panel), HEL-TERT cells after 6 (middle panel) and 100 (right middle panel), and HEL-TERT-T (far right panel) after approximately 30 population doublings. (B) HEL-TERT cells fail to exhibit at least one sign of senescence. HEL-299 cells at 6 (left panel) and 33 (left middle panel), HEL-TERT cells after 42 (right middle panel), and HEL-TERT-T cells at approximately 70 (right panel) population doublings were stained for β-galactosidase activity.

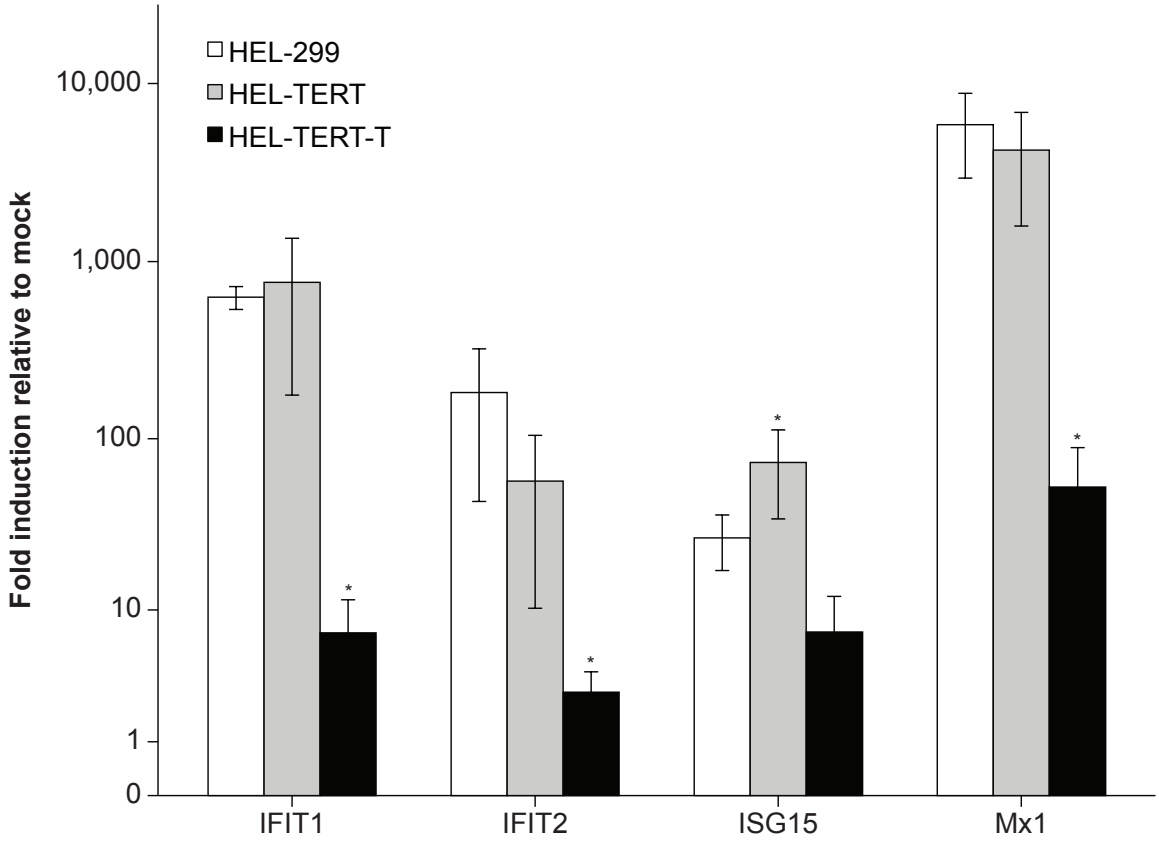


**Figure 3.4. HEL-TERT but not HEL-TERT-T cells show ISG induction at levels similar to HEL-299 cells after IFN stimulation.**

HEL-299s and HEL-TERT cells were treated or mock treated with 1000 U/mL of human IFN-β. At 9 hs post treatment, total RNA was isolated from cells and reversed transcribed into cDNA for qRT-PCR analysis to monitor *ISG15*, *IFIT1*, *IFIT2*, and *Mx1* transcript levels. Data represents the means of 6 samples; error bars represent the standard errors of the means. $*p < 0.05$, one-way ANOVA, Bonferroni's multiple comparison post-test, compared to HEL-299 levels.

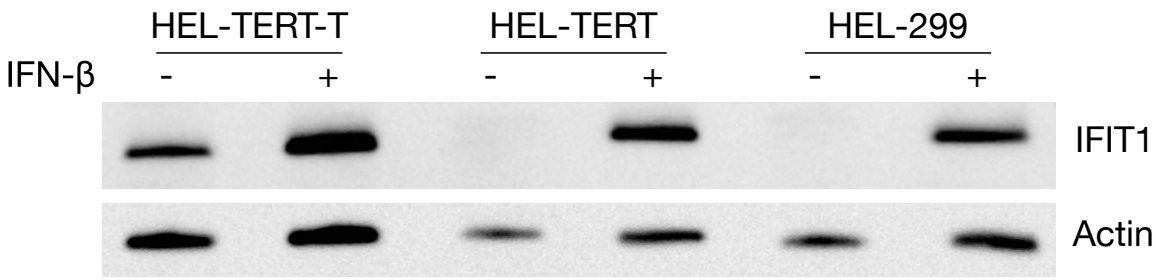


**Figure 3.5. IFIT1 protein production is induced to similar levels by IFN-β in HEL-299 and HEL-TERT cells.**

HEL-299, HEL-TERT, and HEL-TERT-T cells were mock treated or treated with 1000 U/mL of IFN-β and harvested 9 hs later. Cell lysates were analyzed for IFIT1 or β-actin protein production by western blotting.

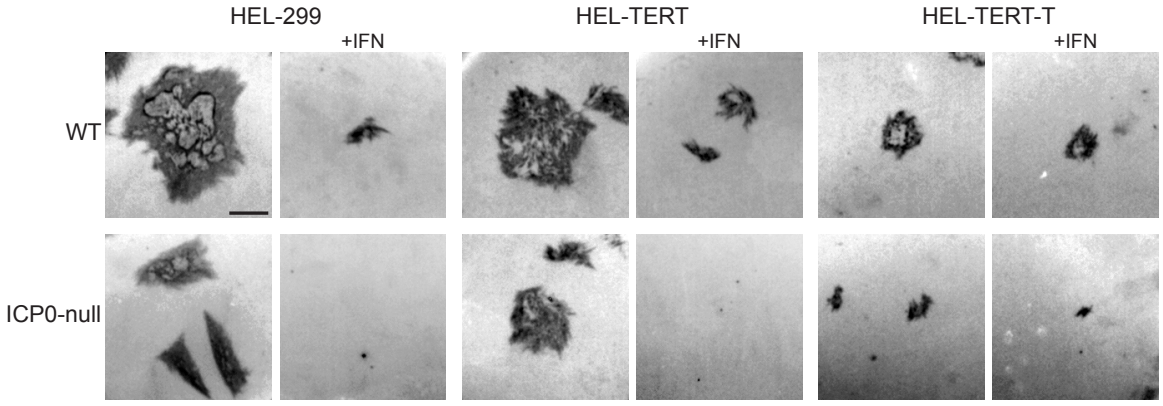


**Figure 3.6. HSV-1 shows similar plaque size and morphology on HEL-299 and HEL-TERT cells.**

HEL-299, HEL-TERT, and HEL-TERT-T cells were mock or pretreated with IFN-β for 16 hs and then infected with WT HSV-1 or an ICP0-null mutant and plaques for both viruses were visualized by immunohistochemistry three days post-infection. Bar = 1 mm.

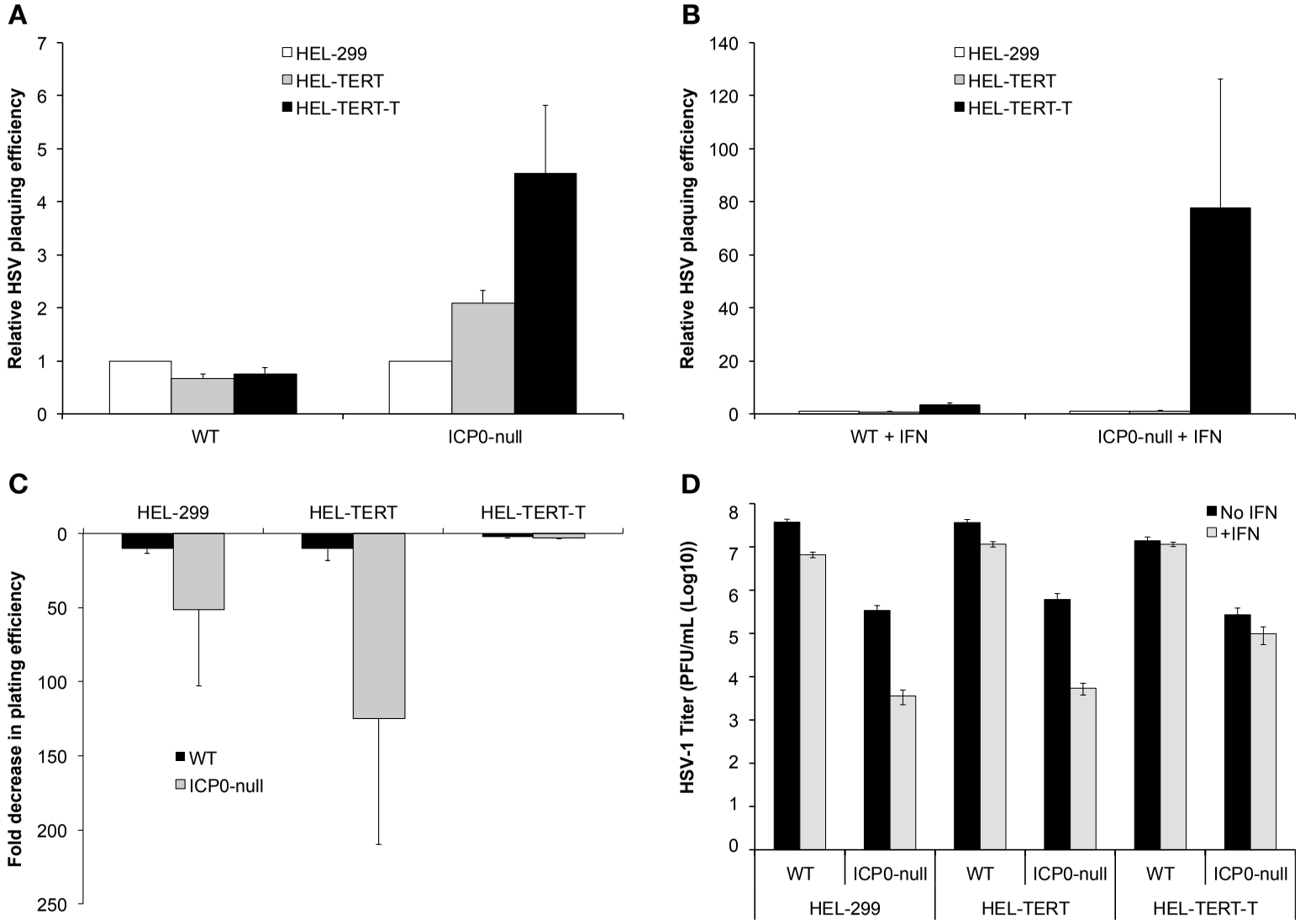
A
Relative HSV plaquing efficiency
HEL-299
HEL-TERT
HEL-TERT-T
WT
ICP0-null
B
Relative HSV plaquing efficiency
HEL-299
HEL-TERT
HEL-TERT-T
WT + IFN
ICP0-null + IFN
C
HEL-299
HEL-TERT
HEL-TERT-T
Fold decrease in plating efficiency
WT
ICP0-null
D
HSV-1 Titer (PFU/mL (Log10))
No IFN
+IFN
WT
ICP0-null
HEL-299
HEL-TERT
HEL-TERT-T

**Figure 3.7. Replication of HSV-1 is diminished by IFN-β in HEL-299 HEL-TERT but not HEL-TERT-T cells.**

(A) and (B) HEL-299, HEL-TERT, and HEL-TERT-T cells were mock (A) or pre-treated with IFN-β (1000 U/mL) (B) and were infected 16 hs post treatment with 10-fold serially diluted stocks of WT HSV-1 or an ICP0-null mutant. Plaques were visualized by immunohistochemistry 3 days post-infection. An average of three experiments is shown. Data is presented as the ratio of plaques formed on the indicated cell line to that on HEL-299 cells.

(C) Data generated for A and B, but presented as a ratio of the number of plaques formed on mock-treated cells compared to that on IFN-treated cells.

(D) HEL-299, HEL-TERT, and HEL-TERT-T cells were mock or pre-treated with IFN-β (1000 U/mL) and were infected (16 hs post treatment) with either WT HSV-1 or the ICP0-null mutant at an MOI of 5 PFU/cell. Samples were harvested 24 hs post-infection. Viral titers were determined by plaque assays. An average of three experiments is shown. In all cases, error bars represent the standard errors of the means.

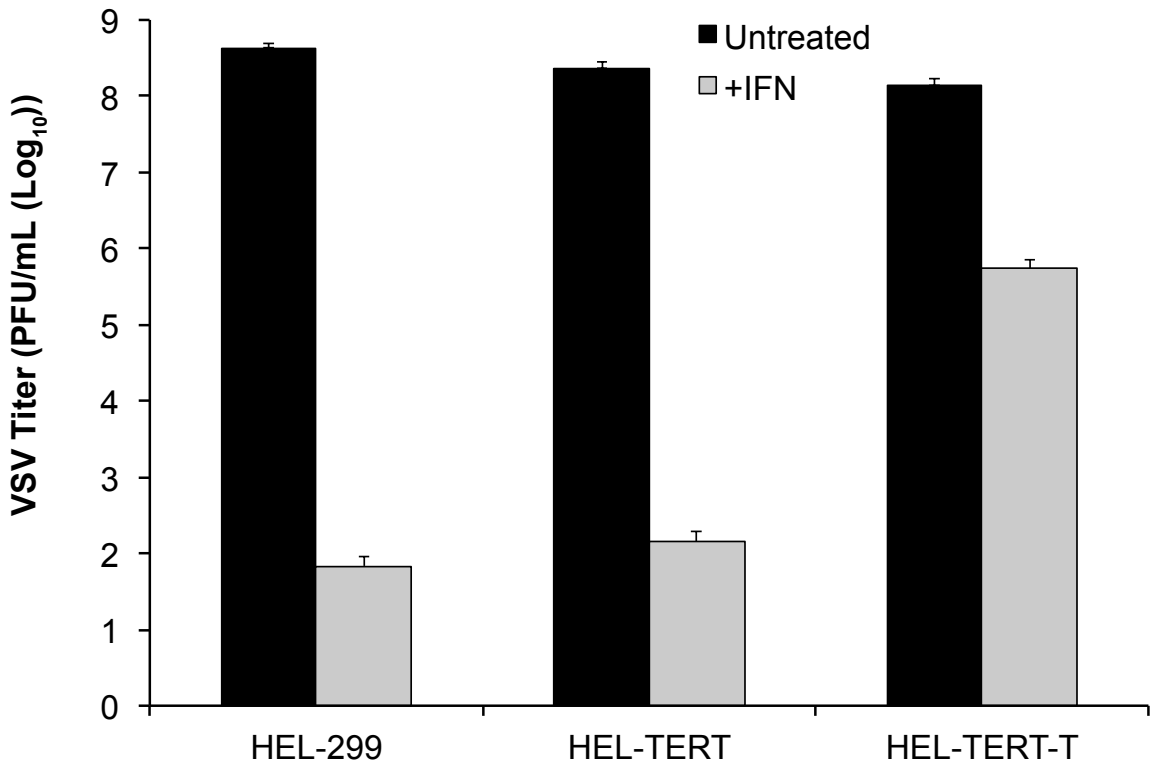


**Figure 3.8. Replication of VSV is diminished by IFN-β in HEL-299 and HEL-TERT but not HEL-TERT-T cells**

HEL-299, HEL-TERT, and HEL-TERT-T cells were mock or pre-treated with IFN-β (1000 U/mL) and were infected (16 hs post treatment) with VSV-eGFP at an MOI of 0.1 PFU/cell. Samples were harvested 24 hpi. Viral titers were determined by plaque assays. An average of three experiments is shown. In all cases, error bars represent the standard errors of the means.

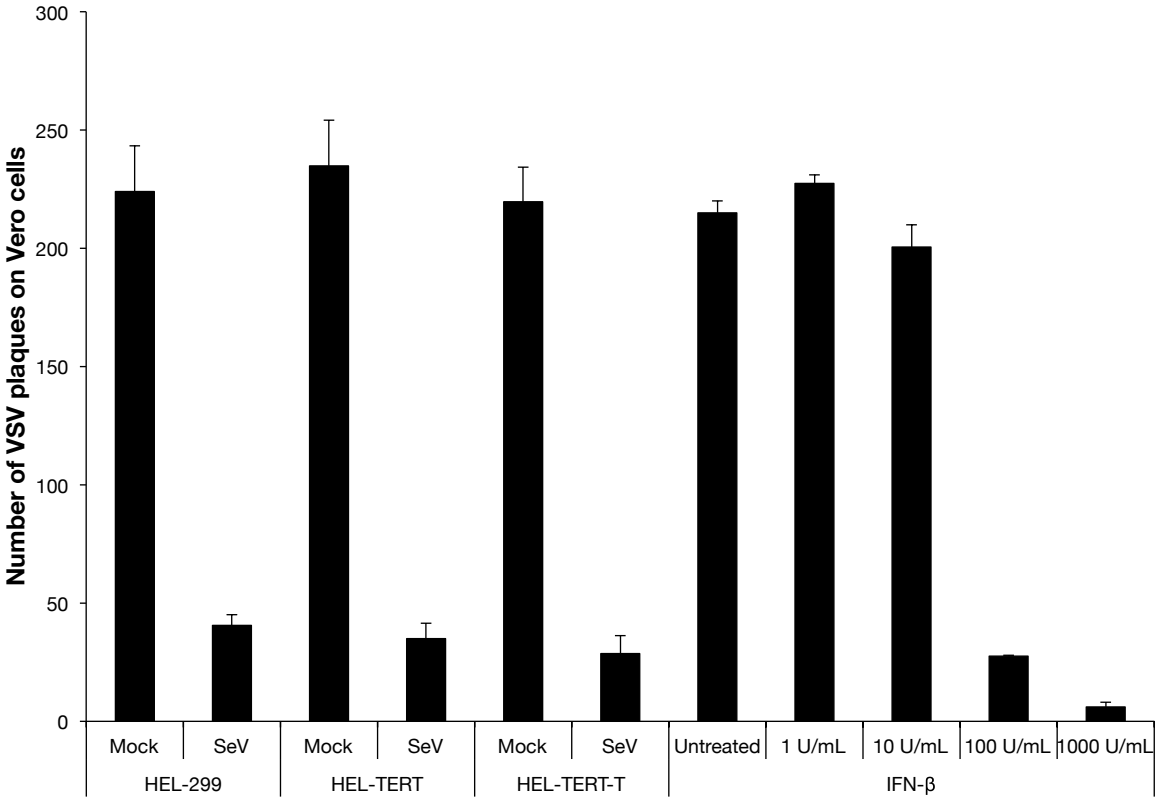


**Figure 3.9. Ectopic hTERT expression does not affect the ability of HEL cells to produce antiviral cytokines.**

HEL-299, HEL-TERT, and HEL-TERT-T cells were mock- or SeV-infected at 100 HAU/$10^6$ cell. At 24 hpi, the media were transferred to naïve Vero cell monolayers. 6 hs later, the Vero cells were infected with 200 PFU of VSV-eGFP per well. At 24 hpi with VSV-eGFP, the Vero cells were fixed and the number of fluorescent plaques counted. Data shown represents the average of two experiments performed in duplicate (6 standard errors of the means).

# Chapter 4: Role of phosphorylation in the antiviral activity of the promyelocytic leukemia protein in response to herpes simplex type I infection

## 4.1 Introduction

PML has been shown to affect aspects of the HSV-1 life cycle [30,33,286–288]. Upon nuclear entry of viral DNA, preexisting ND10s disassemble and reform near the sites of the incoming viral genomes [26,289]. At these sites, certain ND10 members assist in the loading of chromatin on viral DNA and form a shell that prevents the initiation of viral gene expression, presumably by occluding the ability of transcription factors from interacting with viral DNA and initiating transcription [148]. The recruitment of PML to viral genomes is contingent upon its SUMOylation, as forms that cannot be SUMOylated fail to appreciably respond to the nuclear entry of viral DNA and remain positionally stable [290]. Furthermore, these SUMOylation-deficient mutants fail to restrict the ability of HSV-1 mutants that are sensitive to intrinsic defense mechanisms. HSV-1, however, overcomes these defenses through the activity of its E3 ubiquitin ligase, ICP0, which induces the ubiquitination and proteasomal destruction of PML [291,292]. Here again, PML SUMOylation influences the course of infection as ICP0 favors interaction with and degradation of certain SUMOylated forms of PML [292,293].

While the mechanisms are unclear, phosphorylation at a number of sites on PML influence its SUMOylation [178,186]. Additionally, during mitosis and upon double strand DNA breaks, ND10s undergo a PML phosphorylation-dependent disassembly and/or relocalization [196]. Furthermore, phosphorylation of a region near the SIM, which is required for recruitment to incoming viral genomes and restriction of viral plating [286], has been reported to influence the affinity of the SIM for SUMO [191,192]. However, the role of phosphorylation in the control of its antiviral activities, particularly toward HSV-1, has received little attention.

Herein we report that we have identified several regions of phosphorylation within PML that influence its stability in the presence of ICP0 and that mutation of phosphoacceptor sites near the SIM impairs the ability of PML to be recruited to incoming viral genomes.

## 4.2 Methods

### 4.2.1 Cells

Human embryonic lung (HEL-299) cells were obtained from the American Type Culture Collection (CCL-137) and were maintained in Minimum Essential Medium Eagle Alpha Modification (αMEM) containing 10% fetal bovine serum (FBS), 2 mM L-glutamine, 10 U/mL penicillin, and 10 U/mL streptomycin. A549 and A549-based cell lines were maintained in Dulbecco's modified Eagle's medium containing 5% FCS, 2 mM L-glutamine, 10 U/mL penicillin, and 10

U/mL streptomycin. HepaRG [294], HA-shNeg, HA-shPML [295], and all HA-shPML-derivative cell lines were maintained in William's E media containing 10% FBS, 2 mM L-glutamine, 10 U/mL penicillin, 0.5 μM hydrocortisone, and 5 μg/mL insulin. Cells transduced with shRNA-encoding lentivirus were kept under antibiotic selection with puromycin at 1 μg/mL; HA-shPML+LNGY, HA-shPML+LNGY-PML.I, and HA-shPML+LNGY-PML.I-derivative cell lines were additionally maintained under selection with G418 at 200 μg/mL.

GP2-293, U2OS, HEp-2 cells and HEp-2 derivative cell lines were maintained in Dulbecco's modified Eagle's medium (DMEM) containing 5% FBS, 2 mM L-glutamine, 10 U/mL penicillin, and 10 U/mL streptomycin.

A549 and HEp-2 cells depleted of PML or the luciferase-depleted control line were created by transducing cells with LKO-shPML or LKO-shLuci [30,287] lentiviral stocks using four sequential 1-hour incubations, replacing the previous round of incubation with fresh lentiviral supernate. After the fourth round of transduction, the cells were incubated at 37°C overnight. The next day, cells were washed three times with PBS and incubated in fresh medium. Two days post-transduction, the cells were placed under selection using puromycin at 1 μg/mL and thereafter maintained in puromycin.

A549 and HepaRG-based cells expressing FLAG- and CFP-tagged PML were created by transducing cells as above with retrovirus in the presence of 10 μg/mL polybrene as described above.

HepaRG-based cells expressing eYFP-tagged PML were created as described for the creation of shRNA-expressing A549 cells. Two days post

transduction, the cells were placed under antibiotic selection using G418 at 800 μg/mL. The resistant outgrowth was expanded before being enriched by fluorescence activated cell sorting as previously described [286].

### 4.2.2 Plasmids

Vectors encoding the PML ORF were constructed as follows. CFP was subcloned in the place of GFP by replacing the NotI-BamHI fragment of pMX-eGFP (a gift from Toshio Kitamura) with that from pECFP-N1 (Clontech). PML and eCFP were placed An EcoRI-MfeI fragment containing a myc-tagged PML isoform 4 from the vector pCImycPML-fl [293] was subcloned into the EcoRI site of pMX-eCFP to create pMX+mycPML4+eCFP. A MluI-MfeI fragment of pMX+mycPML4+eCFP was replaced with that from pSG5PML-L, which encodes the C-terminus of PML isoform 3, to give rise to pMX+mycPML3+eCFP. To place PML and eCFP in frame, the C-terminus of PML3 was amplified by PCR using Phusion polymerase (New England Biolabs) and the primers 5'-aaaacgcgttgtggtgatcagcagctc-3' 5'aaaaccgcggagcgcgggctggtgggga-3', which removes the stop codon from PML3 and adds a SacII site. This PCR product was then used to replace the MluI-SacII fragment of pMX+mycPML3+eCFP to create pMX+mycPML3_eCFP.

The myc-tag was replaced with a FLAG-tag sequence by first subcloning the EcoRI-SphI fragment of pMX+mycPML3_eCFP into the same sites of pUC19 to create pUC19-(Nterm)mycPML. An oligomer encoding a 3xFLAG sequence (5'-atggactacaaagaccatgacggtgattataaagatcatgacatcgattacaaggatgacgatgacaa-

c-3') was TOPO-cloned into pCR4Blunt-TOPO (Invitrogen) according to the manufacturer's instructions to create pCR4Blunt-TOPO+3xFLAG. The BamHI-NcoI fragment from pCR4Blunt-TOPO+3xFLAG was used to replace the BamHI-NcoI fragment of pUC19+(Nterm)mycPML to create pUC19+(Nterm)3xFLAG_PML, the EcoRI-SphI fragment of which was then subcloned back into pMX+mycPML3_eCFP.

To enable interferon-inducibility of the integrated transgene, a quadruple repeat of the ISRE from *ISG15* flanked by XbaI restriction sites sites (5'-tcta-gacccgccccatgcctcgggaaagggaaaccgaaacgggaaagggaaaccgaaac-gggaaagggaaaccgaaacgggaaagggaaaccgaaactgaagccaatctagaaaa-3') was inserted into the XbaI site of the 3'U3 element of pMX+3xFLAG_PML3_eCFP, giving rise to p3'415MX+3xFLAG_PML3_eCFP.

To create a form of PML that is resistant to silencing by shRNA produced in HA-shPML cells, a BamHI-fragment of pMX+3xFLAG_PML3_eCFP was subcloned into the vector, pAlter-1, and silent mutations were introduced using the Altered Sites Mutagenesis system (Promega) using the primer 5'-tgcatcacccaggggaaGgaCgcGgcGgtGAGTaaAaaGgccagcccagaggct-3' (with upper case letters representing introduced mutations) as per the manufacturer's instructions. The BamHI fragment was then subcloned back into the parental vector to generate p3'415MX+3xFLAG_PML3R_eCFP.

To create a vector that encoded PML isoform 1, the C-terminus of PML-I was amplified by PCR (using the primers 5'- aaagcatgcagtgccccatctgc-3' and 5'-aaaaaaccgcgggctctgctgggaggccctctc-3') from a HEL-299 cDNA library and

subcloned between the SacII and SbfI sites of p3'415MX+PML3R_eCFP to create p3'415MX+3xFLAG_PML1R_eCFP.

The PML phosphorylation knockout mutants were created using PCR mutagenesis with the following primers:

| | |
|---|---|
| S8A forward | 5'-ggagcctgcacccgcccgaGctccgaggccccagc-3' |
| S8E forward | 5'-ggagcctgcacccgcTcgaGAAccgaggccccagcag-3' |
| S8 reverse | 5'-atggcgttgtcatcgtcatccttg-3' |
| T28;S36/38/40A forward | 5'-atgcctccccccgagGcGccctctgaaggccgccagcccGCTcccG-CGccGGCccctacagagcgagc-3' |
| T28;S36/38/40E forward | 5'-atgcctccccccgagGAAccctctgaaggccgGcagcccGAAccc-GAAcccGAAcctacagagcgagcc-3' |
| T28;S36/38/40 reverse | 5'-ggtgggctcctggggccgggcggg-3' |
| S117A | 5'-agtctgcagcggcgcTtAGcggtgtaccggcaga-3' |
| S117E forward | 5'-tctgcagcggcgcctCGAggtgtaccggcagat-3' |
| S117E reverse | 5'-ctctcgaaaaagacgttatccagggcggg-3' |
| S399/403;T409A forward | 5'-aaGgaCgcGgcGgtGGCTaaAaaGgccGCcccagaggctgcca-gcGctcccagggacccta-3' |
| S399/403;T409E forward | 5'-aaGgaCgcGgcGgtGGAGaaAaaGgccGAAccTgaggctgcc-agcGAAcccagggaccctatt-3' |
| S399/403;T409 reverse | 5'-cccctgggtgatgcaagagctgag-3' |
| S480;T482;S493A forward | 5'-cagaagaggaagtgcGCGcagGcccagtgccccaggaaggtcatca-agatggagGctgaggaggggaagg-3' |
| S480;T482;S493E forward | 5'-cagaagaggaagtgcGAGcagGAAcagtgcccTaggaaggtcatc-aagatggagGAAgaggaggggaaggag-3' |
| S480;T482;S493 | 5'-ggctgtcgttgtattggagacatc-3' |
| S504/505A forward | 5'-ggcaaggttggctcgAGCcGccccggagcagccca-3' |
| S504/505A reverse | 5'-tccttcccctcctcagactccatc-3' |
| S504/505E forward | 5'-gcaaggttggctcggGAAGAGccggagcagcccagg-3' |
| S505/505E reverse | 5'-ctccttcccctcctcagactccat-3' |
| S518A forward | 5'-cagcacctccaaggcagtcGcaccTccTcacctggatggaccg-3' |
| S518E forward | 5'-cagcacctccaaggcCgtGGAaccaccccacctgga-3' |
| S518 reverse | 5'-ggcctgggctgctccgg-3' |
| S527/530A | 5'-ctggatggaccgcctGCccccaggGCccccgtcataggaag-3' |
| S527/530E | 5'-ctggatggaccgcctGAAccTaggGAAcccgtcataggaagt-3' |

| | |
|---|---|
| forward | |
| S527/530E reverse | 5’-gtggggtggtgagactgccttggag-3’ |
| S560/561/562/565A forward | 5’-cgcgttgtggtgatcGCGGCcGcggaagacGcagatgccgaaaact-3’ |
| S560/561/562/565A reverse | 5’-ttcctctgcctccccggcgccact-3’ |
| S560/561/562/565E forward | 5’-ggaggcagaggaacgTgttgtggtgatcGAAGAAGAggaagacGA-Agatgccgaaaactcg-3’ |
| S560/561/562/565E reverse | 5’-ccggcgccactggccacgtggttg-3’ |
| S565A forward | 5’-agcagctcggaagacGcagatgccgaaaact-3’ |
| S565A reverse | 5’-gatcaccacaacgcgttcctctgc-3’ |
| S565E forward | 5’-gttgtggtgatcagcTCTtcggaagacGAagatgccgaaaactc-3’ |
| S565E reverse | 5’-gcgttcctctgcctccccggcgcc-3’ |
| V556/557/558A;I559S forward | 5’-aggcagaggaacgcgCtgCggCTaGcagcagctcggaaga-3’ |
| Δ476-490 forward | 5’-gaggcaaggttggctcgga-3’ |
| Δ476-490 reverse | 5’-ctgggctgtcgttgtattggaga-3’ |
| K65R | 5’-atgccaggcggaagcGCGCtgcccgaagctgctg-3’ |
| K160R forward | 5’-acaccagtggttcctACGTcaTgaAgcccggcccctagca-3’ |
| K160R reverse | 5’-gcctcgaagcacttggcgcag-3’ |
| K490R | 5’-cccaggaaggtcatcCGgatggagtctgagga-3’ |
| K616R forward | 5’-gttttctttgacctcCGgattgacaatgaaa-3’ |
| K616R reverse | 5’-cagaggtctgtcttctgcttggg-3’ |

In some cases, sequential rounds of PCR mutagenesis were required to introduce the desired mutations. All constructs were verified by sequencing.

Certain PML mutants were subcloned into pLNGY (a gift from Roger Everett) [286]. To enable rapid subcloning of the PML mutations from the p3’415MX+3xFLAG_PML1R_eCFP background, a PsiI-PsiI fragment (spanning the F1 origin of replication) from pLNGY was removed by restriction digest and the vector was re-ligated to eliminate an AvrII restriction site. An AvrII-StuI region of the PML phosphorylation knockout mutants from p3’415MX+3xFLAG_PML1R_eCFP were subcloned into pLNGY(F1-).

### 4.2.3 Viruses

KOS [201] and Syn17+ [296] are wild type HSV-1 strains used in these studies. 7134 is an ICP0-null mutant in which the *ICP0* open reading frame of KOS is replaced by the *E. coli lac*Z gene [202]. dl1403/CMV*lacZ* is a Syn17+ ICP0-null virus containing a 2 kb deletion in both copies of the *ICP0* gene [281]. Both dl1403/CMV*lacZ* and another Syn17+ mutant, in1863 (which is otherwise similar to wild type Syn17+), encode *lacZ* under the control of the HCMV IE promoter inserted into the *tK* locus [287,297]. KOS, Syn17+, and in1863 viral stocks were prepared in Vero cells, and 7134 and dl1403/CMV*lacZ* were grown in U2OS cells; all viruses were titered as previously described [91,203,287].

Retroviruses were generated the Pantropic Retroviral Expression System (Clontech) as recommended by the manufacturer. Lentiviral stocks were generated essentially as for retroviral stocks except for the inclusion of the packaging vector, psPAX2 (Addgene plasmid 12260), and the use of HEK-293T cells for packaging [298].

### 4.2.4 Reagents

The CK2 inhibitor 2-dimethylamino-4,5,6,7-tetrabromo-1*H*-benzimidazole (DMAT) was purchased from EMD Chemicals and 2-(4,5,6,7-tetrabromo-2-(dimethylamino)-1H-benzo[d]imidazol-1-yl)acetic acid (TMCB) from Ascent Scientific. The CK2 inhibitors were constituted in DMSO (Fisher Scientific).

### 4.2.5 PML immunoprecipitation

HEL-299 cells were transduced with pseudotyped pMX+3xFLAG_PML3_eCFP such that the cells were 70% positive for PML3_eCFP. For uninfected samples, cells were plated in 10 100-mm dishes and grown to confluency. Twenty-two µg of anti-FLAG (M2) were added to 165 µL Dynabeads protein G (Invitrogen), which were washed and prepared according to the manufacturer's instructions, and allowed to incubate together at 4°C overnight. The cells from each plate were washed with 1 mL PBS containing protease inhibitors (1 µg/mL aprotinin, 1 µg/mL leupeptin, 10 mM phenylmethanesulfonylfluoride, 1 mM $Na_3VO_4$, 1x Complete protease cocktail inhibitor (Roche)), and scraped into PBS, centrifuged to pellet cells, and resuspended in 200 µL lysis buffer (4% SDS, 10 mM dithiothreitol, 300 mM NaCl, 100 mM HEPES (pH 7.5)) [299] containing inhibitors. The samples were solubilized by incubation at 100°C for 5 minutes, vortexing, and sonication at 100 W for 1 minute using a cup sonicator. The samples were then combined and diluted with 13 mL of diluent buffer (1.7% Thesit, 150 mM NaCl, 50 mM Hepes (pH 7.5)) containing the protease inhibitors. The anti-FLAG-conjugated Dynabeads were added to the lysate and incubated at 4°C overnight. The next day, the beads were precipitated using a magnet and washed with 2 mL of the diluent buffer (containing inhibitors) 4 times. After the final wash, the beads were resuspended in 50 µL of Laemmli buffer [206], boiled for 5 minutes, and resolved on 4-20% Tris-glycine SDS-PAGE gels. The gels were stained with

Coomassie blue, thoroughly destained, and the desired bands were excised and washed with a 50% acetonitrile/water solution.

PML from infected cells was prepared essentially as above except that cells were pretreated with 10 μM MG132 for 1 h, infected with KOS at an estimated 5 PFU/cell in the presence of MG132, and cells were collected at 5 hpi.

Peptides were analyzed for phosphorylation by tandem mass spectrometry at the Harvard University Microchemistry and Proteomics Analysis Facility.

### 4.2.6 Western blots

To examine the ability of ICP0 to induce degradation of PML or its mutant forms, HEp-2 cells were plated at $1\times10^5$ cells per well of a 24-well plate. The cells were transfected 24 hs later with either 100 ng of p3'415MX+3xFLAG_PML1R_eCFP or one of the PML phosphorylation mutants along with 1 μg of pcDNA3.1, pcDNA3.1+n212, or pcDNA+ICP0 using Lipofectamine 2000 (Invitrogen) as per the manufacturer's recommendation. At 24 hs post transfection, the cells were washed once with PBS and lysed into 50 μL of boiling Laemmli buffer containing 1 μg/mL aprotinin, 1 μg/mL leupeptin, 1 mM PMSF, 10 mM sodium vanadate, 50 mM sodium fluoride, and 20 mM N-ethylmaleimide. One-fifth of each sample was resolved on 4-12% Bis-tris polyacrylamide gels, transferred to nitrocellulose, blocked at room temperature for 1 h with 2% nonfat dry milk in Tris-buffered saline with 0.1% Tween 20 (TBS-

T). The blots were probed either overnight at 4°C or for 2 hs at room temperature with primary antibodies. Primary antibodies used included those directed against FLAG (M2, Sigma Aldrich) or β-actin ((I-19)-R, Santa Cruz Biotechnology). Antibodies were diluted in 2% non-fat dry milk/TBS-T. Membranes were then washed three times with TBS-T and probed at room temperature with goat-anti-mouse IgG, or goat-anti-rabbit IgG conjugated to HRP (Jackson Immunoresearch). Membranes were again washed with TBS-T and developed with chemiluminescent substrate (Femto ECL, Pierce Laboratories). Chemiluminescence was detected using an Image Station 4000R (Kodak) and Carestream Molecular Imaging software. Images were assembled using Adobe Photoshop and Illustrator (Adobe Systems) and band intensities were measured by densitometry analyses using ImageJ.

To examine SUMOylation levels of PML, $1\times10^5$ HEp-2-shPML cells were plated per well in 24-well plates. The next day, the cells were transfected with 100 ng of p3'415MX+3xFLAG_PML1R_eCFP or one of the PML phosphorylation mutants along with 900 ng of pGEM-3 using Lipofectamine 2000 according to the manufacturer's instructions. At 24 hs post transfection, the cells were lysed as above. One fifth of each sample was resolved, transferred, and probed as above except that proteins were resolved using 6% Tris-glycine polyacrylamide gels. Images were assembled using Adobe Photoshop and Illustrator (Adobe Systems) and band intensities were measured by densitometry analyses using ImageJ.

### 4.2.7 Immunofluorescence

To examine the ability of exogenous PML to recruit Sp100 and Daxx to ND10s, A549-shPML or HA-shPML cells were transduced with retroviral vectors encoding 3xFLAG_PML1R_eCFP or one of the phosphorylation site mutants generally as described for the creation of depleted cells. These cells, as well as A549 and HA-shNeg cells, were plated on collagen coated coverslips and the next day were washed once with PBS, fixed for 5 minutes with 5% formaldehyde in PBS at room temperature, washed three times with PBS, permeabilized at 4°C for 15 minutes with 0.5% NP-40 in PBS, and washed an additional three times with PBS. Coverslips were the probed for 30 minutes at 37°C with antibodies against Sp100 (mAb1380, Millipore) and Daxx (S-20, Santa Cruz Biotechnology) diluted in 1% FCS, 1% BSA, 0.05% Tween-20 in PBS; A549 and HA-shNeg cells were probed with antibodies against PML (A301-167A, Bethyl Laboratories) and Sp100. Cells were washed three times with PBS and stained for 30 minutes at 37°C with donkey-anti-mouse IgG Dylight 594 and cow-anti-goat IgG Dylight 488 diluted in the same buffer; A549 and HA-shNeg cells were stained with donkey-anti-rabbit IgG Dylight 594 and donkey-anti-mouse IgG Dylight 488. Coverslips were washed three times with PBS, air dried, and mounted onto glass slides using ProLong antifade (Invitrogen). Proteins were viewed by confocal fluorescent microscopy (Nikon) and captured with a digital camera (Photometrics). Images were assembled using Adobe Photoshop and Illustrator (Adobe Systems). ND10 reformation in HA-shPML was examined in a similar manner, except that the antibodies used against

Sp100 and Daxx (sc-16328, Santa Cruz Biotechnology and mAB 5.14 [300], respectively).

To examine colocalization between PML-I and ICP0, A549-shPML and HA-shPML cells were transduced as above. Two days post transduction, the cells, as well as A549 and HA-shNeg cells, were infected with KOS at an estimated 2.5 PFU/cell. To determine a time point at which to examine colocalization, an initial set of cells was fixed at 1, 2, 3, 4, 5, and 6 hpi as described above and all subsequent studies were examined at 2 hpi. The transduced and infected cells were probed first with antibodies against ICP0 (H11060, Santa Cruz Biotechnology) and ICP4 (EastCoastBio) diluted in 5% rabbit serum in PBS and then probed with goat-anti-mouse IgG1 Dylight 594 and goat-anti-mouse IgG2b Dylight 488 as listed above for Sp100 and Daxx staining; A549 and HA-shNeg cells were stained first for endogenous PML (A301-167A) and ICP0 (H11060) and then with donkey-anti-rabbit IgG Dylight 594 and goat-anti-mouse IgG2b Dylight 488.

To examine the recruitment of PML-I or the PML-I mutants to incoming viral genomes, HA-shPML cells were transduced described above. Three days post transduction, the medium was removed, and cells were infected with dl1403/CMVlacZ at an estimated MOI of 0.1. At 1 hpi, the cells were overlaid with growth medium containing 0.5% methylcellulose. At 24 hpi, the medium was removed, the cells were washed with PBS, and the cells fixed and permeabilized by incubation at -20°C in cold 20% acetone diluted in methanol for 15 minutes. Samples were then washed and stained with an antibody

against ICP4 as described above. HA-shNeg cells were also infected as described and were additionally stained with antibody against PML as described for the ICP0 colocalization studies. For PML recruitment studies in CK2-inhibitor treated cells, the medium on the cells was replaced 1 h prior to infection with fresh medium containing 0.4% DMSO, 20 μM DMAT, or 100 μM TMCB, with the subsequent infection and incubation taking place in the presence of these chemicals.

### 4.2.8 HSV-1 β-galactosidase foci assay

Cells were seeded at $1.5\times10^5$ cells/well in 24-well plates. Twenty-four hs later, viral suspensions were created by preparing 3-fold serial dilutions of in1863 or dl1403/CMVlacZ such that target wells would receive between an estimated 0.5 to 140 or 45 to 3600 PFU for in1863 or dl1403/CMV*lacZ*, respectively. Most of the medium was removed, cells were infected with 100 μL of viral inoculum, incubated at 37°C with shaking every 15 minutes, overlaid with growth medium containing 0.5% methylcellulose at 1 hpi, and incubated at 37°C. At 24-30 hpi, the wells were washed twice with PBS, fixed with 3.7% formaldehyde/PBS for 15 minutes at room temperature, washed three times with PBS, and stained using X-gal containing solution (1 mg/mL 5-bromo-4-chloro-3-indolyl-β-D-galactopyranoside, 5 mM $K_4Fe(CN)_6$, 5 mM $K_3Fe(CN)_6$, 2 mM $MgCl_2$, 0.01% NP40, diluted in PBS). Groupings of ≥4-6 blue cells (which was found to be roughly equivalent to foci that were visible by the naked eye) were counted as plaques.

## 4.3 Results

### 4.3.1 Identification of phosphorylated residues of PML in uninfected and HSV-1 infected cells

While PML is known to be phosphorylated on a number of sites when this project began, a full mapping of phosphorylated sites on PML had not been performed. Additionally, PML phosphorylation during infection had not been examined. To address these questions, we created an HEL-299 cell line that exogenously expresses a FLAG- and CFP-tagged form of PML-III. PML was immunoprecipitated from cells mock-infected or infected with HSV-1 for 6 hs and subjected to mass spectrometry analysis. As detailed in Table 4.1, we identified 19 phosphorylated serines and threonines in uninfected cells and 11 in infected cells, though we noted that there were significant gaps in the coverage of our scans. All of the sites located within regions shared among the different isoforms were either previously identified or have been reported in subsequent studies, though we did find several novel sites within a C-terminal region specific to PML-III. Of the sites identified, we found that S504 was phosphorylated only in uninfected cells while S565 was only detected as phosphorylated in infected cells. Thus, we have identified a number of novel sites of phosphorylation on PML and found that isoform specific sites of phosphorylation exist and that there appears to be changes in the phosphorylation status of PML upon infection.

### 4.3.2 Phosphorylation at sites near the SIM alter ND10 morphology and influences Sp100 and Daxx recruitment to ND10s

To examine the effect that phosphorylation at these sites has on PML, we created a series of retroviral constructs encoding FLAG- and CFP-tagged phosphorylation knockout and mimetic mutants, changing residues to alanine or glutamic acid, respectively. During the course of this work, it was shown that PML-I is the most widely expressed of the PML isoforms [301] and, unlike PML-III, has antiviral activity toward certain HSV-1 mutants [286]. Thus, these mutants were created in a PML-I background. Because exogenous PML forms heterodimers with endogenous PML, which would complicate interpretation, we created cell lines that express shRNAs directed against PML and introduced the mutant forms of PML (which contained additional silent mutations to enable shRNA-resistance) into them. Initially, we chose A549 cells, a human lung epithelial carcinoma cell line, because they are immortalized, have a functional interferon-based antiviral response to a number of viruses, and we found them to be amenable to depletion of PML using shRNAs.

We first examined the ability of exogenous PML to form ND10s and to recruit the major ND10 constituents, Sp100 and Daxx. As expected, cells transduced with the shRNA targeting PML were largely devoid of PML and Sp100 was largely diffuse in the nucleoplasm in contrast to the parental A549s (Figure 4.2A). In cells transduced with the PML-I-expressing retrovirus, however, ND10s were clearly present along with, to a degree, colocalized Sp100 and Daxx (Figure 4.2B). An initial examination of the mutants failed to reveal

large differences in ND10 size or number for most of the PML phosphorylation mutants, with the exception being those bearing mutations near the SIM, S560/561/562/565A and –E, in which case the ND10s were larger; likewise, none of the mutants completely failed to recruit Sp100 or Daxx, though, again, those mutated near the SIM appeared to recruit both Sp100 and Daxx much more efficiently. These results were also true when PML expression was restored in a HepaRG-based PML-depleted cell line (Figure 4.4), though the PML-I(K65/160/490R) SUMOylation-deficient mutant failed to recruit Sp100 and Daxx in these cells.

A closer examination revealed subtle differences among the PML-phosphorylation mutants in their ability to recruit Sp100 and Daxx (Figure 4.3). Notably, the S117E and S518E mutants were much more likely to recruit Sp100 and somewhat better at recruiting Daxx, and specifically for S117E, Sp100 colocalized with it in all cells that were examined. Of the remaining mutants, we also found that S8/T28/S36/38/40A, S480/T482/S493A, S480/T482/S493E, and S504/505A mutants were marginally better at recruiting Sp100. These data suggest that phosphorylation near the SIM, and potentially S117, has a large effect on Sp100 and Daxx recruitment and that phosphorylation at several other sites on PML may subtly influence ND10 member recruitment.

### 4.3.3 Phosphorylation does not largely impact SUMOylation levels

As previous reports suggested interplay between phosphorylation and SUMOylation and current evidence suggest that PML acts as an E3 SUMO

ligase, perhaps on itself, we decided to examine the SUMOylation state of the PML phosphorylation mutants. HEp-2 cells depleted for PML (HEp-2-shPML) (Figure 4.5A) were used to allow us to examine the E3 ligase activity of PML without endogenous PML confounding our results. The cells were transfected with the various phosphorylation mutants, one of two SUMOylation-deficient mutants, the NLS mutant, or the SIM mutant and the next day cell lysates were prepared and examined by western blot. While FLAG-, CFP-tagged wild type PML-I exhibited the laddering typical of multiply SUMOylated proteins (Figure 4.5B), both the K65/160/490R and K65/160/490/616R mutant forms of PML-I were largely devoid of SUMO modification, though a small amount of SUMOylation was detected. These bands likely represent SUMOylation of minor, non-preferred or non-canonical sites [166,167]. Likewise, the NLS-deletion mutant was essentially non-SUMOylated while the SIM-mutant was slightly less SUMOylated than wild type. Of the phosphorylation mutants, while no gross differences in SUMOylation patterns were obvious, densitometric analysis showed that the S518A mutant was more highly SUMOylated while the S565A mutant was slightly less so, resembling the SIM-mutant. These results indicate that the phosphorylation sites examined do not greatly affect SUMOylation levels of PML in resting cells.

### 4.3.4 Phosphorylation is not required for the colocalization of PML-I and ICP0

The ability of ICP0 to interact with PML has been reported to be facilitated by PML SUMOylation. Forms of ICP0 that do not colocalize with PML either fail to or are inefficient at inducing the degradation of PML. As phosphorylation of PML can influence PML SUMOylation and potentially block or create a binding site for ICP0, we wished to determine whether PML phosphorylation affected PML:ICP0 colocalization. While ICP0 induces the proteasomal-dependent degradation of PML, the use of proteasome inhibitors has been reported to change ND10 composition. To determine a time point at which ICP0 levels were high enough for detection but had not yet induced substantial ND10 disassociation, PML-I-transduced HA-shPML cells were infected with HSV-1 and processed for immunofluorescence assays at 1, 2, 3, 4, 5, and 6 hpi (data not shown). We found that 2 hpi was an ideal time at which to examine PML:ICP0 colocalization. HA-shPML cells were transduced with retroviral vectors encoding PML-I or one of the PML-I phosphorylation knockout mutants and two days later infected with HSV-1 at 2.5 PFU per cell to ensure all cells were infected. At 2 hpi, the cells were fixed and processed for immunofluorescence staining for ICP0, with PML detected by autofluorescence. As expected, we found that in infected cells expressing PML-I, ICP0 was present at all ND10s (Figure 4.6). When we examined infected cells transduced with the PML-I phosphorylation mutants, we again found that ICP0 was present at a majority of ND10s, with the sole exception being those formed by the

S8;T28;S36/38/40A mutant, in which a small number of ND10s appeared not to colocalize with ICP0 foci. To confirm that ICP0 was at ND10s due to the presence of PML and not another ND10 constituent (such as SUMOylated Sp100), we also tested the ability of a PML NLS-deletion mutant to retain ICP0 in the cytoplasm. PML-I(ΔNLS) was, as expected, restricted to the cytoplasm, where it formed 2-3 puncta per cell. In cells transduced with this construct, ICP0 was strongly retained in the cytoplasm. We also examined colocalization between ICP0 and PML-I, the PML-I phosphorylation, SIM, NLS, and K65/160/490/616R mutants in the HA-shPML cells (Figure 4.7) and found that they recapitulated those in the A549-shPMLs. These assays indicate that either none of the phosphorylation sites we examined greatly influence the ability of ICP0 to localize with PML-I or that there are multiple sites on or regions in PML to facilitate this process.

### 4.3.5 PML phosphorylation has minor effects on ICP0-induced degradation

Phosphorylation of PML has been shown to contribute to its the stability through a number of mechanisms. To more directly assay whether any of the phosphorylation sites influence the stability of PML in the presence of ICP0, we cotransfected the retroviral constructs that express PML-I or its mutant forms along with either an empty control vector, a vector encoding ICP0, or a vector encoding the n212 truncation mutant of ICP0 (which is incapable of inducing PML degradation) into HEp-2 cells, which have previously been used in assays

examining ICP0-induced PML degradation [293]. Twenty-four h later, the levels of exogenous PML were examined by western blot. As expected, expression of ICP0 lead to the near total loss of PML while expression of the n212 mutant did not (Figure 4.8). Interestingly, while the NLS mutant and ICP0 colocalize (Figure 4.6 and 4.7), ICP0 was unable to induce its degradation. Examination of the phosphorylation mutants revealed that ICP0 was capable of reducing the levels all of these mutants; however, we noted that levels of the S480;T482;S493E, S504/505A, S504/505E, and S518E mutants, while lower in the presence of ICP0, were not diminished to the same degree as wild type PML-I. These results indicate that phosphorylation may play a role in determining PML stability in the presence of ICP0.

### 4.3.6 Mutation of the phosphoacceptor sites in the phosphoSIM of PML-I prevents recruitment to incoming viral genomes

As viral DNA is injected into the nucleus, it is recognized as either foreign or damaged DNA and as such, the cell mounts a response involving DNA damage factors, components of the SUMOylation machinery, and ND10 members. In the case of ND10s, preexisting ND10s breakdown and recoalesce around viral genomes, preventing these factors from accumulating around viral DNA correlates with a loss in their antiviral activity towards HSV-1. In the case of PML, it has been shown that both SUMOylation of PML and the integrity of its SIM are required for relocalization at incoming genomes. Consequently, we

wished to determine whether phosphorylation of PML played a role in this process.

The recruitment of intrinsic antiviral effectors to incoming viral genomes can most easily be seen at the edge of spreading plaques on monolayers infected at low MOIs with ICP0-null mutant viruses. Cells at the plaque edge experience a directional infection, with viral capsids primarily docking and injecting the viral DNA on one side of the cell. This can be visualized by staining for the major viral transactivator, ICP4, which binds to the viral DNA. Therefore, HA-shPML cells were transduced with the various PML-I retroviral constructs. Four days later, they were infected with an ICP0-null virus at a low multiplicity of infection, and overlaid with methylcellulose to restrict viral spread. The next day, the cells were fixed and stained for ICP4, with PML detected by autofluorescence. As expected, along the edges of plaques we observed cells in which ICP4 was found as a front along one side of the nuclear envelope (Figure 4.9A). In cells transduced with PML-I, we found a strong recruitment to ICP4 foci whereas PML-I(V556/557/558A;I559S), in which the SIM is inactivated and cannot be recruited to incoming genomes, or PML-I(K65/160/490R), in which the major SUMOylation acceptor sites are mutated, failed to show any relocalization to ICP4 fronts (Figure 4.9A). Of the various PML phosphorylation mutants, we found that only those that were mutated at sites in the phosphorylation region adjacent to in the SIM failed to relocalize to incoming genomes. In all cases observed, both the S560/561/562/565A and S560/561/562/565E mutants failed to colocalize with ICP4, indicating that

phosphorylation of the SIM may be required for PML's antiviral activity. Indeed, it has previously been shown that mutation of these serines to alanine decreases the ability of PML to interact with SUMOylated proteins in yeast two-hybrid assays [192] and in bioluminescence resonance energy transfer assays [191]. As these sites are phosphorylated by the cellular kinase CK2, we then wished to determine whether the use of a CK2 inhibitor would prevent the recruitment of PML to incoming genomes. PML-I- or PML-I SIM mutant- [PML-I(V556/557/558A;I559S)] transduced HA-shPML cells were pretreated with DMSO (as vehicle control) or the CK2 inhibitor DMAT at 20 μM for 1 h, infected with the ICP0-null mutant at 0.1 PFU/cell in the presence of either DMSO or DMAT, overlaid with methylcellulose at 1 hpi, and processed for immunofluorescence assays at 24 hpi. As expected, DMSO did not affect the ability of PML1 to respond to the presence of viral DNA nor did it change the inability of the PML-I-SIM mutant to do so (Figure 4.9B). In the DMAT-treated cells, however, we unexpectedly found that PML-I could relocalize to incoming viral genomes. Similar results were found when we used a second CK2 inhibitor, TMCB. While these findings were unexpected, we nonetheless have found that of the phosphorylation sites observed in PML, only mutation of those in the phosphoSIM appears to compromise the ability of PML to be recruited to incoming viral genomes.

### 4.3.7 Phosphorylation plays a minor role in the antiviral activity of PML toward HSV

While ICP0-null mutant HSV-1 is at least 100-fold less likely than wild type HSV-1 to productively initiate an infection, it shows an increased likelihood to plaque on cells depleted of PML. Reintroduction of PML isoforms I and II has been reported to partially restore the restriction of plaquing with an ICP0-null virus. Thus, we wished to determine whether phosphorylation of PML was responsible for controlling its antiviral activity by examining whether expressing the PML-I phosphorylation mutants in PML depleted cells had an effect on the plating efficiency of HSV-1. Initial testing showed that restoration using the retroviral constructs did not affect the plaquing efficiency of an ICP0-null virus (data not shown). As overexpression of PML can result in a loss of its antiviral activity (Roger Everett, personal communication), we moved three of the mutants into a lentiviral expression system in which PML is under the control of the weak HSV-1 gD promoter, a construct that has been used in previous reports [286,290,292,295]. We chose to examine the S117A, S480;T482;S493A, and S560/561/562/565A mutants as S117 is phosphorylated by CHK2, the activity of which is stimulated by ICP0; S480;T482;S493 is predicted to be phosphorylated by PI3KKs, whose activities are modulated by HSV-1 infection; and S560/561/562/565A due to its inability to localize to incoming viral genomes. HA-shNeg, HA-shPML, or HA-shPML cells expressing PML-I or one of these mutants were infected with one of two strains of serially diluted HSV-1, in1863 (ICP0+) or dl1403/CMVlacZ (ICP0-). in1863 is an essentially wild type

virus that expresses the *Escherichia coli* β-galactosidase gene under the control of the HCMV major immediate-early promoter while dl1403/CMVlacZ is its ICP0-null counterpart. With these viruses, β-galactosidase activity serves as a marker for successful establishment of infection, independent of viral transactivator-dependent gene expression. While depletion of PML indeed resulted in a partial complementation of plaquing for dl1403/CMVlacZ, we were unable to achieve complementation to the same degree as in previous reports, with our results showing a roughly 3.5-fold increase in plating of dl1403/CMVlacZ (Figure 4.10); this result contrasts with a nearly 10-fold increase previously reported [292]. In our hands, restoration of PML-I alone resulted in little to no decrease in plating efficiency for dl1403/CMVlacZ as compared to that on PML-depleted cells. Two of the mutants – the S117A and S480;T482;S493A – demonstrated a slight decrease in dl1403/CMVlacZ plating, indicating that these sites may play a minor role in PML's antiviral activity. In line with previous reports that mutant forms of PML that fail to relocalize to incoming viral genomes have no effect on viral plating, dl1403/CMVlacZ plated nearly equally efficiently on cells that were transduced with the S560/561/562/565A mutant as it did on cells depleted of PML expression. While not expected, we also consistently observed a nearly 2-fold decrease in plating efficacy for in1863 in PML-depleted cells.

## 4.4 Discussion

PML is constitutively expressed and as such, can respond immediately to cellular insults; however, to do so, it must be regulated in a dynamic manner. One method of quickly controlling proteins includes altering their post-translational modification state. PML is known to be extensively modified and, in some instances, its post-translational state is changed in response to various stimuli when functioning in particular cellular pathways. For instance, phosphorylation of PML has been tied to its role in cell cycle control [183], differentiation [195], and the DNA damage response [193]. In these cases, phosphorylation can alter the stability of PML, its ability to interact or recruit partner proteins, its localization within the cell, or influence other types of post-translational modification. While PML has been demonstrated to have antiviral activity towards a number of viruses, the role of phosphorylation in this response has received little attention.

When this work was began, only a few studies had been performed that mapped phosphorylation on PML. Those studies were limited to examining only a few sites that matched kinase consensus phosphorylation sites. We and others have since made use of advances in mass spectrometry technology to perform precise mapping studies of PML phosphorylation [176,302]. While many of the phosphorylation sites we identified have also been noted in subsequent reports, we have identified a number of unique phosphorylation sites. Furthermore, we are the first group to examine PML phosphorylation during viral infection. Notably, we have mapped a cluster of sites that match the

S/T-Q phosphoinositide 3-kinase-related kinase (PI3KK) consensus motif [303]. These sites are interesting, as PML has previously been demonstrated to be a substrate of ATR, a phosphorylation event that results in a translocation of PML from ND10s to nucleoli, transporting MDM2 with it, which results in the stabilization of p53. In addition to these potential PI3KK acceptor sites, we found that serine 504 was phosphorylated only in uninfected cells and serine 565 was so only in infected cells. Phosphorylation of S565 by CK2 has previously been shown to promote PML polyubiquitination as well as increase the affinity of the SIM for SUMO [183,191]; however, as noted in Chapter 2, the use of pharmacological inhibitors of CK2 does not prevent the degradation of PML by ICP0 and we failed to observe that mutation of S565 increases the stability of the PML-I in the presence of ICP0. The mechanism by which CK2 induces degradation of PML, however, is unknown. While phosphorylation at S504 has only been previously observed in a large scale phosphoproteome screen and thus its role has not been explored [304], it is located amongst a number of other residues that function in promoting the association of PML with Pin1, an interaction that destabilizes PML [181,189]; however, whether phosphorylation at S504 influences PML stability is unknown.

A major function of PML is the nucleation and recruitment of other ND10 member proteins. Two proteins of note, particularly in terms of the antiviral effect mediated by ND10s, are Sp100 and Daxx, especially as these proteins cooperate to limit HSV-1 replication [295]. When we examined exogenous PML-I expressed in PML depleted cells, we found that only a small proportion of the

reformed ND10s strongly recruited Sp100 and Daxx. This is in agreement with previous results showing that expression of individual isoforms of PML failed to fully restore recruitment of Sp100 and Daxx. The PML-I phosphorylation mutants generally behaved like wild type PML-I when it came to the recruitment of Sp100, although the ND10s formed by the S117E, S480;T482;S493E, and S504/505A mutants appeared to have higher levels of Sp100. For the most part, Daxx recruitment followed a similar trend to that of Sp100, though overall it appeared to be much more likely to be nucleoplasmic. The most notable exceptions were the S560/561/562/565A and S560/561/562/565E mutants, both of which were more likely to have intense Daxx staining at the reformed ND10s and Sp100 was more likely to localize with PML. Little is understood about the mechanisms involved in targeting Sp100 to ND10s. Some reports have suggested that they do not physically interact [164] and super-resolution microscopy shows them occupying separate portions of ND10s [136]. In some instances, particularly in stressed or senescence-inducing conditions, Sp100 is capable of forming foci independently of PML, and thus it may be that either PML and Sp100 nucleate around a common structure autonomously or that another protein serves as an adaptor between the two [305]. Phosphorylation of PML might influence its ability to either localize to the structure or interact with the adaptor protein and results in an indirect effect on PML:Sp100 colocalization. Notably, cytoplasmic localization of PML does not result in the cytoplasmic localization of Sp100 (Figure 4.2 and 4.3), unlike with Daxx (Figure 4.2 and 4.3) or ICP0 (Figure 4.6 and 4.7). Daxx, however, directly interacts with

PML in a manner that requires both SUMOylation of PML and a SIM present in Daxx [143,173]. In other studies involving depletion and restoration of PML expression, it was noted that either PML-VI, which lacks the SIM, or mutants of the other isoforms in which the PML SIM was mutated recruited Sp100 and Daxx more readily than wild type versions of PML-I though –V. Unexpectedly, SUMOylation of Sp100 is not necessary for recruitment of Sp100 to ND10s [290]. It seems likely that the PML SIM is required for interaction with another protein that negatively regulates the interaction between Sp100 and Daxx with PML; however, the only proteins known to require the PML SIM for interacting with PML are subunits of the proteasome [306].

Early during infection, ICP0 colocalizes with PML and induces the proteasomal degradation of PML as well as the loss of certain forms of Sp100 [291]. Though not strictly required for the ability of ICP0 to induce the loss of PML, forms that fail to localize to ND10s are inefficient at doing so [307]. We found that mutation of phosphorylation sites in PML-I did not noticeably affect the colocalization between PML and ICP0. Recent work has shown SUMOylation of PML-II, -III, -IV, -V, and –VI is necessary for their interaction with ICP0, while a region in the C-terminus unique to PML-I has the ability to interact with ICP0 in a SUMOylation-independent manner [292]. Little is known about this region other than it is predicted to have an exonuclease-III domain and that it is necessary for nucleolar-localization of PML-I in senescent cells or those that have been induced to have double stranded DNA breaks [144]. As we used PML-I in these studies, it is likely that we were unable to distinguish between

phosphorylation-dependent effects from those of the motif with which ICP0 interacts in the PML-I C-terminus. Indeed, while inactivation of the PML RING or B-boxes typically results in nuclear diffuse PML, they form puncta when in the presence of ICP0 [292]. It would be interesting in the future to examine how the phosphorylation sites influence interactions between ICP0 and the other PML isoforms and to determine whether the C-terminus of PML-I harbors unique phosphorylation sites of its own.

As noted above, colocalization between ICP0 and PML is not absolutely necessary for ICP0 to be able to induce the degradation of PML. Phosphorylation of PML can result it its destabilization [176,183] and certain cellular factors that control the stability of PML have been shown to interact with PML in a phosphorylation-dependent manner. When we examined the ability of ICP0 to induce the degradation of PML-I or the PML-I phosphorylation mutants, we found a number that appear to be somewhat more stable in the presence of ICP0, though none were completely resistant. Of interest, mutation of S505 and S518, the latter site implicated in mediating interaction with Pin1 upon its phosphorylation by CDK1, CDK2, or ERK2 which results in the polyubiquitination of PML by the Cullin3-KLHL20 E3 ligase [181], appeared to result in increased stability. In contrast, mutation of S565, which is implicated in the control of PML protein levels by PIAS1/CK2/RNF4 [141], had no effect. As noted in Chapter 2, the use of CK2 inhibitors does not prevent the degradation of PML by ICP0 during the course of infection. For Pin1, mutation of S403/505/518/527A has been found to be necessary to abrogate interaction

between PML and Pin1 [176]; nonetheless, as the region to which ICP0 binds is both C-terminal to these sites and specific to PML-I, it is intriguing to hypothesize that ICP0 may act in concert with Pin1, though it is known that CDK1 and CDK2 are not necessary for ICP0-induced PML degradation [308] nor do any of the immediate early HSV-1 proteins induce ERK2 activation [309,310]. Additionally, it will be of interest to determine what, if any, effects these phosphorylation sites have on the stability of other isoforms of PML.

Entry of viral DNA into the nucleus triggers the deposition of DNA damage response factors, SUMOylation machinery, and ND10 components at or near the viral DNA [19,26,284]. While the specific host cell activator of these factors in response to viral infection has not been identified, it is notable that many of the same factors assemble around sites of DNA damage [311]. Recruitment of PML to incoming viral genomes, which is essential for its antiviral function, requires the RING-finger, B-box 1, coiled-coil, SIM, and SUMOylation on either K160, K490, or both [290]. In the case of DNA damage, ND10s undergo an ATM-, CHK2-, and ATR-dependent fragmentation where portions of preexisting ND10s bud off and move to sites of damage, indicating that phosphorylation of PML may play a role in this process [312]. It is unknown whether this phosphorylation-dependent breakdown of ND10s is also required for recruitment to viral DNA, though the deposition of ND10 components near viral DNA does first require the exchange between ND10s and the nucleoplasm [26].

Of the phosphorylation mutants examined, we found that only sites near the SIM detectably influence recruitment of PML to incoming viral genomes. Phosphorylation of the phosphoSIM motifs of Daxx and PIAS1 have been shown to affect the ability of the SIM-domain containing protein to interact with SUMO, and in the case of Daxx, determining SUMO paralog preference [313], although this was not the case for PML [191]. It was also reported that the SUMO conjugation pathway components Ubc9, PIAS2β, and SUMO2/3 are found juxtaposed to viral genomes and depletion of Ubc9 compromises the ability of PML, Sp100, and Daxx to respond to the entry of viral DNA [19]. As SUMOylation of PML is also required for this response, it is unclear whether Ubc9 is needed to SUMOylate a PML-interacting partner with which PML binds in a SIM-dependent manner or if it is needed to SUMOylate PML and allow for PML's exit from ND10s [172]. Curiously, mutation of the serines of the phosphoSIM motif to either alanine, which would block phosphorylation, or glutamic acid, which should mimic phosphorylation, both lead to the same phenotype. In this instance, it might be that the reversible phosphorylation of the phosphoSIM is necessary for recruitment, as the introduction of glutamic acid may disrupt the proper folding near the SIM and results in its inactivation, or that glutamic acid fails to fully mimic the steric and electrostatic properties of phosphorylation at these sites. Previous work using a PML-III S560/561/562/565D mutant in bioluminescence resonance energy transfer assays, however, showed that mutation of these sites to aspartic acid does not compromise the ability of the SIM to interact with unconjugated SUMO1, unlike

their mutation to alanine [191]; this result suggests that it is dynamic phosphorylation of the phosphoSIM which is required for recruitment to viral genomes. These sites have previously been demonstrated to act as a substrate for CK2-mediated phosphorylation [183] and the phosphoSIM motifs of both PIAS1 and Daxx have been found to be phosphorylated by CK2 [192,313]. In both cases, the use of CK2 inhibitors resulted in a reduction in the ability of the proteins to bind to SUMO. We observed that treating cells with CK2 inhibitors did not compromise the ability of PML-I to relocalize to incoming viral genomes. While it is possible that the levels of the CK2 inhibitors used were insufficient to block CK2 activity, these inhibitors were used at the same concentration as in Chapter 2 and previous reports [314,315] and we did note that the number of plaques was decreased and their sizes were smaller suggesting an effect on CK2 activity. It is also possible that the inhibitors failed to prevent recruitment of PML due to PML being phosphorylated before treatment with the inhibitors; this seems unlikely, however, as phosphorylation at these sites also promotes degradation of PML [183]. While none of the other phosphorylation mutants demonstrated a defect in their recruitment, this does not rule out a role for overall PML phosphorylation or these sites in this activity. Multiple sites may serve redundant roles, as has been seen for the interaction between PML and Pin1 [176]. Additionally, our assays might not be sensitive enough to detect differences imposed by the mutations. Another possibility is that mutation of one site leads to a shift in phosphorylation to secondary sites, as HIPK2 phosphorylates S36 when its preferred residue at S38 on PML is mutated to

alanine [178]. Finally, our mass spectrometry failed to map a large portion of the N-terminus of PML, and this region might contain novel sites that contribute to the recruitment of PML to viral genomes.

PML has previously been established to have antiviral activity toward HSV-1, particularly for ICP0-null mutants [30,33,148,286,287,295]. While depletion of PML indeed resulted in a partial complementation of plaquing for dl1403/CMVlacZ, we were unable to achieve complementation to the same degree as in previous reports, with our results showing a roughly 3.5-fold increase in plating for dl1403/CMVlacZ, unlike a previous report of a ~10-fold increase [292]. This degree of complementation makes determining the antiviral activity of knocked in PML mutants limited, especially as the expression of a single PML isoform fails to completely restore the restriction of the ICP0-null virus. We are unable to explain the differences between our data and that of the Everett group, though it should be noted that our results were reproducible. Likewise, we have had difficulty establishing that the expression of PML-I or its mutant forms in PML-depleted cell lines restores restriction of an ICP0-null virus, or other assays that measure viral replication or gene expression (data not shown). Given these limitations, of the three mutants examined here, the S560/561/562/565A mutant, as expected due to its inability to be recruited to incoming genomes, had little to no antiviral activity while the S480;T482;S493A mutant appeared to have the strongest antiviral effect. It is unclear how preventing phosphorylation at S480, T482, and S493 might contribute to PML's

antiviral activity, as mutations of these sites did not lead to an obvious phenotype in our functional assays for PML activities.

In sum, we have mapped a number of phosphorylation sites on PML. An examination of these, as well as a number of other sites already reported in the literature, revealed that only those in the phosphoSIM motif appear to play a significant role in either the ability of PML to form ND10s or in its response to viral infection; however, we failed to observe these forms of PML have a substantial effect on viral replication. It is possible that our lack of a replication phenotype is due to PML isoform specific mechanisms, and as such further investigation should focus on other isoforms or in cells in which multiple isoforms have been restored. It is also possible that the difference in plating efficiency between control- and PML-depleted cell lines is too small to observe an effect and that such differences might be more obvious in other contexts. For instance, the simultaneous depletion of PML, Sp100, and Daxx results in a 50-fold increase in the plating efficiency for an ICP0-null virus and restoration into these cells may make differences among the phosphorylation mutants more obvious [295]. Additionally, as the requirement for ICP0 is much greater in primary or primary-like cells, these cell types may be more appropriate for examining restrictions on viral replication. Also, differences in the ability to restrict HSV-1 replication might also be more apparent in combination with other viral mutations, such as in the viral transactivator, VP16, as the lack of functional VP16 leads to a greater requirement for ICP0 in viral replication. Lastly it is

plausible that one or more phosphorylation sites of PML contribute to novel and combinatory antiviral mechanisms that have not yet been identified.

## 4.5 Tables

**Table 4.1: Sites of Phosphorylation on PML-III**

| Uninfected | | HSV-1 infected | |
|---|---|---|---|
| | Coverage gaps | | Coverage gaps |
| S399 | 1-44 | S403 | 1-7 |
| S403 | 57-86 | T409 | 18-44 |
| T409 | 147-149 | S505 | 57-97 |
| S480 | 212-216 | S518 | 132-153 |
| T482 | | S527 | 206-216 |
| S493 | | S565 | 336-337 |
| S504 | | T594 | 395-399 |
| S505 | | S598 | 478-486 |
| S518 | | S603 | |
| S527 | | S613 | |
| T594 | | S637 | |
| S598 | | | |
| S603 | | | |
| S608 | | | |
| S613 | | | |
| S616 | | | |
| S619 | | | |
| T620 | | | |
| S637 | | | |

HEL-299 cells were transduced with a retrovirus encoding FLAG-, CFP-tagged PML-III. Protein was then isolated from uninfected cells or those infected with HSV-1 for 5 h in the presence of the proteasome inhibitor MG132. Sites of phosphorylation were identified by tandem mass spectrometry.

## Table 4.2: Properties of PML-I and PML-I mutants

| | Sp100 recruitment | | Daxx recruitment | | SUMOylation | ICP0 colocalization | | Resistance to ICP0-induced degradation | Recruitment to incoming genomes | Restriction of ICP0-null plating |
|---|---|---|---|---|---|---|---|---|---|---|
| | A549 | HepaRG | A549 | HepaRG | | A549 | HepaRG | | | |
| endogenous PML | ++ | +++ | ND | ++ | ND | +++ | +++ | ND | +++ | +++ |
| PML-I | + | ++ | - | - | ++ | +++ | +++ | - | +++ | - |
| K65/160/490R | ++ | - | + | - | - | +++ | +++ | - | +++ | ND |
| S8;T28;S36/38/40A | ++ | ++ | + | + | ++ | +++ | + | - | +++ | ND |
| S8;T28;S36/38/40E | ++ | ND | + | ND | ++ | +++ | ND | - | +++ | ND |
| S117A | ++ | ++ | + | - | ++ | +++ | +++ | - | +++ | + |
| S117E | +++ | ND | ++ | ND | ++ | +++ | ND | - | +++ | ND |
| S480;T482;S493A | ++ | ++ | - | - | ++ | +++ | +++ | - | +++ | ++ |
| S480;T482;S493E | ++ | ND | + | ND | ++ | +++ | ND | + | +++ | ND |
| S504/505A | ++ | ++ | + | + | ++ | +++ | +++ | + | +++ | ND |
| S504/505E | ++ | ND | - | ND | ++ | +++ | ND | + | +++ | ND |
| S518A | ++ | ++ | - | + | +++ | +++ | +++ | - | +++ | ND |
| S518E | ++ | ND | + | ND | ++ | +++ | ND | + | +++ | ND |
| S527/530A | + | ++ | - | ++ | ++ | +++ | +++ | - | +++ | ND |
| S527/530E | + | ND | - | ND | ++ | +++ | ND | - | +++ | ND |
| S560/561/562/565A | ++ | +++ | ++ | +++ | + | +++ | +++ | - | - | - |
| S560/561/562/565E | ++ | ND | ++ | ND | ++ | +++ | ND | - | - | ND |
| S565A | ND | +++ | ND | +++ | + | +++ | +++ | - | +++ | ND |
| S565E | ++ | ND | ++ | ND | ++ | +++ | ND | - | +++ | ND |
| V556/557/558A;I559S | +++ | +++ | +++ | +++ | + | +++ | +++ | ND | - | ND |
| Δ476-490 | - | | + | | - | +++ | ++ | ++ | - | ND |

PML-I and the PML-I mutants were scored for their relative ability to recruit Sp100 or Daxx, their levels of SUMOylation, their ability to colocalize with ICP0, their resistance to ICP0-mediated degradation, their recruitment to incoming viral genomes, and ability to suppress viral plaque formation as detailed in Figures 4.1-4.9. ND, not determined; -, unable; +, weak; ++, moderate; -+++, strong

## 4.6 Figures

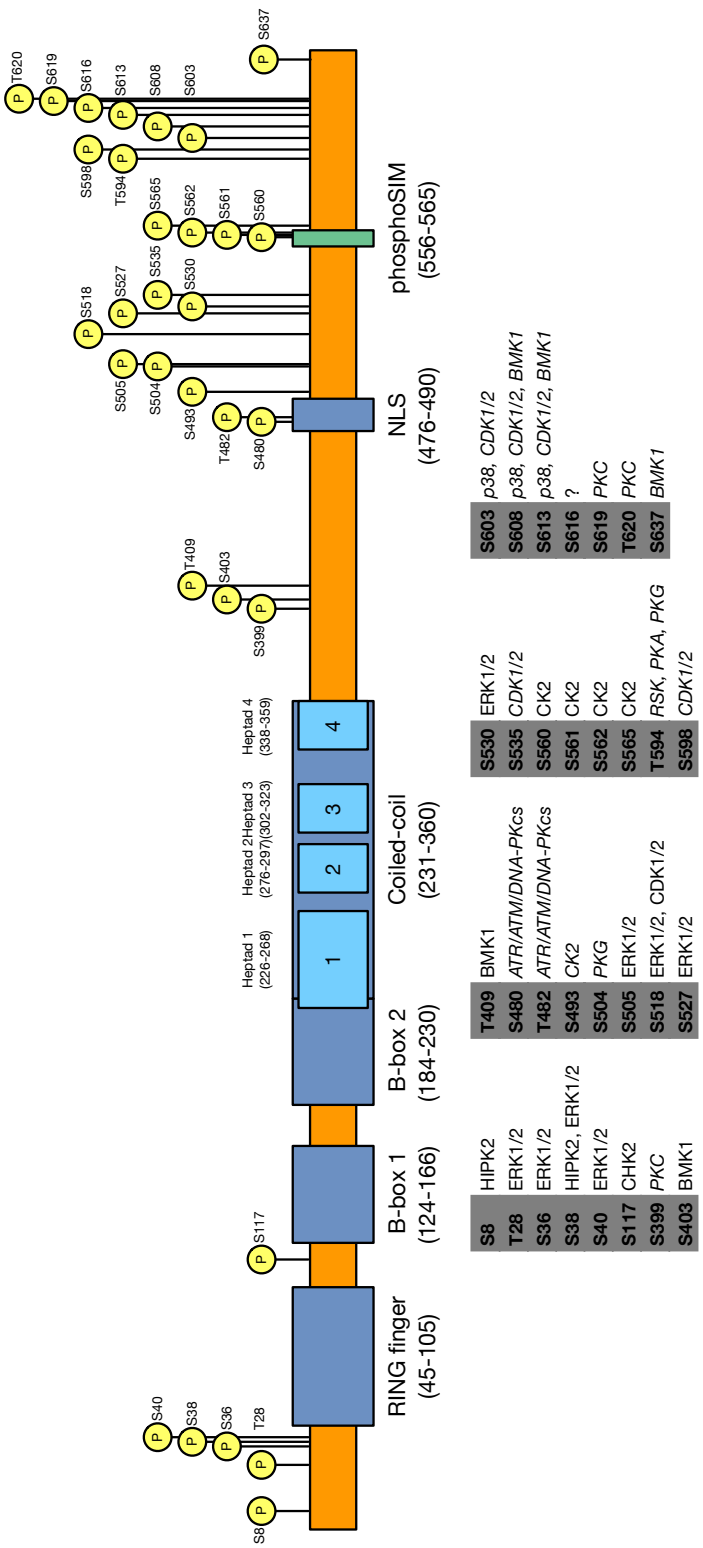
RING finger (45-105)
B-box 1 (124-166)
B-box 2 (184-230)
Coiled-coil (231-360)
Heptad 1 (226-268)
Heptad 2 (276-297)
Heptad 3 (302-323)
Heptad 4 (338-359)
NLS (476-490)
phosphoSIM (556-565)
S8 HIPK2
T28 ERK1/2
S36 ERK1/2
S38 HIPK2, ERK1/2
S40 ERK1/2
S117 CHK2
S399 PKC
S403 BMK1
T409 BMK1
S480 ATR/ATM/DNA-PKcs
T482 ATR/ATM/DNA-PKcs
S493 CK2
S504 PKG
S505 ERK1/2
S518 ERK1/2, CDK1/2
S527 ERK1/2
S530 ERK1/2
S535 CDK1/2
S560 CK2
S561 CK2
S562 CK2
S565 CK2
T594 RSK, PKA, PKG
S598 CDK1/2
S603 p38, CDK1/2
S608 p38, CDK1/2, BMK1
S613 p38, CDK1/2, BMK1
S616 ?
S619 PKC
T620 PKC
S637 BMK1

**Figure 4.1. Map of known and novel sites of PML-III phosphorylation and the kinases that target these residues.**

Sites of phosphorylation from published studies and Table 4.1. Table below lists kinases that phosphorylate or are predicted by either NetPhos 2.0 [316] or PROSITE [317,318] (in italics) to phosphorylate the indicated residues.

## 4.2A

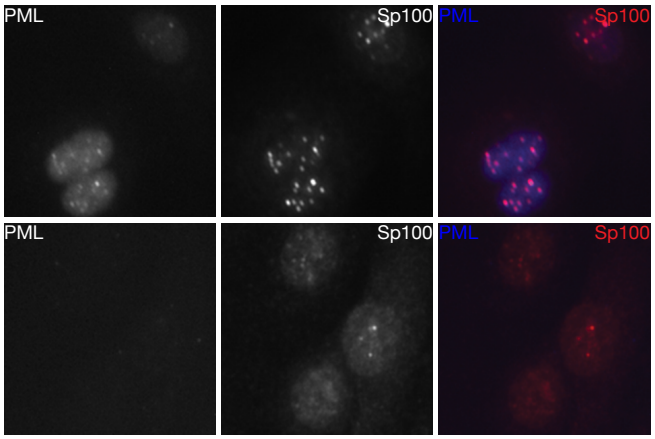


## 4.2B part 1

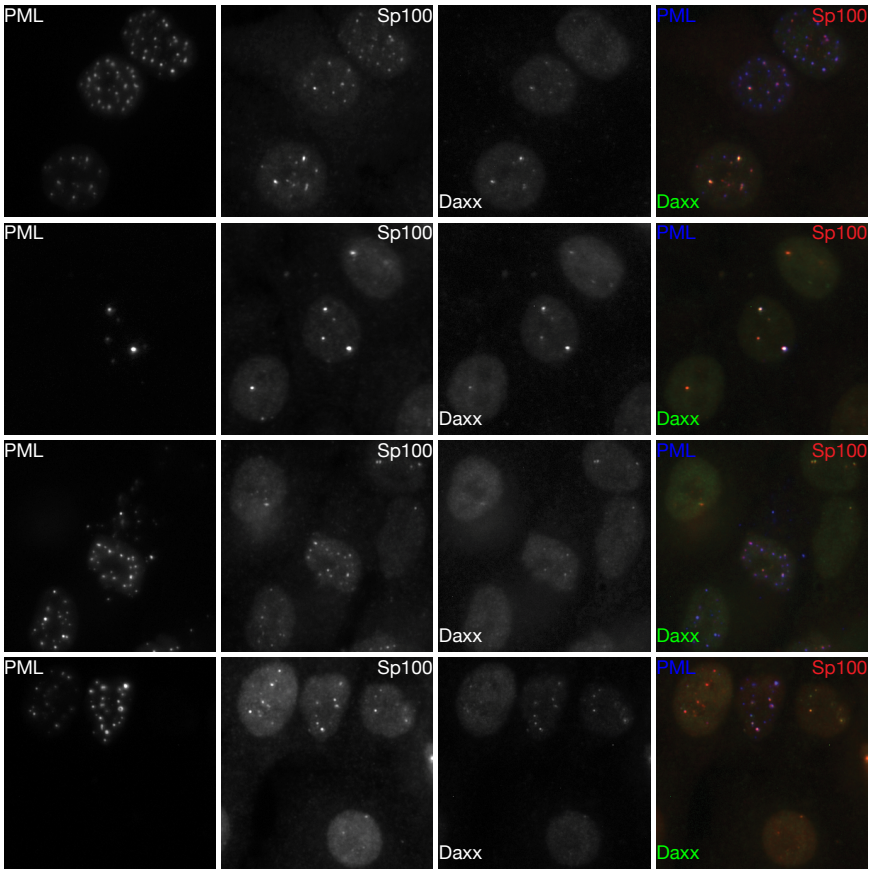

**4.2B part 2**

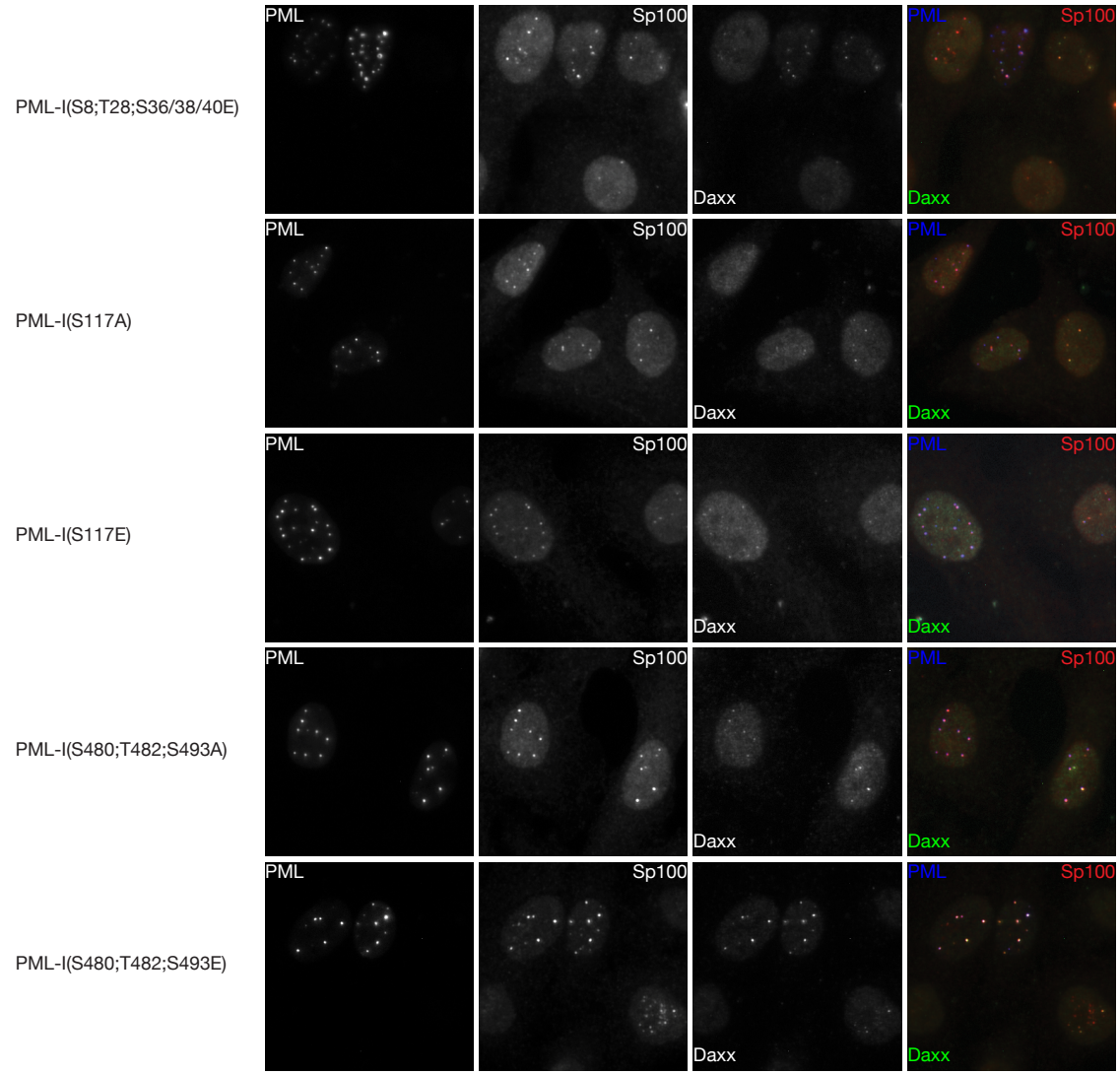
PML-I(S8;T28;S36/38/40E)
PML-I(S117A)
PML-I(S117E)
PML-I(S480;T482;S493A)
PML-I(S480;T482;S493E)
PML
Sp100
Daxx
PML
Sp100
Daxx

**4.2B part 3**

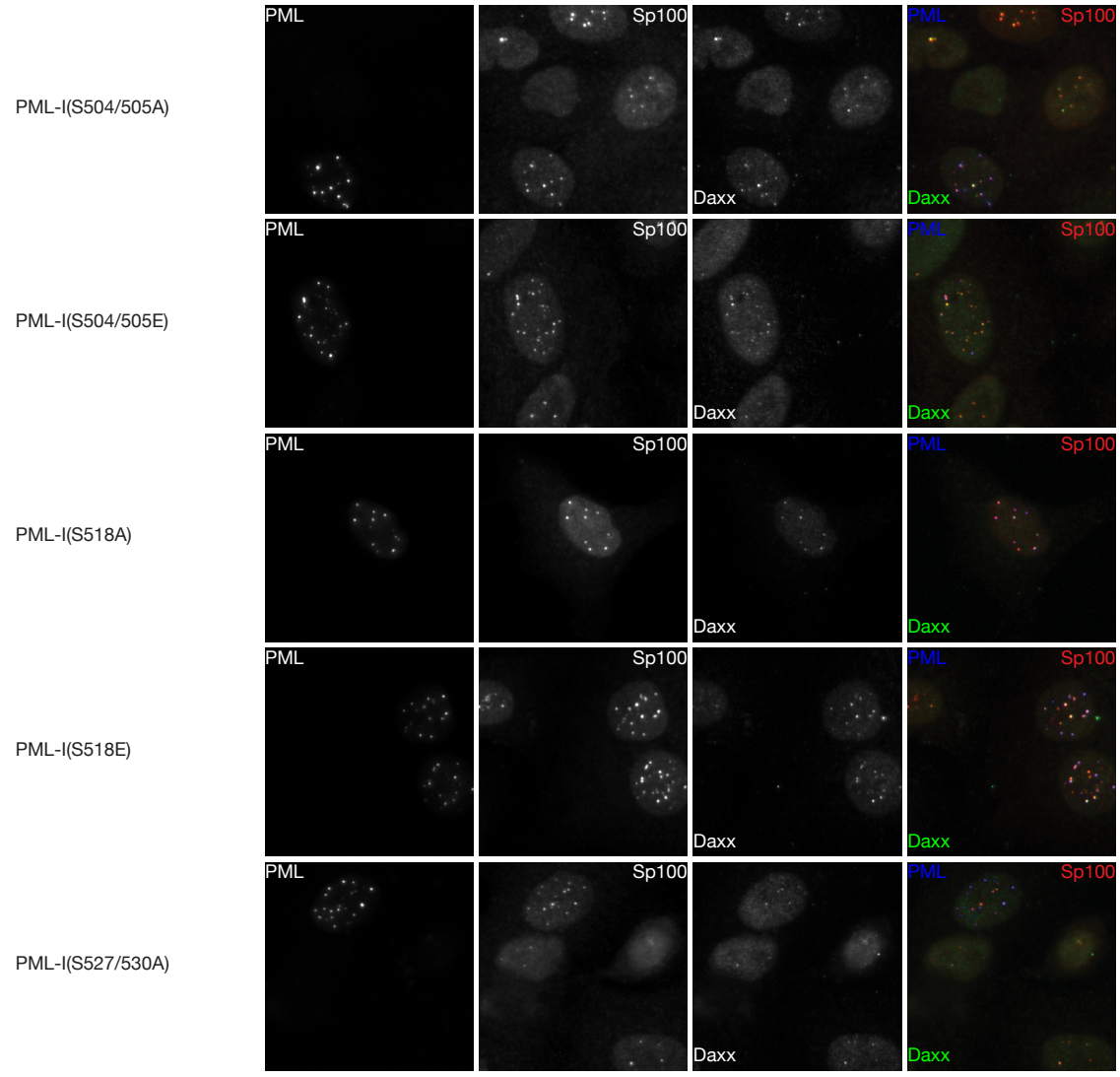
PML
Sp100
Daxx
PML
Sp100
Daxx
PML-I(S504/505A)
PML-I(S504/505E)
PML-I(S518A)
PML-I(S518E)
PML-I(S527/530A)

**4.2B part 4**

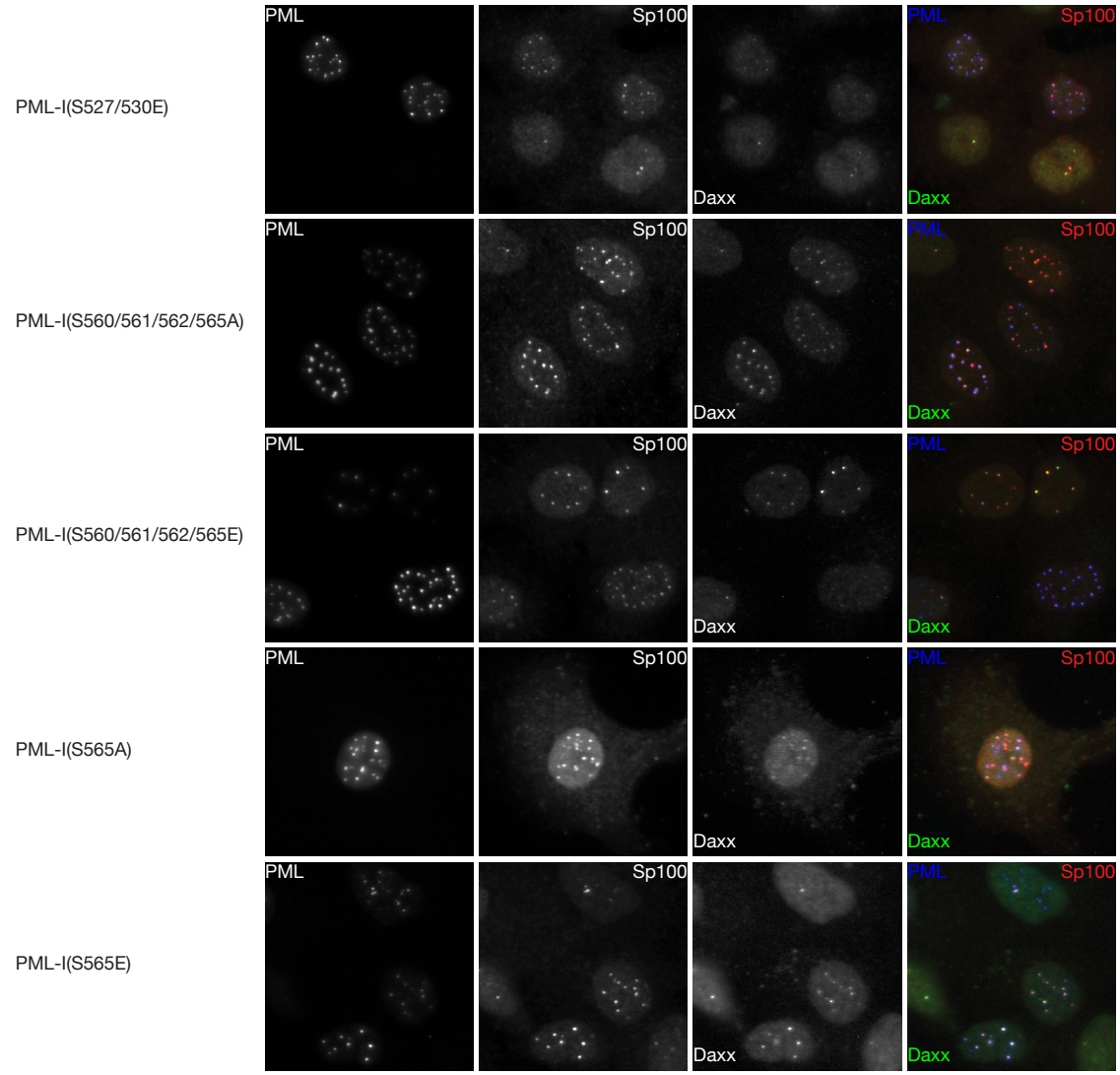
PML-I(S527/530E)
PML-I(S560/561/562/565A)
PML-I(S560/561/562/565E)
PML-I(S565A)
PML-I(S565E)
PML
Sp100
Daxx

**4.2B part 5**

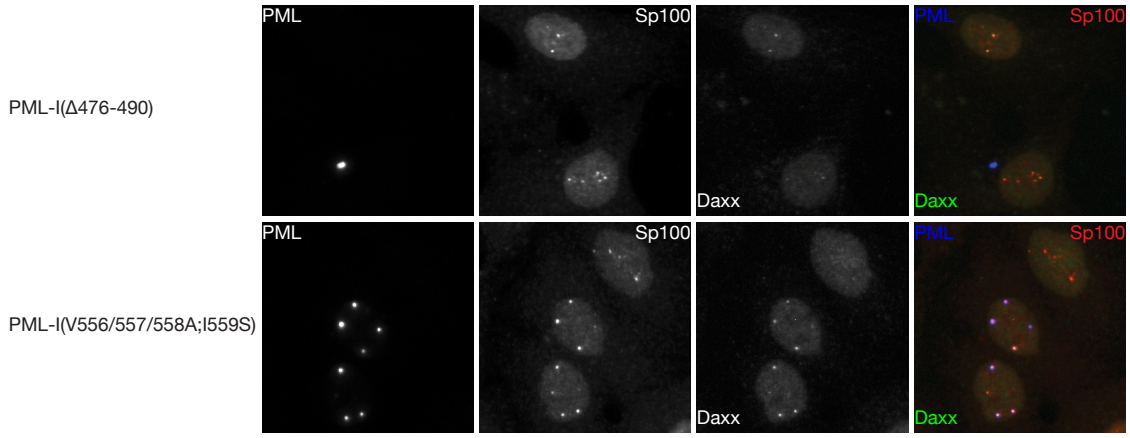


**Figure 4.2. Recruitment of Sp100 and Daxx to PML-I and PML-I phosphorylation mutants in PML-depleted A594 cells.**

(A) A549 or A549 cells that express an shRNA that targets PML (A549-shPML) and antibody stained to detect PML and Sp100 by immunofluorescence.

(B) A549-shPMLs were transduced with FLAG-, CFP-tagged PML-I, or a SUMOylation-deficient, NLS-inactivated, SIM-inactivated, or phosphorylation mutant form of PML-I. Sp100 and Daxx were detected by immunofluorescence, and exogenous PML was detected by autofluorescence.

A

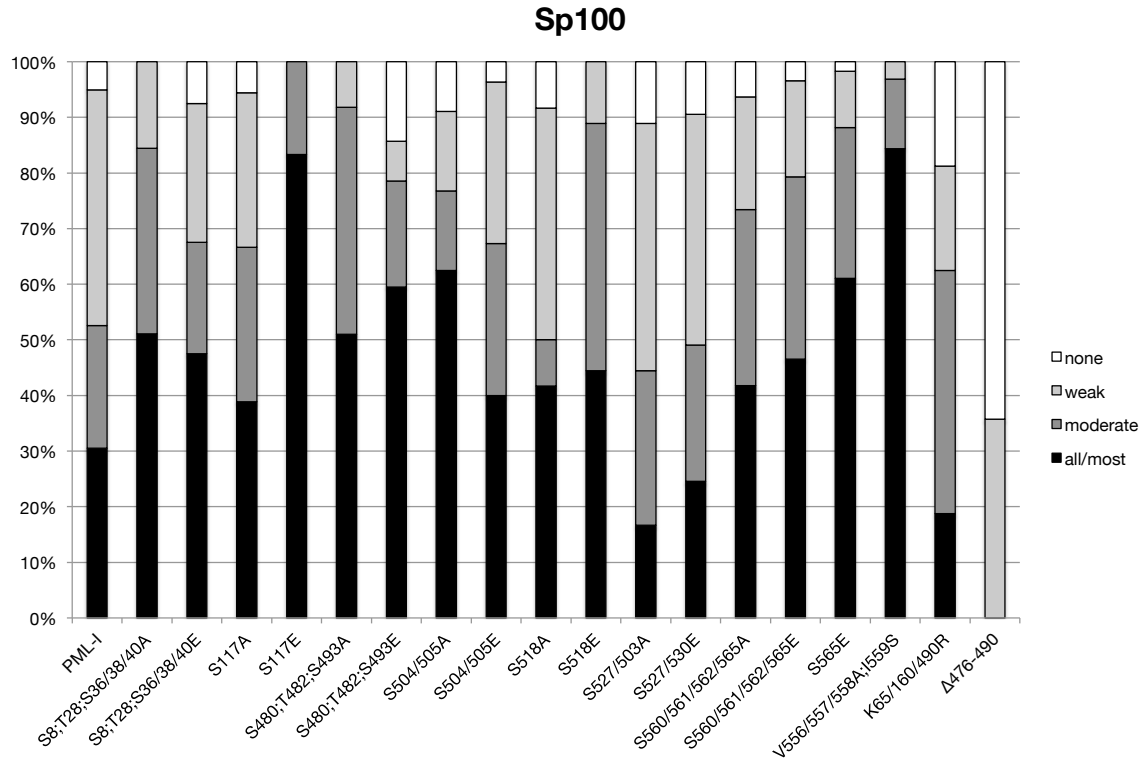
Sp100
100%
90%
80%
70%
60%
50%
40%
30%
20%
10%
0%
none
weak
moderate
all/most
PML-I
S8;T28;S36/38/40A
S8;T28;S36/38/40E
S117A
S117E
S480;T482;S493A
S480;T482;S493E
S504/505A
S504/505E
S518A
S518E
S527/503A
S527/530E
S560/561/562/565A
S560/561/562/565E
S565E
V556/557/558A;I559S
K65/160/490R
Δ476-490

B

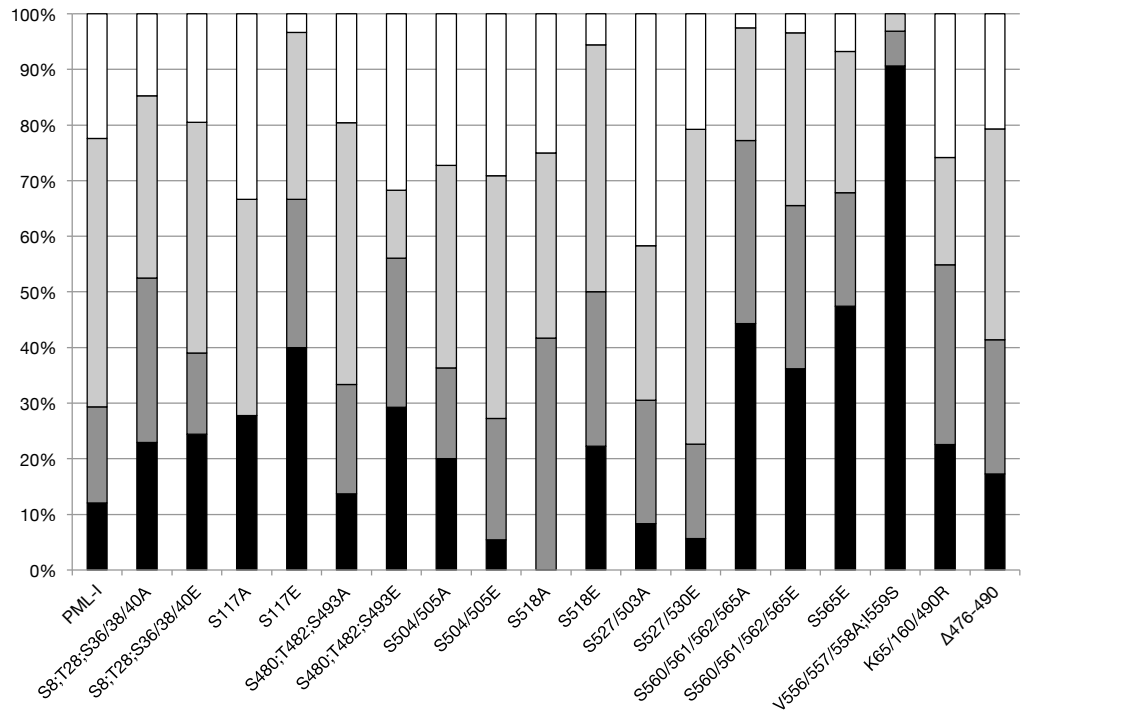
Daxx
100%
90%
80%
70%
60%
50%
40%
30%
20%
10%
0%
PML-I
S8;T28;S36/38/40A
S8;T28;S36/38/40E
S117A
S117E
S480;T482;S493A
S480;T482;S493E
S504/505A
S504/505E
S518A
S518E
S527/503A
S527/530E
S560/561/562/565A
S560/561/562/565E
S565E
V556/557/558A;I559S
K65/160/490R
Δ476-490

**Figure 4.3. Quantification of Sp100 and Daxx recruitment to PML in PML-depleted A549 cells that express wild type and mutant forms of PML-I.**

A549-shPML cells transduced with CFP-tagged PML-I or each PML-I mutant were scored on a four-point scale based on how well they recruited Sp100 (A) or Daxx (B), with either none (none), less than 50% (weak), between 50-90% (moderate), or >90% (all/most) of the protein being localized at ND10s, as judged using fluorescence microscopy.

**4.4A**

HA-shNeg

HA-shPML

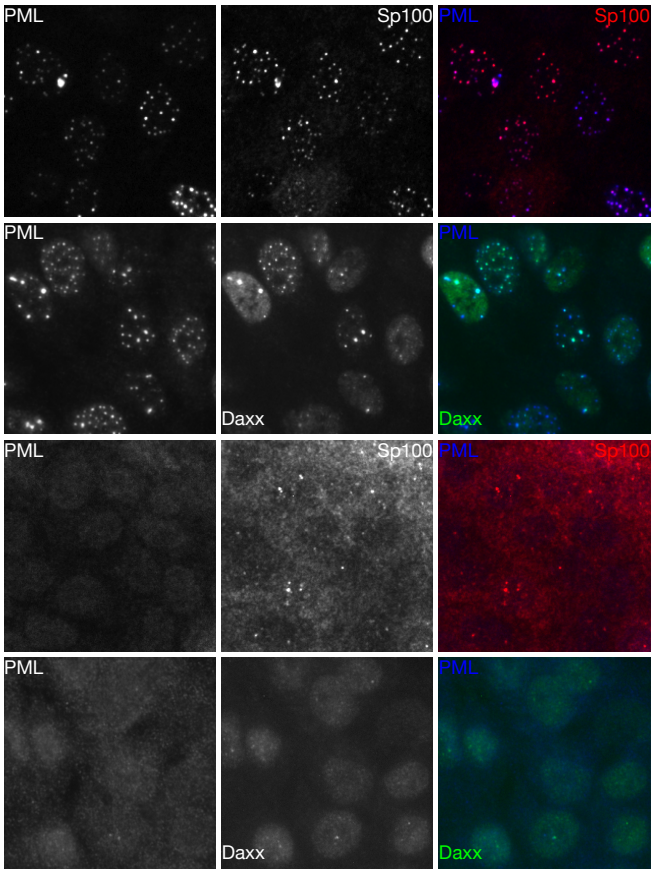


**4.4B part 1**

PML-I

PML-I(K65/160/490R)

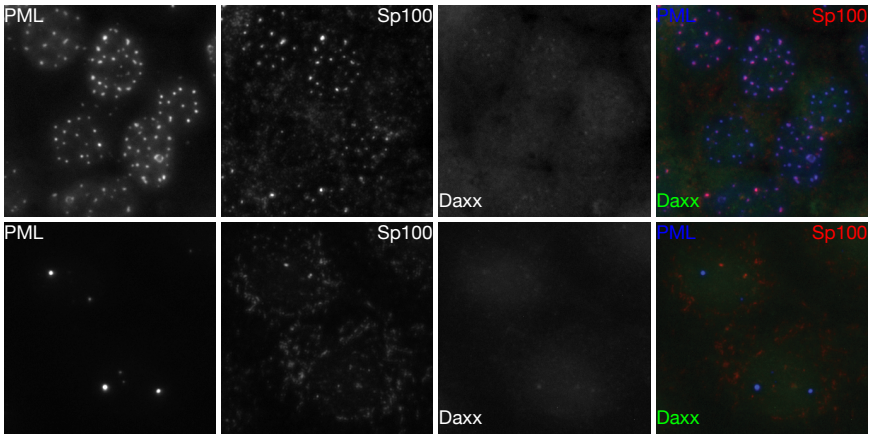

**4.4B part 2**

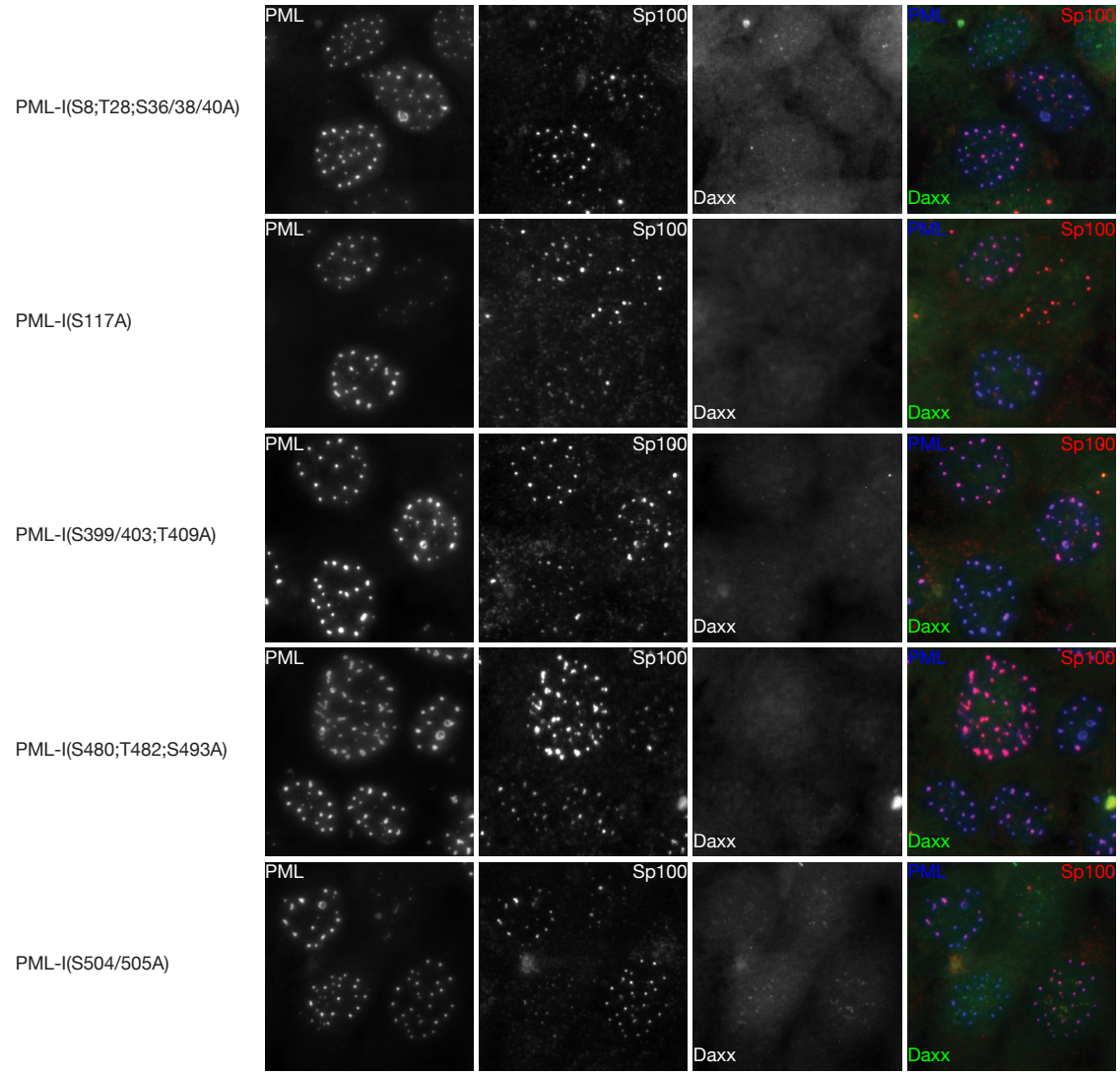
PML-I(S8;T28;S36/38/40A)
PML-I(S117A)
PML-I(S399/403;T409A)
PML-I(S480;T482;S493A)
PML-I(S504/505A)
PML
Sp100
Daxx

**4.4B part 3**

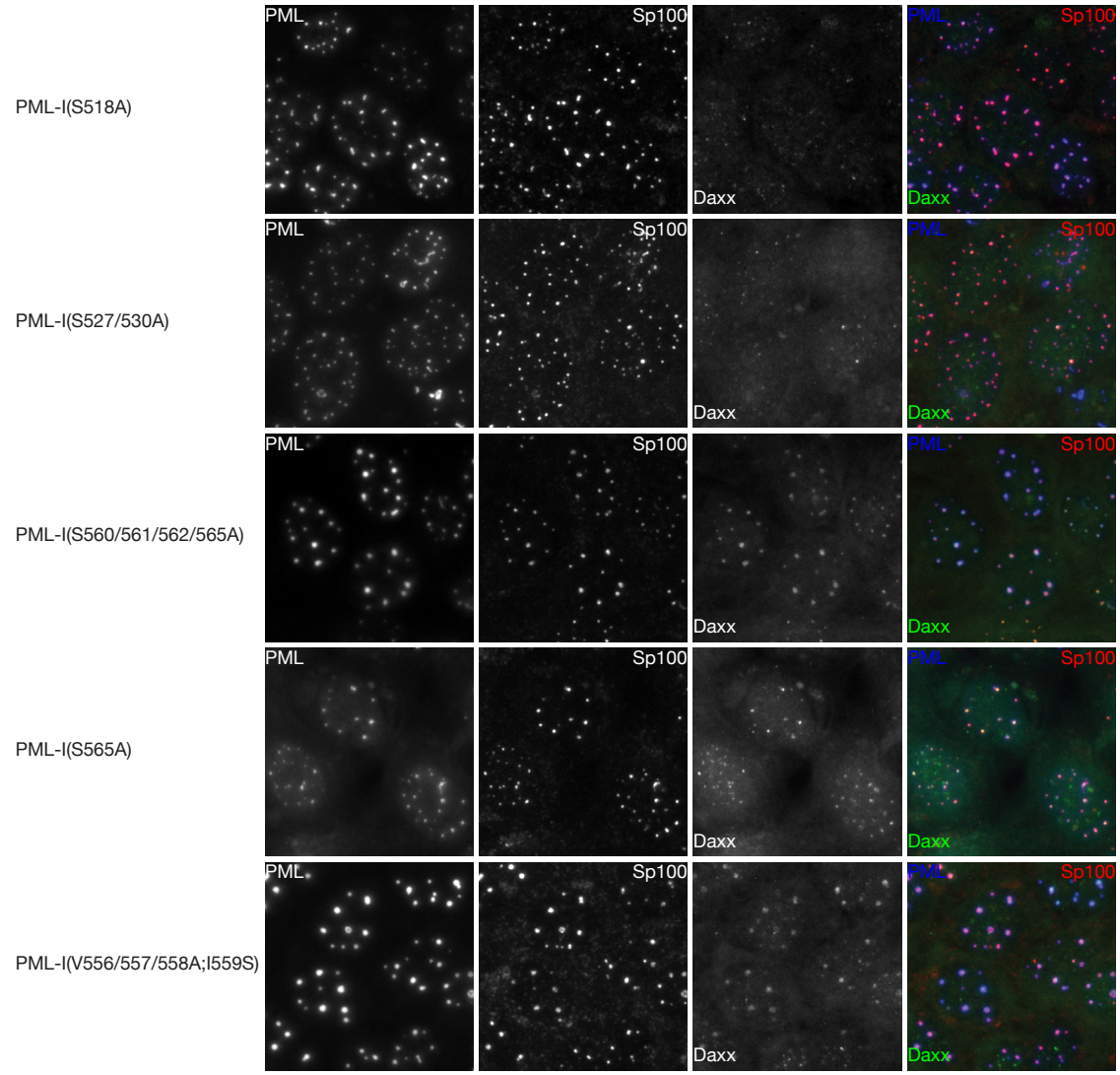


**Figure 4.4. Recruitment of Sp100 and Daxx to PML-I and PML-I mutants in PML-depleted HepaRG cells.**

(A) HepaRG cells that either express a control shRNA (HA-shNeg) or an shRNA that targets PML (HA-shPML) and stained with antibodies to detect PML and Sp100 or Daxx by immunofluorescence.

(B) HA-shPMLs were transduced with FLAG-, CFP-tagged PML-I, or a SUMOylation-deficient, NLS-inactivated, SIM-inactivated, or phosphorylation mutant form of PML-I. Sp100, Daxx, and PML were detected as in Figure 4.2.

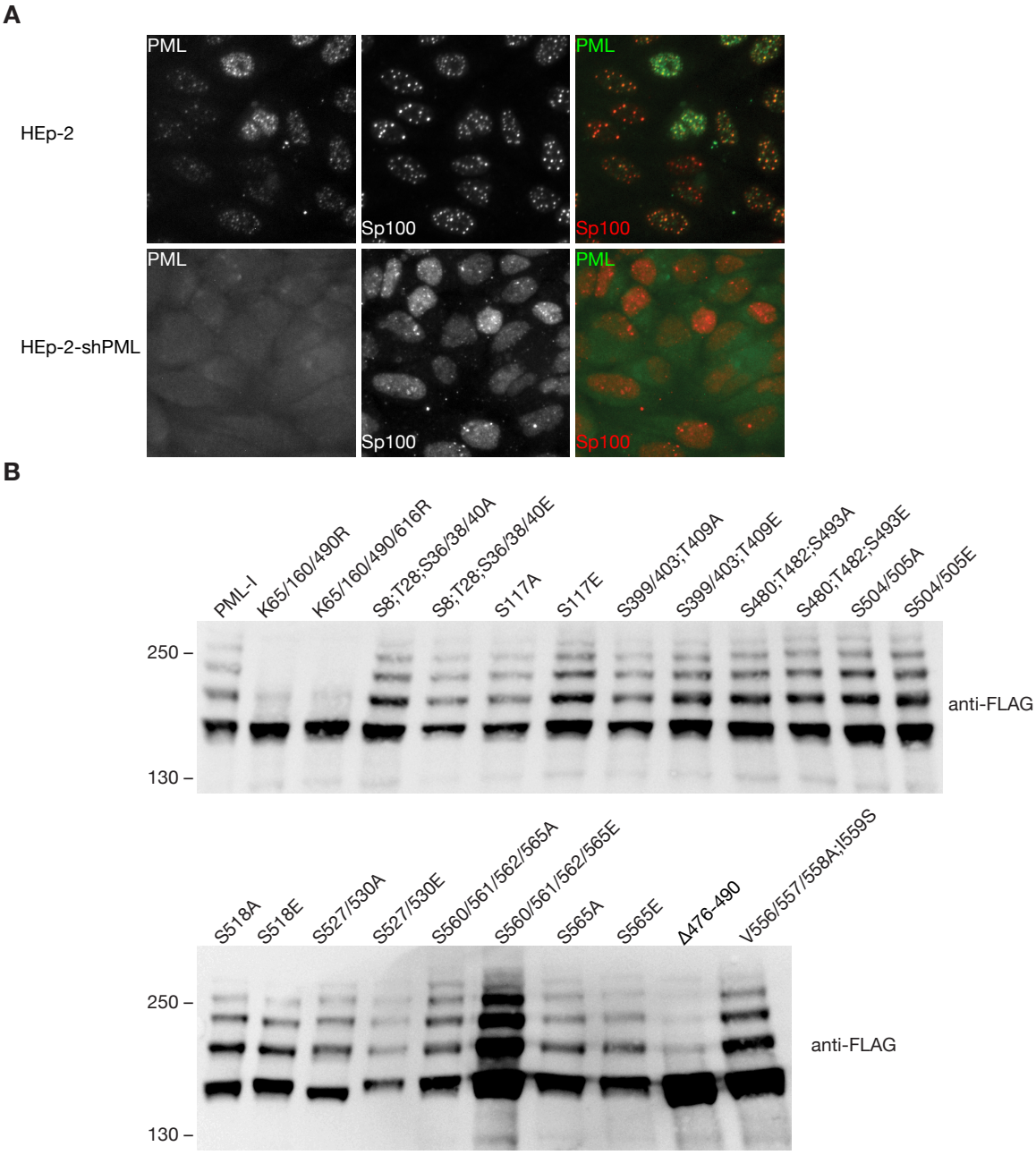


**Figure 4.5. SUMOylation of PML-I or PML-I mutants in PML-depleted cells.**

(A) HEp-2 cells and HEp-2 cells depleted of PML and antibody stained to detect PML and Sp100 by immunofluorescence.

(B) HEp-2-shPML cells were transfected with 900 ng of pGEM-3 (as carrier DNA) and 100 ng of a plasmid encoding FLAG-, CFP-tagged PML-I or a

mutant of PML-I. The next day, the lysates of the cells were prepared, resolved by SDS-PAGE, and analyzed by western blot with an anti-FLAG antibody.

## 4.6 part 1

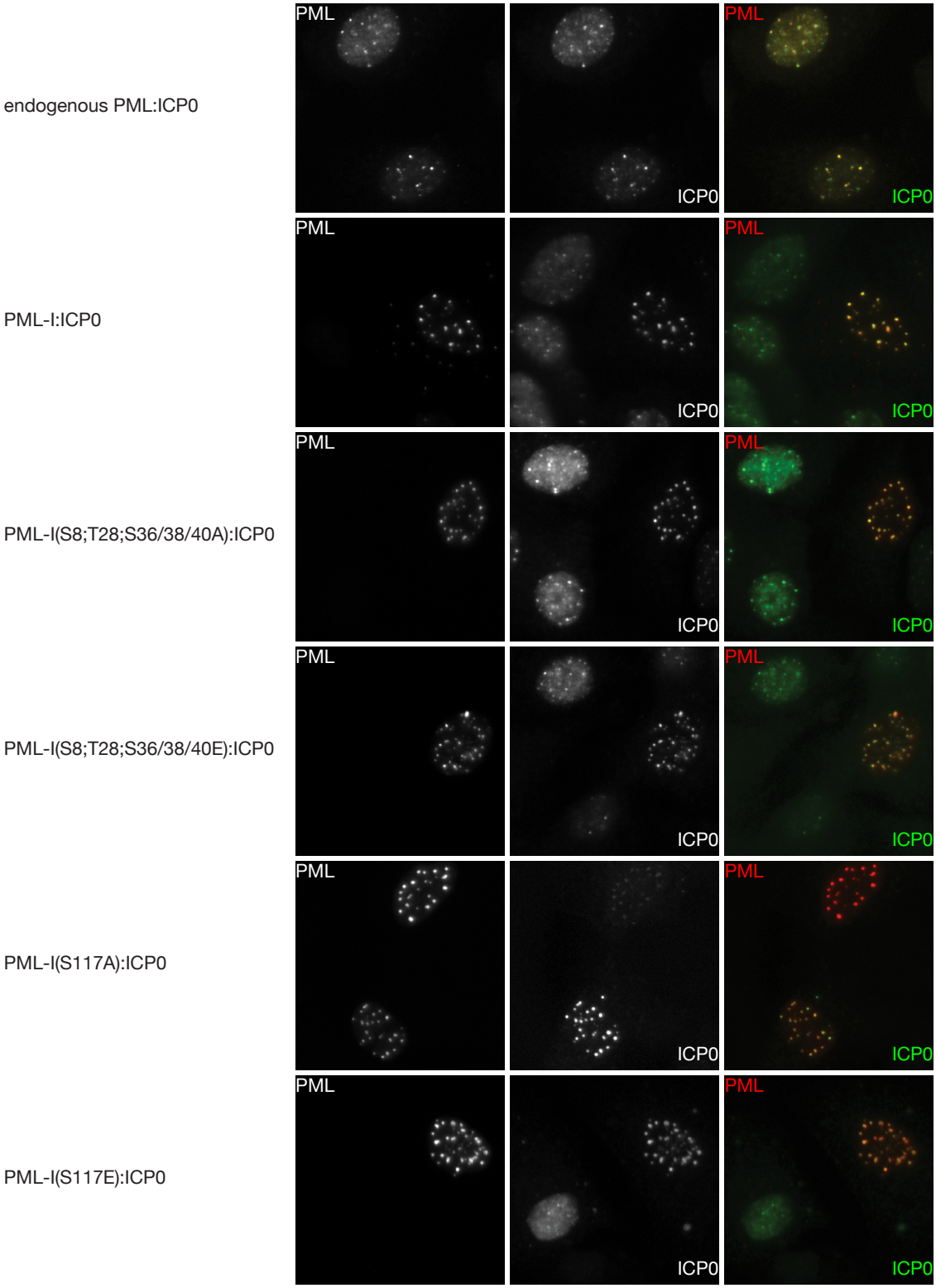
endogenous PML:ICP0
PML-I:ICP0
PML-I(S8;T28;S36/38/40A):ICP0
PML-I(S8;T28;S36/38/40E):ICP0
PML-I(S117A):ICP0
PML-I(S117E):ICP0
PML
ICP0

## 4.6 part 2

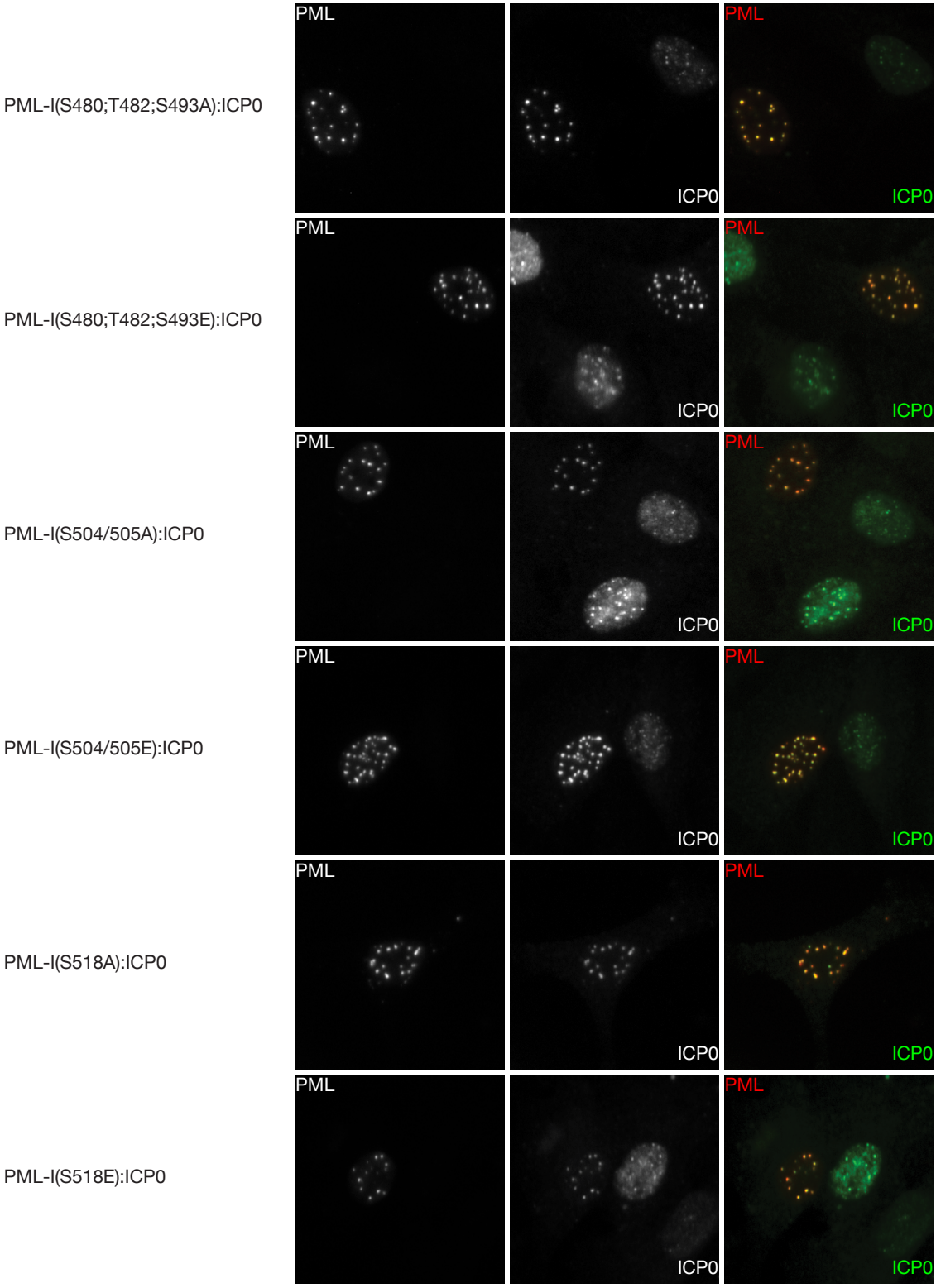
PML-I(S480;T482;S493A):ICP0
PML-I(S480;T482;S493E):ICP0
PML-I(S504/505A):ICP0
PML-I(S504/505E):ICP0
PML-I(S518A):ICP0
PML-I(S518E):ICP0
PML
ICP0

## 4.6 part 3

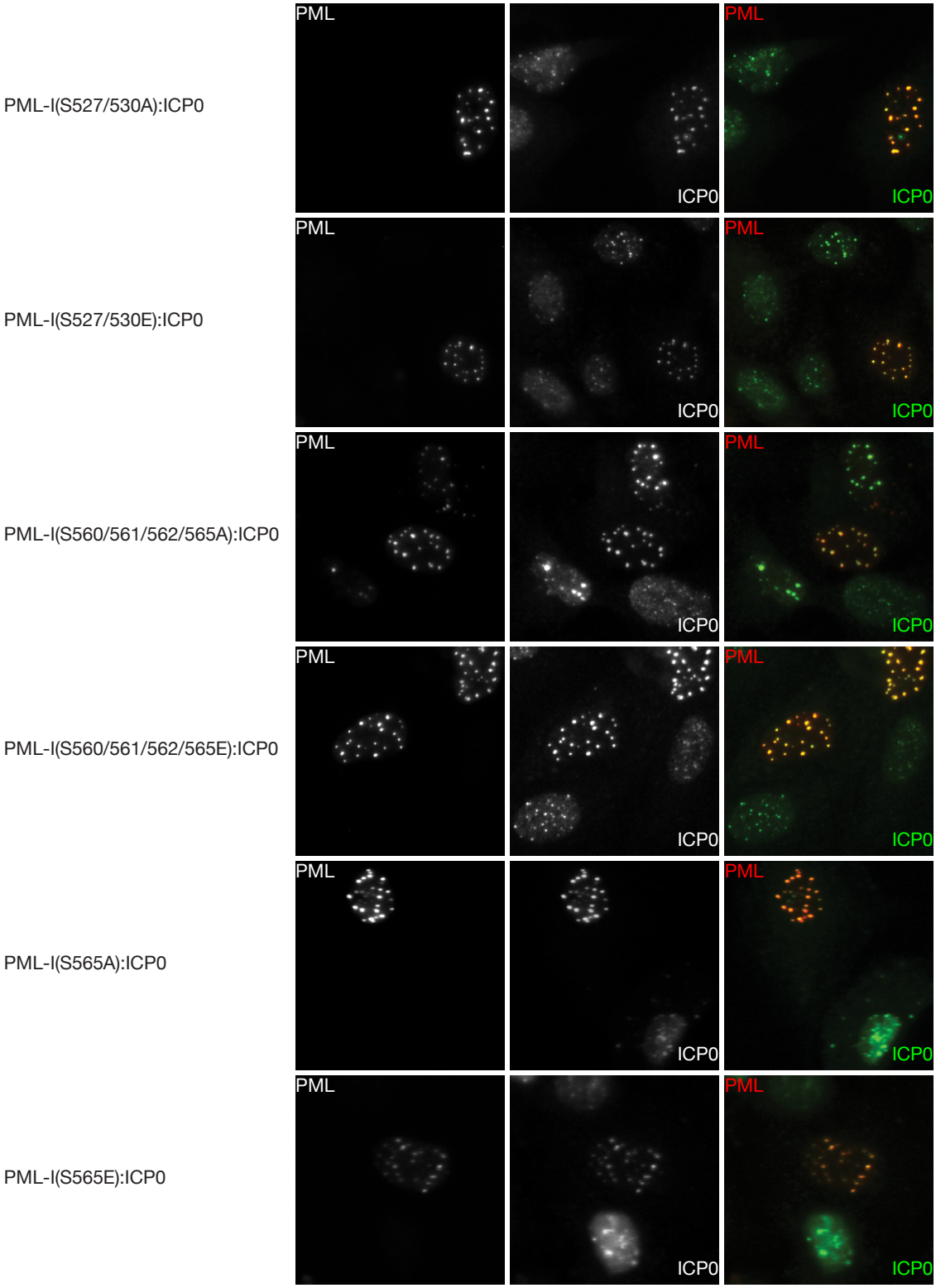
PML-I(S527/530A):ICP0
PML-I(S527/530E):ICP0
PML-I(S560/561/562/565A):ICP0
PML-I(S560/561/562/565E):ICP0
PML-I(S565A):ICP0
PML-I(S565E):ICP0
PML
ICP0

**4.6 part 4**

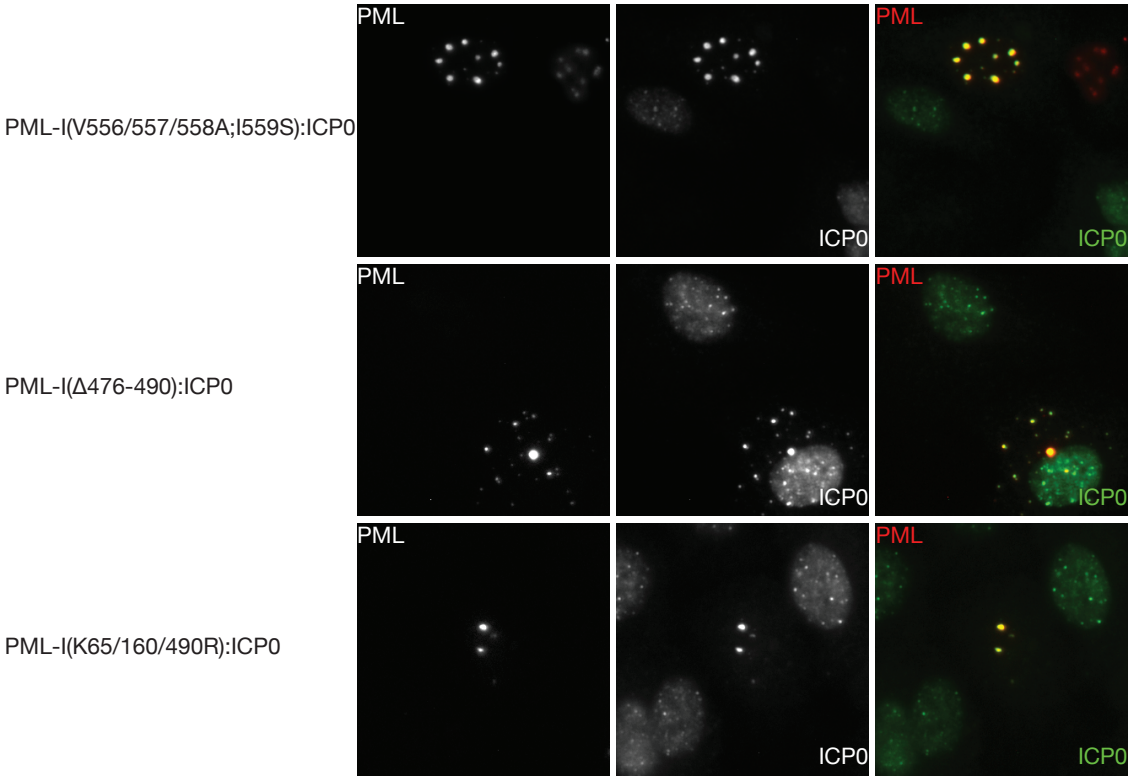


**Figure 4.6. Colocalization between PML-I or PML-I mutants and ICP0 in A549-shPML cells.**

A549-shPML cells transduced with FLAG-, CFP-tagged PML-I or each PML-I mutant were infected with HSV-1 at 2 PFU/cell. At 2 hpi, the cells were fixed and stained with antibodies against ICP0. PML is shown as red and ICP0 as green in the merged image.

**4.7 part 1**

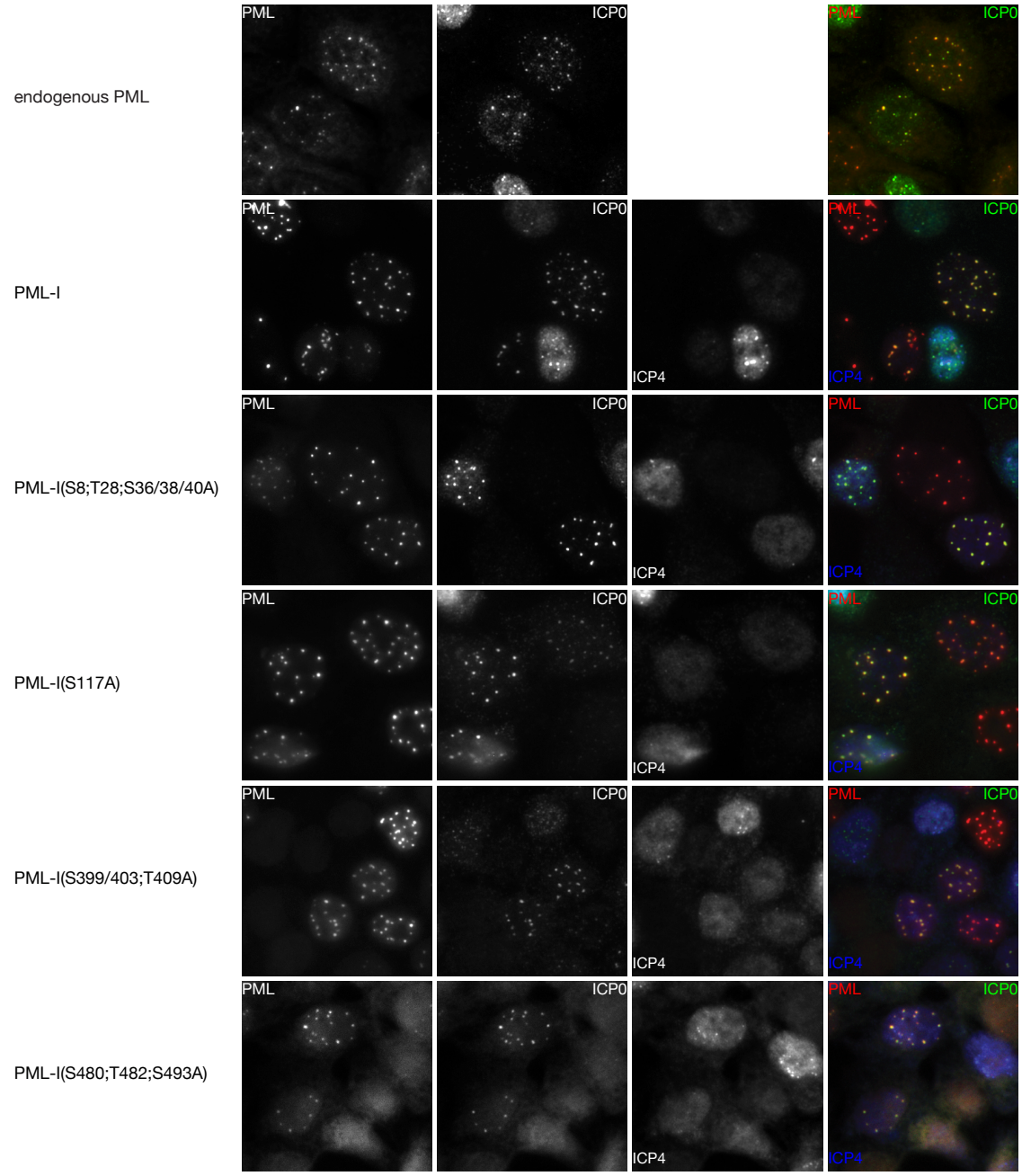
endogenous PML
PML-I
PML-I(S8;T28;S36/38/40A)
PML-I(S117A)
PML-I(S399/403;T409A)
PML-I(S480;T482;S493A)
PML
ICP0
ICP4

**4.7 part 2**

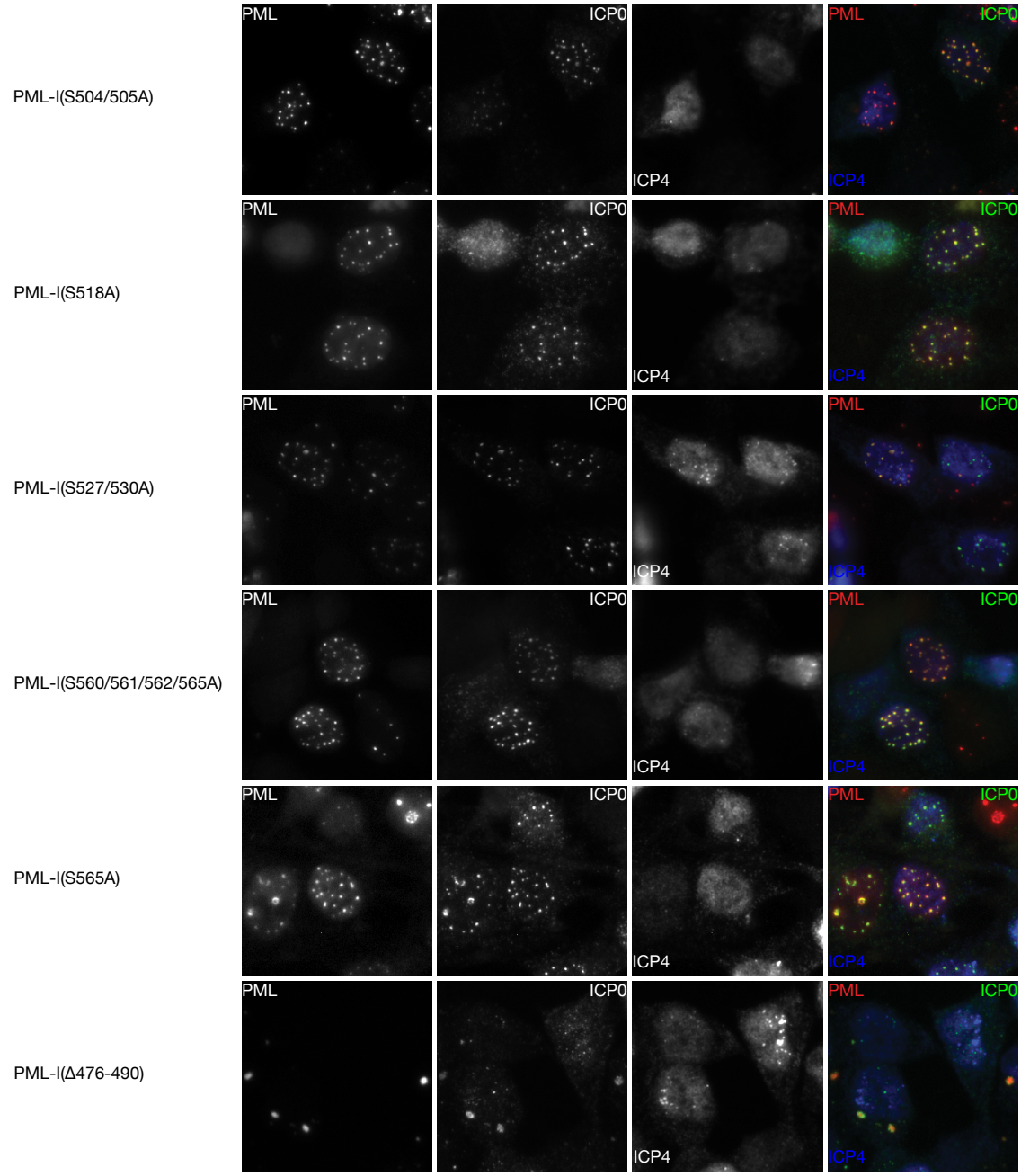
PML-I(S504/505A)
PML-I(S518A)
PML-I(S527/530A)
PML-I(S560/561/562/565A)
PML-I(S565A)
PML-I(Δ476-490)
PML
ICP0
ICP4

**4.7 part 3**

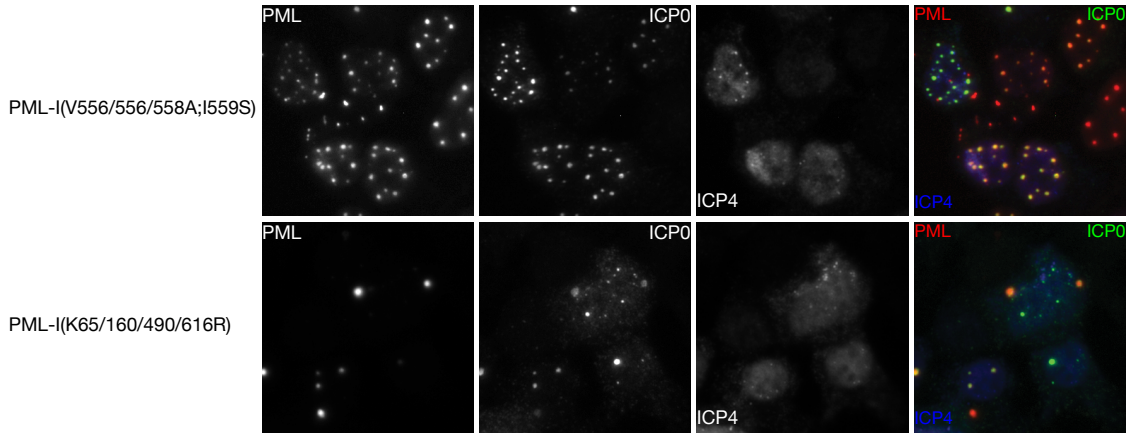


**Figure 4.7. Colocalization between PML-I or PML-I mutants and ICP0 in HA-shPML cells.**

HA-shPML cells transduced with FLAG-, CFP-tagged PML-I or each PML-I mutant were infected with HSV-1 at 2 PFU/cell. At 2 hpi, the cells were fixed and stained with antibodies against ICP0 and ICP4. PML is shown as red, ICP0 as green, and ICP4 as blue in the merged image.

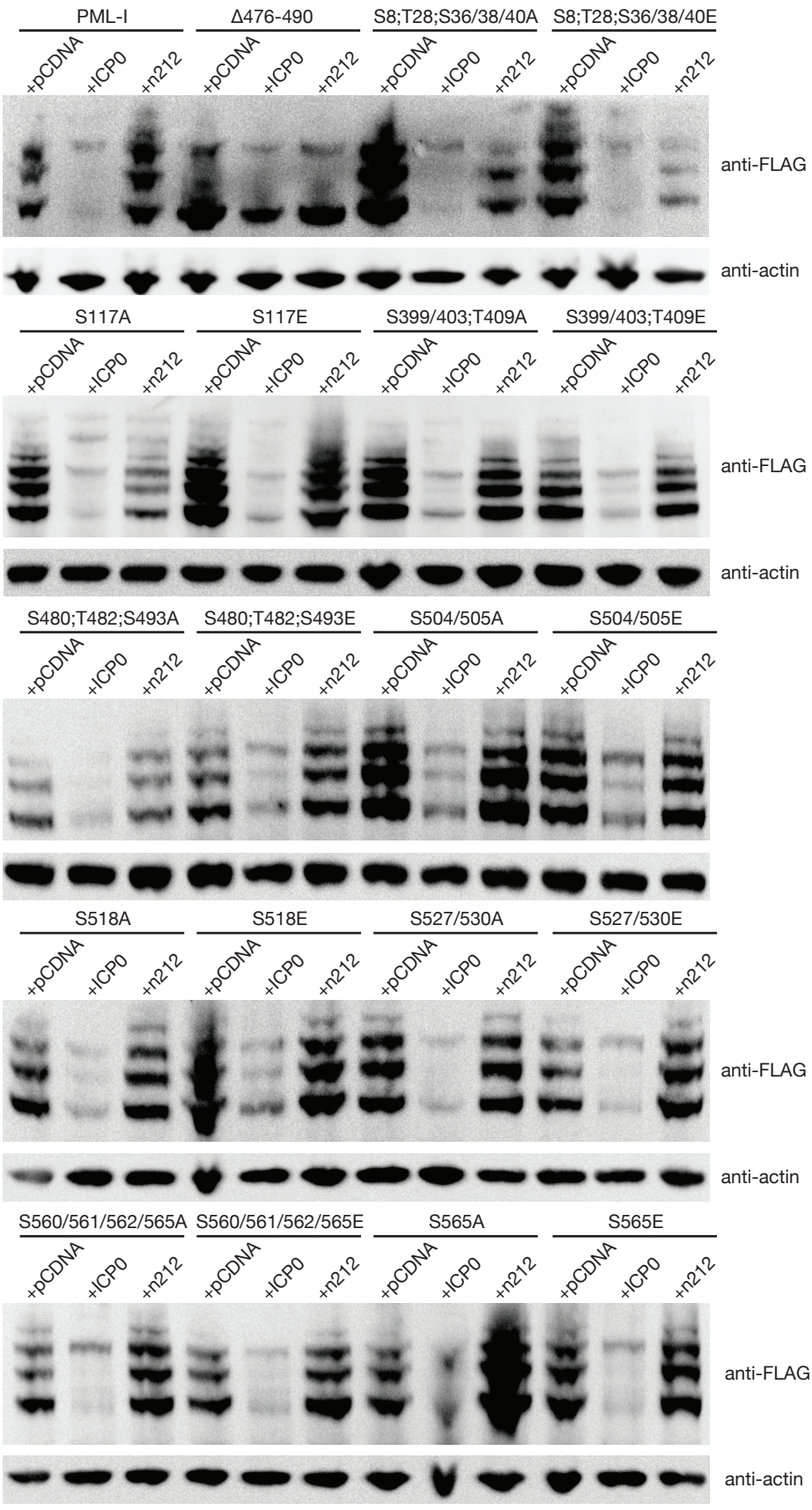
PML-I
Δ476-490
S8;T28;S36/38/40A
S8;T28;S36/38/40E
+pCDNA
+ICP0
+n212
anti-FLAG
anti-actin
S117A
S117E
S399/403;T409A
S399/403;T409E
S480;T482;S493A
S480;T482;S493E
S504/505A
S504/505E
S518A
S518E
S527/530A
S527/530E
S560/561/562/565A
S560/561/562/565E
S565A
S565E

**Figure 4.8. Degradation of PML-I or PML-I mutants by ICP0.**

HEp-2 were transfected with 900 ng of an empty vector (pGEM-3), a vector encoding ICP0, or a vector encoding the ICP0 mutant n212 and 100 ng of a plasmid encoding FLAG-, CFP-tagged PML-I or a PML-I mutant. Twenty-four hs later, cells were lysed, resolved by SDS-PAGE, and analyzed by western blot with an anti-FLAG or anti-β-actin antibody.

**4.9A**

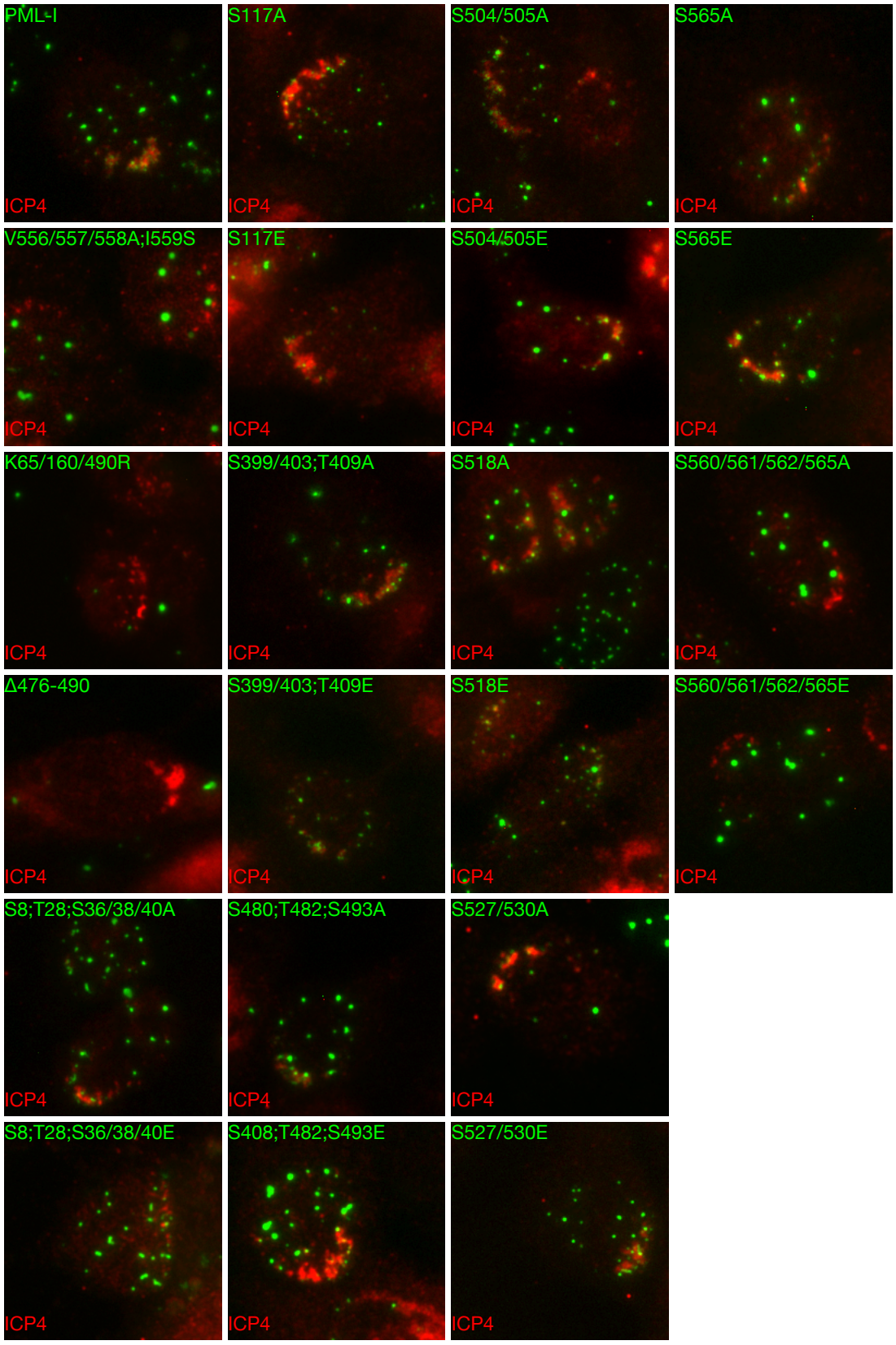
PML-I
ICP4
S117A
ICP4
S504/505A
ICP4
S565A
ICP4
V556/557/558A;I559S
ICP4
S117E
ICP4
S504/505E
ICP4
S565E
ICP4
K65/160/490R
ICP4
S399/403;T409A
ICP4
S518A
ICP4
S560/561/562/565A
ICP4
Δ476-490
ICP4
S399/403;T409E
ICP4
S518E
ICP4
S560/561/562/565E
ICP4
S8;T28;S36/38/40A
ICP4
S480;T482;S493A
ICP4
S527/530A
ICP4
S8;T28;S36/38/40E
ICP4
S408;T482;S493E
ICP4
S527/530E
ICP4

4.9B

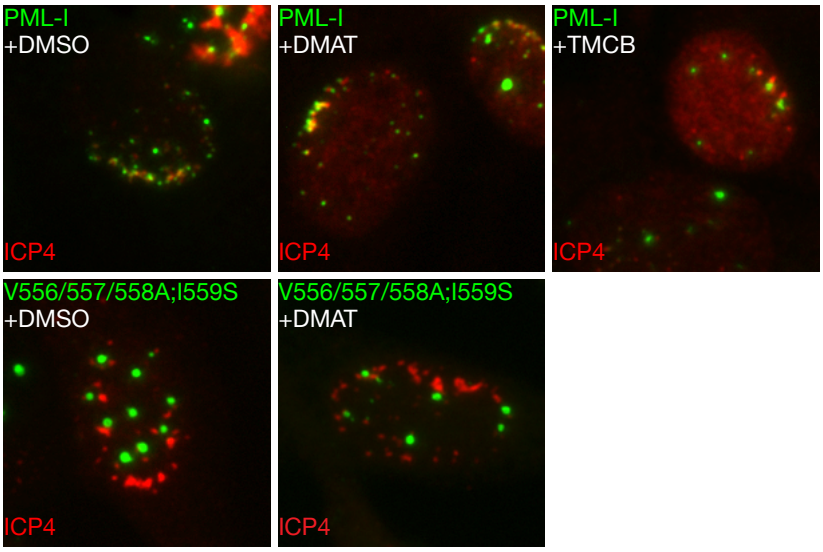


4.9C

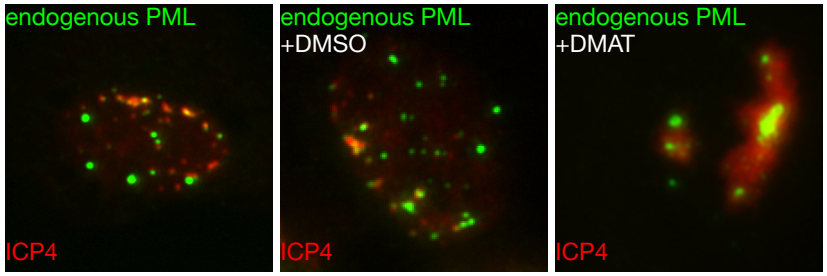


**Figure 4.9. Recruitment of PML-I or PML-I mutants to incoming viral genomes.**

(A) HA-shPML cells transduced with FLAG-, CFP-tagged PML-I or a PML-I mutant were infected with an ICP0-null virus at 0.1 PFU/cell. At 24 hpi, the cells were fixed and stained with antibody against ICP4 as a marker of viral DNA.

(B) Same as in (A), except that 1 h prior to infection, the cells were pretreated with DMSO or one of two CK2 inhibitors, DMAT or TMCB, which were then used throughout infection.

(C) HA-shNeg cells were treated, infected, and stained as described for HA-shPML cells.

**4.10A**

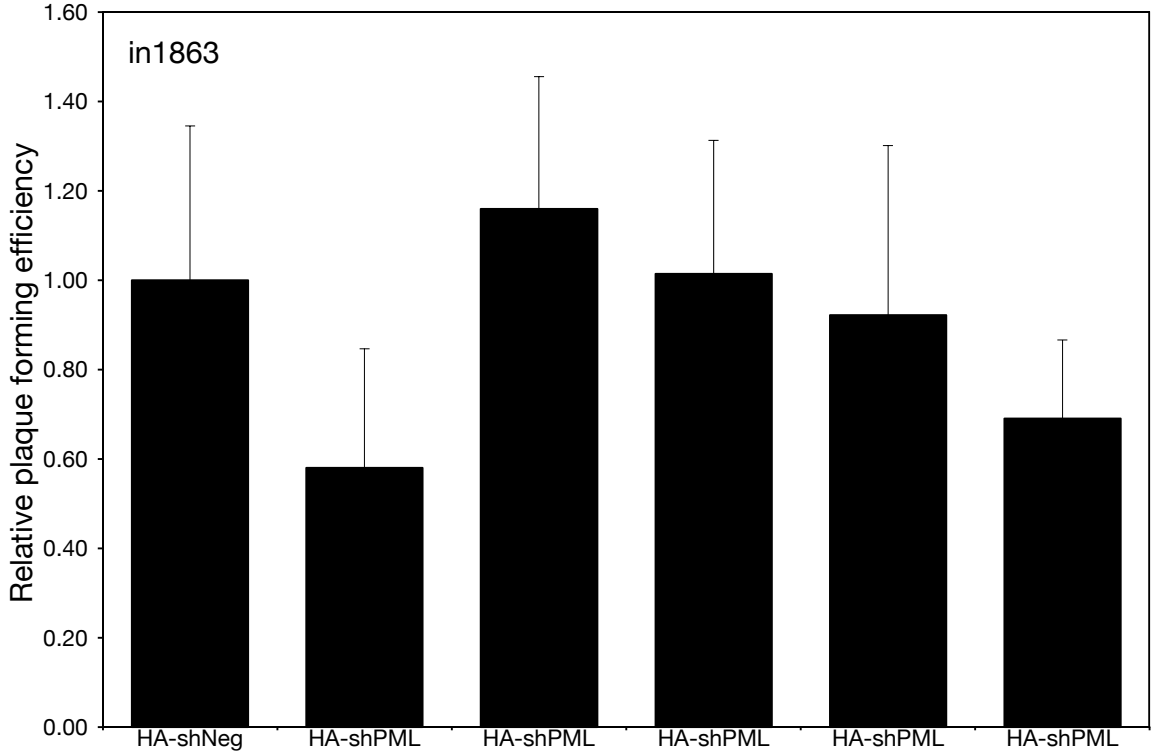
in1863
Relative plaque forming efficiency
1.60
1.40
1.20
1.00
0.80
0.60
0.40
0.20
0.00
HA-shNeg
HA-shPML
HA-shPML +PML.I
HA-shPML +PML.1 (S117A)
HA-shPML +PML.1 (S480;T482;S493A)
HA-shPML +PML.1 (S560/561/ 562/565A)

**4.10B**

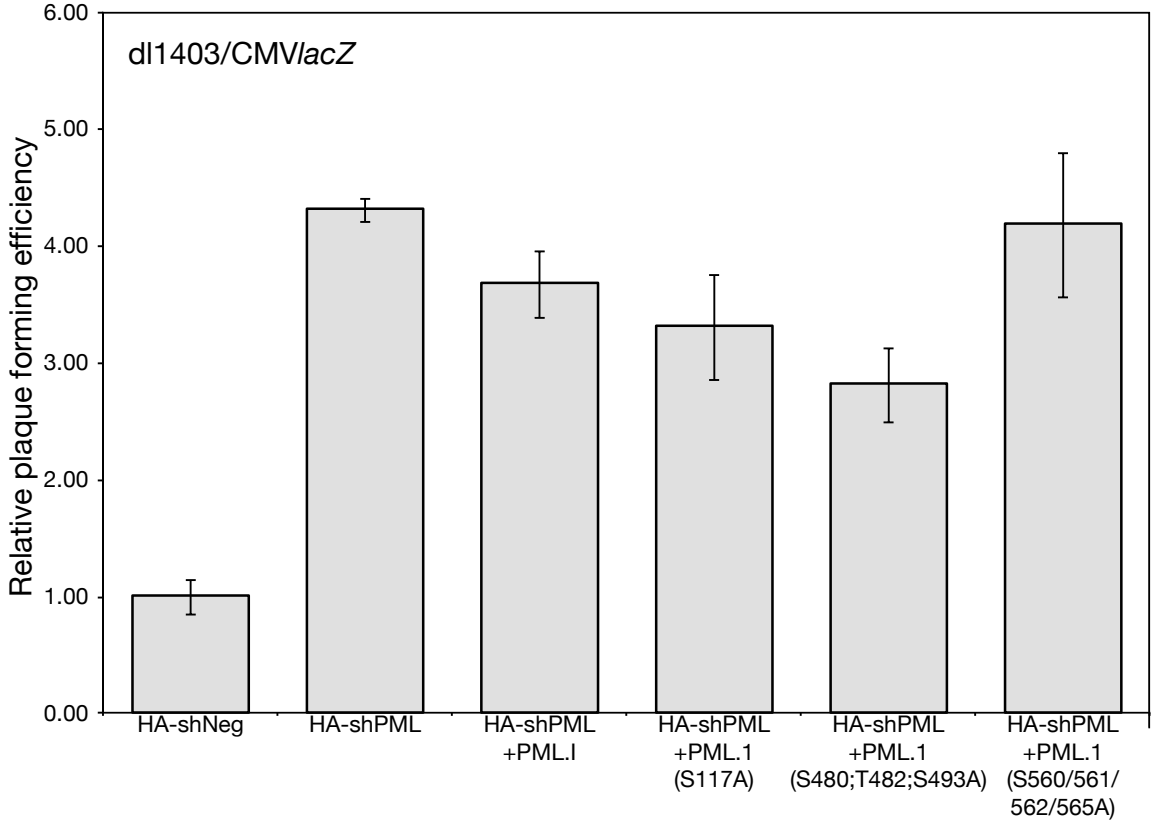
dl1403/CMV*lacZ*
Relative plaque forming efficiency
6.00
5.00
4.00
3.00
2.00
1.00
0.00
HA-shNeg
HA-shPML
HA-shPML +PML.I
HA-shPML +PML.1 (S117A)
HA-shPML +PML.1 (S480;T482;S493A)
HA-shPML +PML.1 (S560/561/ 562/565A)

**Figure 4.10. Plating efficiency of HSV-1 on HepaRG-based cells**

HA-shNeg, HA-shPML, and HA-shPML cells expressing eYFP-tagged PML-I, PML-I(S117A), PML-I(S480;T482;S493A), or PML-I(S560/561/562/565A) cells were infected with 3-fold serial dilutions of in1863 (wild type) or dl1403/CMVlacZ (ICP0-null) and incubated with methylcellulose to restrict viral spread. At 24 hpi, the cells were fixed and stained with X-gal to visualize plaques, and plaques consisting of greater than 4-6 cells were counted. The data are shown as the number of plaques on an individual cell line normalized to that on HA-shNeg cells and represent the average of three separate experiments performed in duplicate.

## Chapter 5: Conclusions and Future Directions

HSV-1 is endemic in the human population. Its success is partially due to its ability to establish a latent infection for the life of the host and because it can overcome cellular antiviral defenses. This dissertation has examined the role of three cellular factors in the host's antiviral response to HSV-1.

Despite the known requirement for cellular kinases and the large number of either known or potential viral substrates, the role of cellular kinase CK2 in the life cycle of HSV-1 has received little attention. In Chapter 2, I have shown that CK2 activity is largely unnecessary for HSV-1 replication. The use of two CK2 inhibitors did not affect the ability of the virus to initiate replication (Table 2.1), the ability to spread from cell to cell (Table 2.1), to or produce viral proteins (Figure 2.2) and there was no affect on the overall amount of virus produced in inhibitor-treated cells (Figure 2.1). However, these same activities were impaired when cells with a pre-existing IFN response where infected in the presence of the CK2 inhibitors (Table 2.1 and Figure 2.1A and 2.1C). I examined one potential viral CK2 substrates that is involved in countering the IFN response, ICP0, and found that in the absence of ICP0, the inhibitors no longer increase the IFN-sensitivity of HSV-1 (Figure 2.1B and 2.1D). Surprisingly, I found that this was independent of ICP0's E3 ligase function (Figures 2.3 and 2.4). There are a number of potential models to explain this outcome (Figure 5.1). ICP0 has been shown to transactivate a number of viral genes independently of its E3 ligase activity [319], which was not examined in this

thesis. It is possible that phosphorylation of ICP0 by CK2 affects its ability to transactivate the expression of another viral gene, such as ICP34.5 or vhs, and that the product of this gene is responsible for overcoming the interferon response (Figure 5.1A). Indeed, the use of the CDK inhibitor, roscovitine, affects ICP0's transactivation activity but not the E3 function in a similar fashion [308]. It would be of interest to examine whether this second function of ICP0 is linked to its anti-IFN counter activity. While ICP0 is phosphorylated on several residues that are present within CK2 consensus sequences, whether CK2 actually phosphorylates ICP0 has yet to be demonstrated. Alternatively, it might be that the product of an ICP0 transactivated gene requires CK2-mediated phosphorylation to impair the IFN response (Figure 5.1B). Another possibility is that ICP0 might interact with a partner protein whose activity it stimulates in a CK2 phosphorylation-dependent manner (Figure 5.1C). Furthermore, it is plausible that ICP0 interacts with CK2 to stimulate its activity toward certain target proteins (Figure 5.1D). Indeed, the EBV protein, EBNA1, interacts with CK2 and utilizes its activity to disrupt ND10s [77]. Finally, while I failed to observe such an effect for PML, it is possible that one or more interferon effector proteins that have activity towards HSV-1, but not Ad5 or VSV, are phosphorylated by CK2, and this phosphorylation is required for ICP0-mediated proteasomal degradation of the target (Figure 5.1E). The above interpretations are not mutually exclusive and several may function during viral infection. Future work will need to be performed to identify the viral target of CK2 responsible for overcoming restriction by IFNs. Also, while CK2-inhibition did

not enhance restriction of IFN-β with adenovirus or vesicular stomatitis virus, it is unknown whether this effect would extend to other herpesvirus family members. As noted above, EBV, a γ-herpesvirus, relocalizes CK2 to ND10s to induce PML degradation [77], suggesting that the use of CK2 to evade host immune responses may be a general feature of herpesviruses. Lastly, while it is unlikely that the compounds used have a non-specific cellular target in common, a stronger argument for CK2 in facilitating HSV-1 replication in the face of an IFN response could be made if CK2's activity was depleted or inhibited using siRNAs or cells that express one or more dominant negative forms of the CK2 enzyme.

A number of previous reports have shown that human fibroblasts could be immortalized through the expression of hTERT. Additionally, several reports demonstrated that HCMV replication was unaffected by hTERT-immortalization. On the other hand, some studies had shown that hTERT has non-telomerase related roles (e.g., anti-apoptotic) and that its expression can lead to changes in gene expression. However, the ability of hTERT-immortalized cells to mount a cellular antiviral response to HSV-1 had not previously been examined. Chapter 2 demonstrates that exogenous hTERT expression does not impair the ability of cells to produce antiviral cytokines (most likely IFNs) (Figure 3.9) in response to viral infection nor does it cause ISG dysregulation (Figures 3.4 and 3.5). This is in contrast to cells that are transformed with a viral oncogene, which leads to a greatly reduced ability to induce ISG expression and persistent ISG protein production. Like HCMV [280,281], hTERT does not affect HSV-1 replication nor

does it change the ability of IFN to restrict the growth of an IFN-sensitive HSV-1 mutant (Figures 3.6 and 3.7). Additionally, unlike in traditionally immortalized cells, the requirement for the HSV-1 protein ICP0 is preserved. Thus, the HEL-TERT cells represent the creation of a reagent that should facilitate future work that examines intrinsic- and IFN-based antiviral responses and aid in the study of certain HSV-1 mutants. Though the interferon response to HSV-1 and VSV were unaffected, it remains possible that the process of immortalization affects other cellular pathways that can impact viral replication. Additionally, there may be other ISGs than the four tested in this thesis that are affected by either hTERT expression or long term culturing, which would be found in an expanded examination of ISG gene expression.

PML is known to function in antiviral pathways, and many of its activities are controlled by post-translational modifications; however, no study to date has examined the role of PML phosphorylation in regulating its antiviral activity. A number of studies have identified sites of PML phosphorylation during the course of this dissertation [176,178,185,187,304] and confirm the authenticity of my mass spectrometry data; nonetheless, my thesis research represents the first study to examine PML phosphorylation during viral infection, using HSV-1 as the pathogen. As I initially examined the phosphorylation status of PML-III, it would be interesting to examine the C-terminus of the remaining PML isoforms, particularly PML-I and –II due to their antiviral activities on HSV-1 and see whether they also have unique sites of phosphorylation. Mutations of the phosphorylation sites resulted, for the most part, in minor effects on a number of

PML properties when these mutants were expressed in PML-depleted cells. Only mutation of sites near the SIM resulted in visible changes to ND10 morphology and the ability to recruit the ND10 associated proteins Sp100 and Daxx. Mutation of the SIM proximal sites also compromised the ability of PML to relocate to incoming viral genomes, though it is unclear at this time whether this is due to a change in phosphorylation at these sites. While phosphorylation has been implicated in the degradation of PML by cellular factors, mutation of the sites examined in this thesis did not, for the most part, inhibit the ability of ICP0 to induce PML degradation. This might be due to the ability of ICP0 to physically interact with a C-terminal portion of PML-I and future work should examine whether these phosphorylation sites differentially control the ability of ICP0 to induce the loss of other PML isoforms, much like polySUMOylation at K160 [293]. When PML-I and several of the PML-I phosphorylation knockout mutants were assayed for antiviral activity toward HSV-1 infection, they all failed to substantially restrict the establishment of infection. It should be said, however, that not only did restoration of PML-I expression itself fail to restrict the plaquing of an HSV-1 ICP0-null mutant but that, in my hands, knock-down of endogenous PML did not result in the same increase in plaquing as in previous reports. While HepaRG cells, the line used for these assays, have a high requirement for ICP0, they are transformed and thus the use of another cell line, such as the HEL-TERT cells created in Chapter 2, may prove more suitable in an examination of intrinsic defense. Additionally, using a technology such as transcription activator-like effector nucleases or zinc finger nucleases to knock

out, instead of knocking down, *PML* may result in a larger degree of complementation for plaquing with an ICP0-null mutant. I expect that switching from PML-I to PML-II or restoring the expression of multiple isoforms simultaneously would likely increase the antiviral activity of PML.

To explain how mutations adjacent to the SUMO interaction motif influence the antiviral activity of PML, I would propose the following model (Figure 5.2). In a resting cell, the localization of PML can be found in equilibrium between the ND10s and the nucleoplasm. This equilibrium serves to allow PML to act as a nuclear sensor that detects SUMOylated proteins and can either recruit them into ND10s or nucleate new ND10s at the site of these SUMOylated proteins. In the absence of a high number of positionally stable, non-ND10-localized SUMOylated proteins, PML favors interacting with itself to form ND10s. When the amount of non-ND10 SUMOylated proteins is high, the localization equilibrium shifts, and PML is gradually lost from ND10s. In the absence of ICP0, foci of SUMOylated proteins as well as Ubc9 and certain SUMO E3 ligases can be found at viral DNA [19,290]. While the SUMOylated targets are unknown, several DDR members, including BRCA1, 53BP1, MDC1, and RNF168 [320–322] have been shown to be modified by the SUMO paralogs. The high concentration of SUMOylated proteins results in nucleoplasmic PML being recruited to areas containing incoming viral genomes and depletes ND10 of PML. PML localization next to viral DNA may play a similar role similar to the one it performs at stem cell telomeres, where PML cooperates with another ND10 member, ATRX, in the establishment of heterochromatin [323].

Additionally, it is possible that PML uses its E3 ligase function to amplify the SUMOylation signal at viral DNA to further recruit effector proteins like RNF168, which amplifies the ubiquitination signal on γH2AX at DNA damage foci and allows for the recruitment of 53BP1 and BRCA1 [324,325]. In support of this model, PML has been found to act as a stabilizing factor in the recruitment of certain DNA damage response proteins [326]. As mutation of the phosphoacceptor sites near the PML SIM compromises its ability to interact with SUMOylated proteins, the amount of time PML spends in the nucleoplasm is short and the localization equilibrium shifts in favor of ND10-resident PML. Additionally, SIM-inactivated forms of PML are unable to detect the signal present at incoming viral DNA, which compromises its ability to effect a repression of viral gene expression. The increase in the residence of PML in ND10s also serves to more strongly recruit other ND10 members it interacts with such as Sp100 and Daxx. While it was not examined in this thesis, it would be interesting to see whether Sp100 and Daxx are still recruited to incoming viral in cells expressing SIM-inactivated PML or whether SIM-deficient forms of PML retain these two proteins at ND10s during infection.

In conclusion, I have established in this thesis that host cells have several defenses (i.e,, IFN-β and PML) to limit or inhibit HSV-1 replication. The virus, in turn, has developed strategies to counteract these defenses, either through the activities of viral encoded proteins (i.e. ICP0) or cellular kinases (i.e. CK2). Ultimately, the interactions between these factors will dictate whether HSV-1 will establish a lytic or latent/quiescent infection in its host.

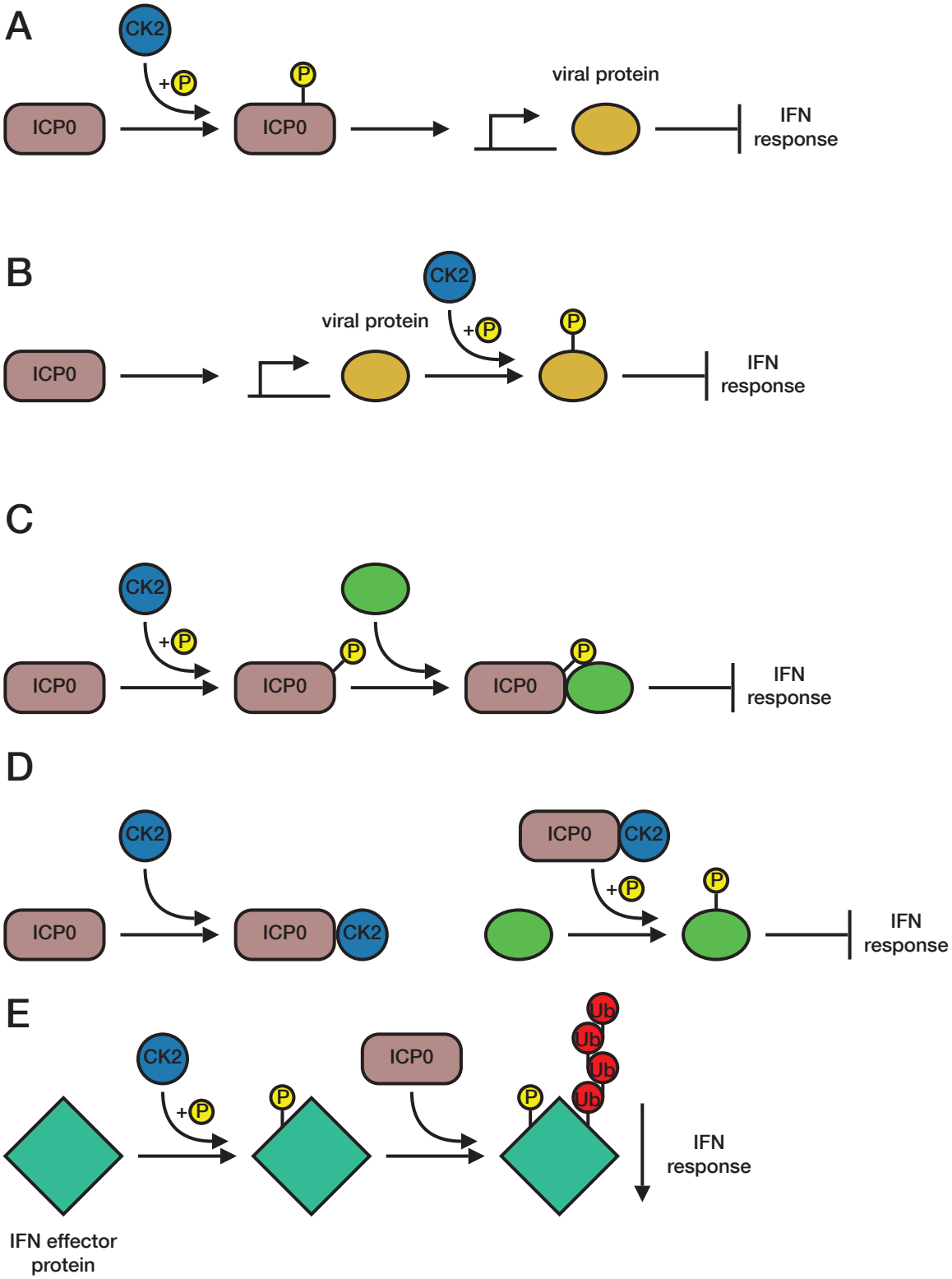
A
CK2
+P
ICP0
P
ICP0
viral protein
IFN
response
B
CK2
viral protein
+P
ICP0
P
IFN
response
C
CK2
+P
ICP0
P
ICP0
P
ICP0
IFN
response
D
CK2
ICP0
ICP0
CK2
ICP0
CK2
+P
P
IFN
response
E
CK2
+P
P
ICP0
Ub
Ub
Ub
Ub
P
IFN
response
IFN effector
protein

**Figure 5.1 Role of CK2 in IFN response impairment during HSV-1 infection**

(A) CK2 phosphorylates ICP0, allowing ICP0 to activate the expression of a viral protein that counteracts the IFN response.

(B) ICP0 transactivates the expression of a viral protein that requires CK2-mediated phosphorylation for its anti-IFN effector activity.

(C) ICP0 is phosphorylated by CK2, enabling it to interact with a partner protein. The complex formed by this partner and ICP0 functions to disarm the IFN response.

(D) ICP0 interacts with CK2 and directs the kinase activity of CK2 toward a viral or cellular target that results in the impairment of the IFN response.

(E) CK2 phosphorylates a cellular IFN effector protein, with this phosphorylation being necessary to enable the ICP0-mediated polyubiquitination and proteasomal degradation of the effector protein.

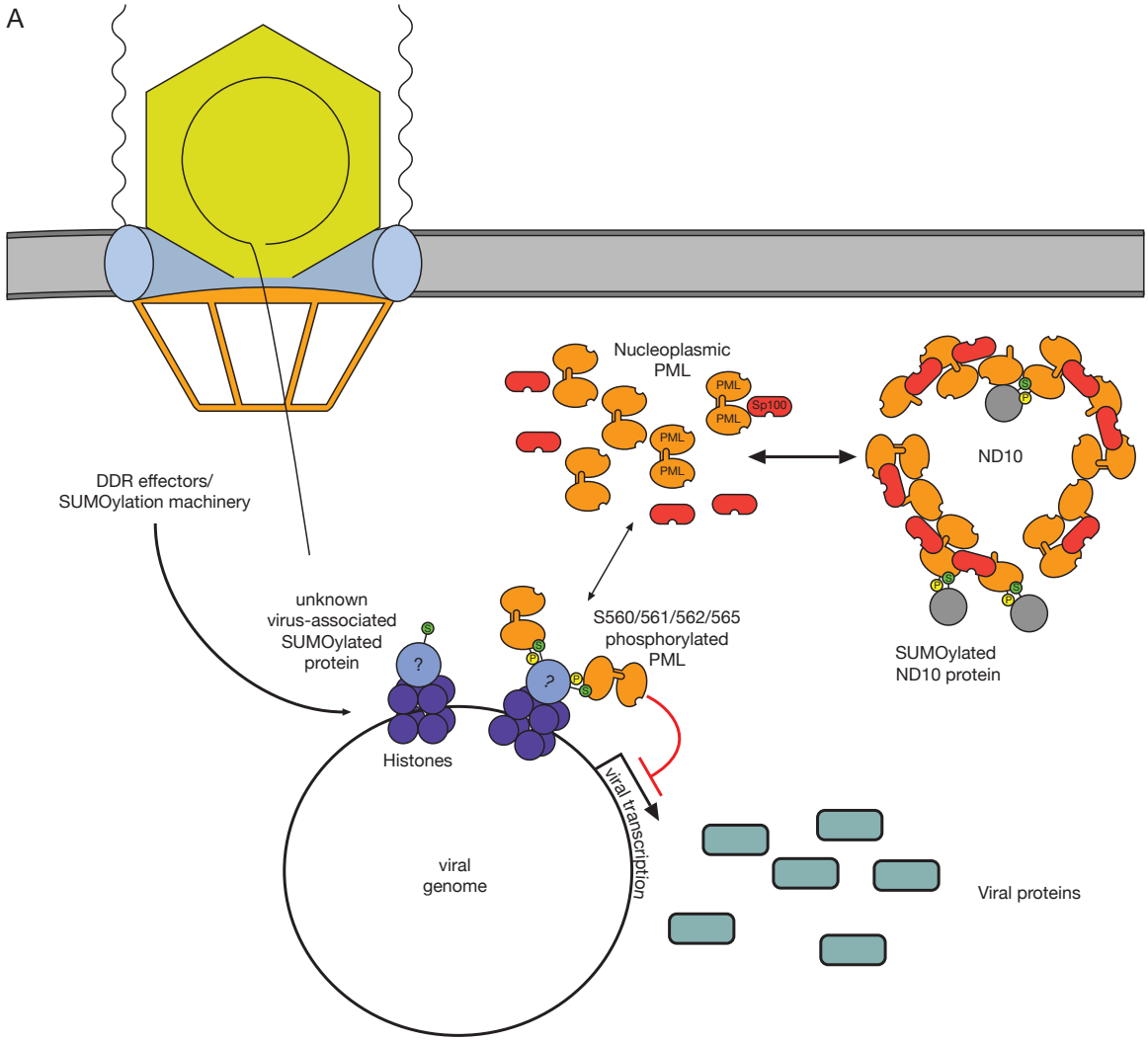
A
Nucleoplasmic
PML
PML
PML
Sp100
PML
PML
ND10
DDR effectors/
SUMOylation machinery
unknown
virus-associated
SUMOylated
protein
S560/561/562/565
phosphorylated
PML
SUMOylated
ND10 protein
?
?
Histones
viral transcription
viral
genome
Viral proteins

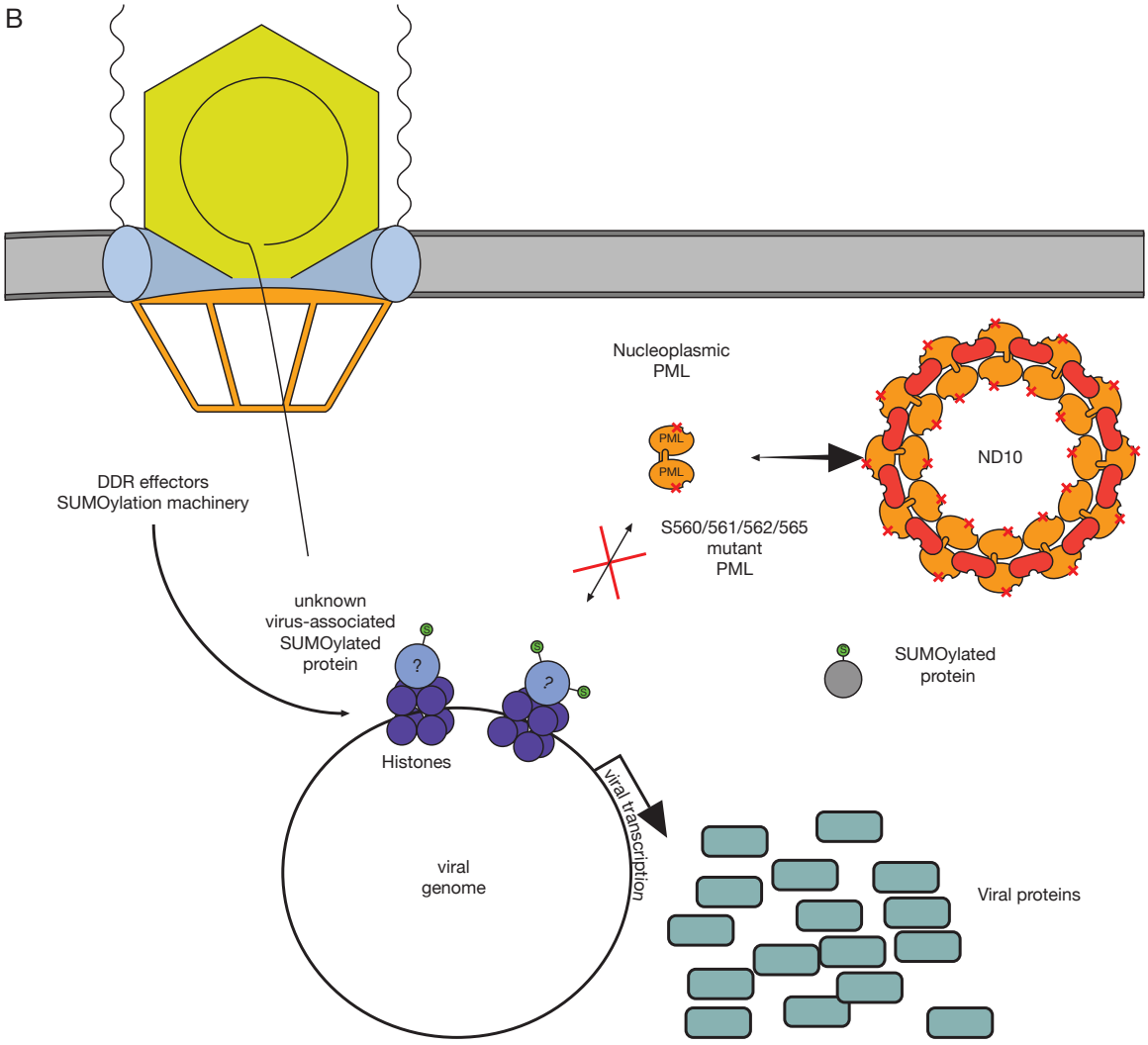


**Figure 5.2 Function of the phosphoSIM in the antiviral activity of PML**

(A) In cells expressing WT PML, injection of the viral genome into the nucleus results in the recruitment of DNA damage response and SUMOylation proteins to sites of viral DNA, leading to chromatinization of the viral genome. A SUMOylation signal on one or more proteins associated with this viral chromatin then recruits nucleoplasmic PML, which promotes the formation of a repressive chromatin state and an impairment of viral gene expression.

(B) In cells expressing a form of PML in which the phosphoSIM cannot be phosphorylated, nucleoplasmic PML fails to interact with the viral chromatin-associated SUMO signal, preventing the formation of a repressive chromatin state and allowing for increased viral gene expression. Consequently, due to the inability of this mutant form of PML to interact with SUMOylated proteins, PML is present in ND10s to a larger degree and produces larger ND10s that more strongly recruit certain ND10 members that it interacts with in a SIM-independent manner.

## Bibliography


[1] B.N. Fields, D.M. Knipe, P.M. Howley, D.E. Griffin, Fields Virology, Lippincott Williams & Wilkins, 2007.

[2] R.J. Whitley, D.W. Kimberlin, B. Roizman, Herpes Simplex Viruses, Clin. Infect. Dis. 26 (1998) 541–555.

[3] C.M. Roberts, J.R. Pfister, S.J. Spear, Increasing proportion of herpes simplex virus type 1 as a cause of genital herpes infection in college students, Sex. Transm. Dis. 30 (2003) 797–800.

[4] S.J. Macdonald, H.H. Mostafa, L.A. Morrison, D.J. Davido, Genome Sequence of Herpes Simplex Virus 1 Strain KOS, J. Virol. 86 (2012) 6371–6372.

[5] S. Loret, G. Guay, R. Lippe, Comprehensive Characterization of Extracellular Herpes Simplex Virus Type 1 Virions, J. Virol. 82 (2008) 8605–8618.

[6] I. Liashkovich, W. Hafezi, J.M. Kühn, H. Oberleithner, V. Shahin, Nuclear delivery mechanism of herpes simplex virus type 1 genome, J. Mol. Recognit. 24 (2011) 414–421.

[7] R.W. Honess, B. Roizman, Regulation of Herpesvirus Macromolecular Synthesis I. Cascade Regulation of the Synthesis of Three Groups of Viral Proteins, J. Virol. 14 (1974) 8–19.

[8] P. Lomonte, K.F. Sullivan, R.D. Everett, Degradation of Nucleosome-associated Centromeric Histone H3-like Protein CENP-A Induced by Herpes Simplex Virus Type 1 Protein ICP0, J. Biol. Chem. 276 (2001) 5829–5835.

[9] P. Lomonte, E. Morency, Centromeric protein CENP-B proteasomal degradation induced by the viral protein ICP0, Febs Lett. 581 (2007) 658–662.

[10] R.D. Everett, W.C. Earnshaw, J. Findlay, P. Lomonte, Specific destruction of kinetochore protein CENP-C and disruption of cell division by herpes simplex virus immediate-early protein Vmw110, Embo J. 18 (1999) 1526–1538.

[11] S. Gross, F. Catez, H. Masumoto, P. Lomonte, Centromere Architecture Breakdown Induced by the Viral E3 Ubiquitin Ligase ICP0 Protein of Herpes Simplex Virus Type 1, Plos One. 7 (2012) e44227.

[12] C.E. Lilley, M.S. Chaurushiya, C. Boutell, S. Landry, J. Suh, S. Panier, et al., A viral E3 ligase targets RNF8 and RNF168 to control histone ubiquitination and DNA damage responses, Embo J. 29 (2010) 943–955.

[13] J. Parkinson, S.P. Lees-Miller, R.D. Everett, Herpes Simplex Virus Type 1 Immediate-Early Protein Vmw110 Induces the Proteasome-Dependent Degradation of the Catalytic Subunit of DNA-Dependent Protein Kinase, J. Virol. 73 (1999) 650–657.

[14] M. Kummer, N.M. Turza, P. Muhl-Zurbes, M. Lechmann, C. Boutell, R.S. Coffin, et al., Herpes Simplex Virus Type 1 Induces CD83 Degradation in Mature Dendritic Cells with Immediate-Early Kinetics via the Cellular Proteasome, J Virol. 81 (2007) 6326–6338.
[15] C. Boutell, M. Canning, A. Orr, R.D. Everett, Reciprocal Activities between Herpes Simplex Virus Type 1 Regulatory Protein ICP0, a Ubiquitin E3 Ligase, and Ubiquitin-Specific Protease USP7, J Virol. 79 (2005) 12342–12354.
[16] L. Diao, B. Zhang, J. Fan, X. Gao, S. Sun, K. Yang, et al., Herpes virus proteins ICP0 and BICP0 can activate NF-[kappa]B by catalyzing I[kappa]B[alpha] ubiquitination, Cell. Signal. 17 (2005) 217–229.
[17] M.H. Orzalli, N.A. DeLuca, D.M. Knipe, Nuclear IFI16 induction of IRF-3 signaling during herpesviral infection and degradation of IFI16 by the viral ICP0 protein, Proc. Natl. Acad. Sci. 109 (2012) E3008–E3017.
[18] Y. Fukuyo, N. Horikoshi, A.M. Ishov, S.J. Silverstein, T. Nakajima, The Herpes Simplex Virus Immediate-Early Ubiquitin Ligase ICP0 Induces Degradation of the ICP0 Repressor Protein E2FBP1, J Virol. 85 (2011) 3356–3366.
[19] C. Boutell, D. Cuchet-Lourenço, E. Vanni, A. Orr, M. Glass, S. McFarlane, et al., A Viral Ubiquitin Ligase Has Substrate Preferential SUMO Targeted Ubiquitin Ligase Activity that Counteracts Intrinsic Antiviral Defence, Plos Pathog. 7 (2011) e1002245.
[20] R.D. Everett, M.K. Chelbi-Alix, PML and PML nuclear bodies: Implications in antiviral defence, Biochimie. 89 (2007) 819–830.
[21] R. Hagglund, B. Roizman, Role of ICP0 in the Strategy of Conquest of the Host Cell by Herpes Simplex Virus 1, J. Virol. 78 (2004) 2169–2178.
[22] K.L. Mossman, A.A. Ashkar, Herpesviruses and the innate immune response, Viral Immunol. 18 (2005) 267–281.
[23] M.D. Weitzman, C.E. Lilley, M.S. Chaurushiya, Genomes in conflict: maintaining genome integrity during virus infection, Annu. Rev. Microbiol. 64 (2010) 61–81.
[24] G.G. Maul, D. Negorev, P. Bell, A.M. Ishov, Review: Properties and Assembly Mechanisms of ND10, PML Bodies, or PODs, J. Struct. Biol. 129 (2000) 278–287.
[25] G.G. Maul, A.M. Ishov, R.D. Everett, Nuclear Domain 10 as Preexisting Potential Replication Start Sites of Herpes Simplex Virus Type-1, Virology. 217 (1996) 67–75.
[26] R.D. Everett, J. Murray, ND10 Components Relocate to Sites Associated with Herpes Simplex Virus Type 1 Nucleoprotein Complexes during Virus Infection, J Virol. 79 (2005) 5078–5089.
[27] R.D. Everett, P. Freemont, H. Saitoh, M. Dasso, A. Orr, M. Kathoria, et al., The Disruption of ND10 during Herpes Simplex Virus Infection Correlates with the Vmw110- and Proteasome-Dependent Loss of Several PML Isoforms, J Virol. 72 (1998) 6581–6591.

[28] J. Parkinson, R.D. Everett, Alphaherpesvirus Proteins Related to Herpes Simplex Virus Type 1 ICP0 Affect Cellular Structures and Proteins, J Virol. 74 (2000) 10006–10017.
[29] V. Lukashchuk, R.D. Everett, Regulation of ICP0-Null Mutant Herpes Simplex Virus Type 1 Infection by ND10 Components ATRX and hDaxx, J Virol. 84 (2010) 4026–4040.
[30] R.D. Everett, S. Rechter, P. Papior, N. Tavalai, T. Stamminger, A. Orr, PML Contributes to a Cellular Mechanism of Repression of Herpes Simplex Virus Type 1 Infection That Is Inactivated by ICP0, J. Virol. 80 (2006) 7995–8005.
[31] P. Härle, B. Sainz, D.J.J. Carr, W.P. Halford, The Immediate-Early Protein, ICP0, Is Essential for the Resistance of Herpes Simplex Virus to Interferon-α/β, Virology. 293 (2002) 295–304.
[32] R.D. Everett, A. Orr, Herpes Simplex Virus Type 1 Regulatory Protein ICP0 Aids Infection in Cells with a Preinduced Interferon Response but Does Not Impede Interferon-Induced Gene Induction, J Virol. 83 (2009) 4978–4983.
[33] A.V. Chee, P. Lopez, P.P. Pandolfi, B. Roizman, Promyelocytic Leukemia Protein Mediates Interferon-Based Anti-Herpes Simplex Virus 1 Effects, J Virol. 77 (2003) 7101–7105.
[34] R.D. Everett, D.F. Young, R.E. Randall, A. Orr, STAT-1- and IRF-3-Dependent Pathways Are Not Essential for Repression of ICP0-Null Mutant Herpes Simplex Virus Type 1 in Human Fibroblasts, J Virol. 82 (2008) 8871–8881.
[35] W. Halford, C. Weisend, J. Grace, M. Soboleski, D. Carr, J. Balliet, et al., ICP0 antagonizes Stat 1-dependent repression of herpes simplex virus: implications for the regulation of viral latency, Virol. J. 3 (2006) 44.
[36] G. Uzé, D. Monneron, IL-28 and IL-29: Newcomers to the interferon family, Biochimie. 89 (2007) 729–734.
[37] M.G. Katze, Y. He, M. Gale, Viruses and interferon: a fight for supremacy, Nat Rev Immunol. 2 (2002) 675–687.
[38] M. Paulson, C. Press, E. Smith, N. Tanese, D.E. Levy, IFN-Stimulated transcription through a TBP-free acetyltransferase complex escapes viral shutoff, Nat. Cell Biol. 4 (2002) 140–147.
[39] H. Kristiansen, H.H. Gad, S. Eskildsen-Larsen, P. Despres, R. Hartmann, The Oligoadenylate Synthetase Family: An Ancient Protein Family with Multiple Antiviral Activities, J. Interferon Cytokine Res. 31 (2011) 41–47.
[40] O. Haller, G. Kochs, Interferon-Induced Mx Proteins: Dynamin-Like GTPases with Antiviral Activity, Traffic. 3 (2002) 710–717.
[41] A. Pindel, A. Sadler, The Role of Protein Kinase R in the Interferon Response, J. Interferon Cytokine Res. 31 (2011) 59–70.
[42] V. Fensterl, G.C. Sen, The ISG56/IFIT1 Gene Family, J. Interferon Cytokine Res. 31 (2011) 71–78.
[43] F. Meggio, L.A. Pinna, One-thousand-and-one substrates of protein kinase CK2?, Faseb J. 17 (2003) 349–368.

[44] L.A. Pinna, Casein kinase 2: an “eminence grise” in cellular regulation?, Biochim. Biophys. Acta. 1054 (1990) 267–284.
[45] G. Vilk, J.E. Weber, J.P. Turowec, J.S. Duncan, C. Wu, D.R. Derksen, et al., Protein kinase CK2 catalyzes tyrosine phosphorylation in mammalian cells, Cell. Signal. 20 (2008) 1942–1951.
[46] T. Buchou, M. Vernet, O. Blond, H.H. Jensen, H. Pointu, B.B. Olsen, et al., Disruption of the Regulatory β Subunit of Protein Kinase CK2 in Mice Leads to a Cell-Autonomous Defect and Early Embryonic Lethality, Mol. Cell. Biol. 23 (2003) 908–915.
[47] E. Schneider, S. Kartarius, N. Schuster, M. Montenarh, The cyclin H/cdk7/Mat1 kinase activity is regulated by CK2 phosphorylation of cyclin H, Oncogene. 21 (2002) 5031–5037.
[48] N. Allende-Vega, S. Dias, D. Milne, D. Meek, Phosphorylation of the acidic domain of Mdm2 by protein kinase CK2, Mol. Cell. Biochem. 274 (2005) 85–90.
[49] D.M. Keller, X. Zeng, Y. Wang, Q.H. Zhang, M. Kapoor, H. Shu, et al., A DNA Damage–Induced p53 Serine 392 Kinase Complex Contains CK2, hSpt16, and SSRP1, Mol. Cell. 7 (2001) 283–292.
[50] N. Watanabe, H. Arai, J. Iwasaki, M. Shiina, K. Ogata, T. Hunter, et al., Cyclin-dependent kinase (CDK) phosphorylation destabilizes somatic Wee1 via multiple pathways, Proc. Natl. Acad. Sci. U. S. A. 102 (2005) 11663–11668.
[51] N. St-Denis, D. Litchfield, From birth to death: The role of protein kinase CK2 in the regulation of cell proliferation and survival, Cell. Mol. Life Sci. 66 (2009) 1817–1829.
[52] T.B. Panova, K.I. Panov, J. Russell, J.C.B.M. Zomerdijk, Casein Kinase 2 Associates with Initiation-Competent RNA Polymerase I and Has Multiple Roles in Ribosomal DNA Transcription, Mol. Cell. Biol. 26 (2006) 5957–5968.
[53] D.J. Hockman, M.C. Schultz, Casein kinase II is required for efficient transcription by RNA polymerase III., Mol. Cell. Biol. 16 (1996) 892–898.
[54] P. Hu, S. Wu, N. Hernandez, A Minimal RNA Polymerase III Transcription System from Human Cells Reveals Positive and Negative Regulatory Roles for CK2, Mol. Cell. 12 (2003) 699–709.
[55] P. Hu, K. Samudre, S. Wu, Y. Sun, N. Hernandez, CK2 Phosphorylation of Bdp1 Executes Cell Cycle-Specific RNA Polymerase III Transcription Repression, Mol. Cell. 16 (2004) 81–92.
[56] K.L. Abbott, M.B. Renfrow, M.J. Chalmers, B.D. Nguyen, A.G. Marshall, P. Legault, et al., Enhanced Binding of RNAP II CTD Phosphatase FCP1 to RAP74 Following CK2 Phosphorylation, Biochemistry (Mosc.). 44 (2005) 2732–2745.
[57] L.R. Martins, P. Lúcio, M.C. Silva, K.L. Anderes, P. Gameiro, M.G. Silva, et al., Targeting CK2 overexpression and hyperactivation as a novel therapeutic tool in chronic lymphocytic leukemia, Blood. 116 (2010) 2724–2731.

[58] H. Lawnicka, M. Kowalewicz-Kulbat, P. Sicinska, Z. Kazimierczuk, P. Grieb, H. Stepien, Anti-neoplastic effect of protein kinase CK2 inhibitor, 2-dimethylamino-4,5,6,7-tetrabromobenzimidazole (DMAT), on growth and hormonal activity of human adrenocortical carcinoma cell line (H295R) in vitro, Cell Tissue Res. 340 (2010) 371–379.
[59] S. Shin, Y. Lee, W. Kim, H. Ko, H. Choi, K. Kim, Caspase-2 primes cancer cells for TRAIL-mediated apoptosis by processing procaspase-8, Embo J. 24 (2005) 3532–3542.
[60] J.P. Turowec, J.S. Duncan, G.B. Gloor, D.W. Litchfield, Regulation of caspase pathways by protein kinase CK2: identification of proteins with overlapping CK2 and caspase consensus motifs, Mol. Cell. Biochem. 356 (2011) 159–167.
[61] J.C. Tapia, V.A. Torres, D.A. Rodriguez, L. Leyton, A.F.G. Quest, Casein kinase 2 (CK2) increases survivin expression via enhanced β-catenin–T cell factor/lymphoid enhancer binding factor-dependent transcription, Proc. Natl. Acad. Sci. 103 (2006) 15079–15084.
[62] Y. Zheng, H. Qin, S.J. Frank, L. Deng, D.W. Litchfield, A. Tefferi, et al., A CK2-dependent mechanism for activation of the JAK-STAT signaling pathway, Blood. 118 (2011) 156–166.
[63] Z. Sun, H. Ren, Y. Liu, J.L. Teeling, J. Gu, Phosphorylation of RIG-I by Casein Kinase II Inhibits Its Antiviral Response, J. Virol. 85 (2011) 1036–1047.
[64] A. Schmidt, T. Schwerd, W. Hamm, J.C. Hellmuth, S. Cui, M. Wenzel, et al., 5′-triphosphate RNA requires base-paired structures to activate antiviral signaling via RIG-I, Proc. Natl. Acad. Sci. 106 (2009) 12067–12072.
[65] S. Veeranki, D. Choubey, Interferon-inducible p200-family protein IFI16, an innate immune sensor for cytosolic and nuclear double-stranded DNA: Regulation of subcellular localization, Mol. Immunol. 49 (2012) 567–571.
[66] L.J. Briggs, R.W. Johnstone, R.M. Elliot, C.-Y. Xiao, M. Dawson, J.A. Trapani, et al., Novel properties of the protein kinase CK2-site-regulated nuclear- localization sequence of the interferon-induced nuclear factor IFI 16, Biochem. J. 353 (2001) 69–77.
[67] J. Friborg, A. Ladha, H. Göttlinger, W.A. Haseltine, E.A. Cohen, Functional analysis of the phosphorylation sites on the human immunodeficiency virus type 1 Vpu protein, J. Acquir. Immune Defic. Syndr. Hum. Retrovirology Off. Publ. Int. Retrovirology Assoc. 8 (1995) 10–22.
[68] E. Haneda, T. Furuya, S. Asai, Y. Morikawa, K. Ohtsuki, Biochemical Characterization of Casein Kinase II as a Protein Kinase Responsible for Stimulation of HIV-1 Protease in Vitro, Biochem. Biophys. Res. Commun. 275 (2000) 434–439.
[69] S. Harada, E. Haneda, T. Maekawa, Y. Morikawa, S. Funayama, N. Nagata, et al., Casein kinase II (CK-II)-mediated stimulation of HIV-1 reverse transcriptase activity and characterization of selective inhibitors in vitro, Biol. Pharm. Bull. 22 (1999) 1122–1126.

[70] K. Ohtsuki, T. Maekawa, S. Harada, A. Karino, Y. Morikawa, M. Ito, Biochemical characterization of HIV-1 Rev as a potent activator of casein kinase II in vitro, Febs Lett. 428 (1998) 235–240.
[71] M. Schindler, D. Rajan, C. Banning, P. Wimmer, H. Koppensteiner, A. Iwanski, et al., Vpu serine 52 dependent counteraction of tetherin is required for HIV-1 replication in macrophages, but not in ex vivo human lymphoid tissue, Retrovirology. 7 (2010) 1.
[72] M.I. Barrasa, N.Y. Harel, J.C. Alwine, The Phosphorylation Status of the Serine-Rich Region of the Human Cytomegalovirus 86-Kilodalton Major Immediate-Early Protein IE2/IEP86 Affects Temporal Viral Gene Expression, J. Virol. 79 (2005) 1428–1437.
[73] Y. Gao, K. Colletti, G.S. Pari, Identification of Human Cytomegalovirus UL84 Virus- and Cell-Encoded Binding Partners by Using Proteomics Analysis, J. Virol. 82 (2008) 96–104.
[74] M.T. Nogalski, J.P. Podduturi, I.B. DeMeritt, L.E. Milford, A.D. Yurochko, The Human Cytomegalovirus Virion Possesses an Activated Casein Kinase II That Allows for the Rapid Phosphorylation of the Inhibitor of NF-κB, IκBα, J. Virol. 81 (2007) 5305–5314.
[75] A.S. El-Guindy, G. Miller, Phosphorylation of Epstein-Barr Virus ZEBRA Protein at Its Casein Kinase 2 Sites Mediates Its Ability To Repress Activation of a Viral Lytic Cycle Late Gene by Rta, J. Virol. 78 (2004) 7634–7644.
[76] C. Medina-Palazon, H. Gruffat, F. Mure, O. Filhol, V. Vingtdeux-Didier, H. Drobecq, et al., Protein Kinase CK2 Phosphorylation of EB2 Regulates Its Function in the Production of Epstein-Barr Virus Infectious Viral Particles, J. Virol. 81 (2007) 11850–11860.
[77] N. Sivachandran, J.Y. Cao, L. Frappier, Epstein-Barr Virus Nuclear Antigen 1 Hijacks the Host Kinase CK2 To Disrupt PML Nuclear Bodies, J Virol. 84 (2010) 11113–11123.
[78] N. Franck, J.L. Seyec, C. Guguen-Guillouzo, L. Erdtmann, Hepatitis C Virus NS2 Protein Is Phosphorylated by the Protein Kinase CK2 and Targeted for Degradation to the Proteasome, J. Virol. 79 (2005) 2700–2708.
[79] A.V. Ivanov, O.A. Smirnova, O.N. Ivanova, O.V. Masalova, S.N. Kochetkov, M.G. Isaguliants, Hepatitis C Virus Proteins Activate NRF2/ARE Pathway by Distinct ROS-Dependent and Independent Mechanisms in HUH7 Cells, Plos One. 6 (2011) e24957.
[80] T.L. Tellinghuisen, K.L. Foss, J. Treadaway, Regulation of Hepatitis C Virion Production via Phosphorylation of the NS5A Protein, Plos Pathog. 4 (2008) e1000032.
[81] M. Yi, Y. Ma, J. Yates, S.M. Lemon, trans-Complementation of an NS2 Defect in a Late Step in Hepatitis C Virus (HCV) Particle Assembly and Maturation, Plos Pathog. 5 (2009) e1000403.
[82] W.-M. Chien, J.N. Parker, D.-C. Schmidt-Grimminger, T.R. Broker, L.T. Chow, Casein Kinase II Phosphorylation of the Human Papillomavirus-18

E7 Protein Is Critical for Promoting S-Phase Entry, Cell Growth Differ. 11 (2000) 425–435.
[83] N.J. Genovese, N.S. Banerjee, T.R. Broker, L.T. Chow, Casein Kinase II Motif-Dependent Phosphorylation of Human Papillomavirus E7 Protein Promotes p130 Degradation and S-Phase Induction in Differentiated Human Keratinocytes, J. Virol. 82 (2008) 4862–4873.
[84] J. Yue, R. Shukla, R. Accardi, I. Zanella-Cleon, M. Siouda, M.-P. Cros, et al., Cutaneous Human Papillomavirus Type 38 E7 Regulates Actin Cytoskeleton Structure for Increasing Cell Proliferation through CK2 and the Eukaryotic Elongation Factor 1A, J. Virol. 85 (2011) 8477–8494.
[85] W. Ching, T. Dobner, E. Koyuncu, The Human Adenovirus Type 5 E1B 55-Kilodalton Protein Is Phosphorylated by Protein Kinase CK2, J. Virol. 86 (2012) 2400–2415.
[86] P. Massimi, D. Pim, A. Storey, L. Banks, HPV-16 E7 and adenovirus E1a complex formation with TATA box binding protein is enhanced by casein kinase II phosphorylation, Oncogene. 12 (1996) 2325–2330.
[87] S. Barik, A.K. Banerjee, Phosphorylation by cellular casein kinase II is essential for transcriptional activity of vesicular stomatitis virus phosphoprotein P, Proc. Natl. Acad. Sci. 89 (1992) 6570–6574.
[88] T. Das, A.K. Gupta, P.W. Sims, C.A. Gelfand, J.E. Jentoft, A.K. Banerjee, Role of Cellular Casein Kinase II in the Function of the Phosphoprotein (P) Subunit of RNA Polymerase of Vesicular Stomatitis Virus, J. Biol. Chem. 270 (1995) 24100 –24107.
[89] A.K. Gupta, T. Das, A.K. Banerjee, Casein kinase II is the P protein phosphorylating cellular kinase associated with the ribonucleoprotein complex of purified vesicular stomatitis virus, J. Gen. Virol. 76 (1995) 365–372.
[90] K. Xia, D.M. Knipe, N.A. DeLuca, Role of protein kinase A and the serine-rich region of herpes simplex virus type 1 ICP4 in viral replication, J. Virol. 70 (1996) 1050–1060.
[91] D.J. Davido, W.F. Zagorski, W.S. Lane, P.A. Schaffer, Phosphorylation Site Mutations Affect Herpes Simplex Virus Type 1 ICP0 Function, J. Virol. 79 (2005) 1232–1243.
[92] C. Potel, G. Elliott, Phosphorylation of the Herpes Simplex Virus Tegument Protein VP22 Has No Effect on Incorporation of VP22 into the Virus but Is Involved in Optimal Expression and Virion Packaging of ICP0, J. Virol. 79 (2005) 14057–14068.
[93] S. Rojas, K.A. Corbin-Lickfett, L. Escudero-Paunetto, R.M. Sandri-Goldin, ICP27 Phosphorylation Site Mutants Are Defective in Herpes Simplex Virus 1 Replication and Gene Expression, J. Virol. 84 (2010) 2200–2211.
[94] H.H. Mostafa, T.W. Thompson, D.J. Davido, N-Terminal Phosphorylation Sites of Herpes Simplex Virus 1 ICP0 Differentially Regulate Its Activities and Enhance Viral Replication, J. Virol. 87 (2013) 2109–2119.

[95] P.A. Bates, N.A. DeLuca, The Polyserine Tract of Herpes Simplex Virus ICP4 Is Required for Normal Viral Gene Expression and Growth in Murine Trigeminal Ganglia, J. Virol. 72 (1998) 7115–7124.
[96] R.M. Sandri-Goldin, The many roles of the regulatory protein ICP27 during herpes simplex virus infection, Front. Biosci. J. Virtual Libr. 13 (2008) 5241–56.
[97] M.D. Koffa, J. Kean, G. Zachos, S.A. Rice, J.B. Clements, CK2 Protein Kinase Is Stimulated and Redistributed by Functional Herpes Simplex Virus ICP27 Protein, J. Virol. 77 (2003) 4315–4325.
[98] K.A. Corbin-Lickfett, S. Rojas, L. Li, M.J. Cocco, R.M. Sandri-Goldin, ICP27 Phosphorylation Site Mutants Display Altered Functional Interactions with Cellular Export Factors Aly/REF and TAP/NXF1 but Are Able To Bind Herpes Simplex Virus 1 RNA, J. Virol. 84 (2010) 2212–2222.
[99] A.L. Fridman, L. Tang, O.I. Kulaeva, B. Ye, Q. Li, F. Nahhas, et al., Expression profiling identifies three pathways altered in cellular immortalization: interferon, cell cycle, and cytoskeleton, J. Gerontol. A. Biol. Sci. Med. Sci. 61 (2006) 879–889.
[100] O.I. Kulaeva, S. Draghici, L. Tang, J.M. Kraniak, S.J. Land, M.A. Tainsky, Epigenetic silencing of multiple interferon pathway genes after cellular immortalization, Oncogene. 22 (2003) 4118–4127.
[101] J. Shou, R. Soriano, S.W. Hayward, G.R. Cunha, P.M. Williams, W.-Q. Gao, Expression Profiling of a Human Cell Line Model of Prostatic Cancer Reveals a Direct Involvement of Interferon Signaling in Prostate Tumor Progression, Proc. Natl. Acad. Sci. 99 (2002) 2830–2835.
[102] G. Untergasser, H.B. Koch, A. Menssen, H. Hermeking, Characterization of Epithelial Senescence by Serial Analysis of Gene Expression Identification of Genes Potentially Involved in Prostate Cancer, Cancer Res. 62 (2002) 6255–6262.
[103] L. Hayflick, The limited in vitro lifetime of human diploid cell strains, Exp. Cell Res. 37 (1965) 614–636.
[104] E. Gilson, V. Geli, How telomeres are replicated, Nat Rev Mol Cell Biol. 8 (2007) 825–838.
[105] T. de Lange, How Telomeres Solve the End-Protection Problem, Science. 326 (2009) 948–952.
[106] Y. Zhao, H. Hoshiyama, J.W. Shay, W.E. Wright, Quantitative Telomeric Overhang Determination Using a Double-Strand Specific Nuclease, Nucleic Acids Res. 36 (2008) e14.
[107] C.B. Harley, A.B. Futcher, C.W. Greider, Telomeres shorten during ageing of human fibroblasts, Publ. Online 31 May 1990 Doi101038345458a0. 345 (1990) 458–460.
[108] E.H. Blackburn, C.W. Greider, E. Henderson, M.S. Lee, J. Shampay, D. Shippen-Lentz, Recognition and elongation of telomeres by telomerase, Genome Natl. Res. Counc. Can. Génome Cons. Natl. Rech. Can. 31 (1989) 553–560.

[109] J. Feng, W.D. Funk, S.-S. Wang, S.L. Weinrich, A.A. Avilion, C.-P. Chiu, et al., The RNA Component of Human Telomerase, Science. 269 (1995) 1236–1241.
[110] P. Neumeister, C. Albanese, B. Balent, J. Greally, R.G. Pestell, Senescence and epigenetic dysregulation in cancer, Int. J. Biochem. Cell Biol. 34 (2002) 1475–1490.
[111] J. Campisi, F. d' Adda di Fagagna, Cellular senescence: when bad things happen to good cells, Nat Rev Mol Cell Biol. 8 (2007) 729–740.
[112] J. Campisi, Cellular senescence as a tumor-suppressor mechanism, Trends Cell Biol. 11 (2001) S27–S31.
[113] M. Braig, C.A. Schmitt, Oncogene-Induced Senescence: Putting the Brakes on Tumor Development, Cancer Res. 66 (2006) 2881–2884.
[114] J.R. Smith, O.M. Pereira-Smith, Replicative Senescence: Implications for in Vivo Aging and Tumor Suppression, Science. 273 (1996) 63–67.
[115] C.M. Beausejour, A. Krtolica, F. Galimi, M. Narita, S.W. Lowe, P. Yaswen, et al., Reversal of human cellular senescence: roles of the p53 and p16 pathways, Embo J. 22 (2003) 4212–4222.
[116] P. Hawley-Nelson, K.H. Vousden, N.L. Hubbert, D.R. Lowy, J.T. Schiller, HPV16 E6 and E7 proteins cooperate to immortalize human foreskin keratinocytes., Embo J. 8 (1989) 3905.
[117] J.B. Hudson, M.A. Bedell, D.J. McCance, L.A. Laiminis, Immortalization and Altered Differentiation of Human Keratinocytes in Vitro by the E6 and E7 Open Reading Frames of Human Papillomavirus Type 18., J. Virol. 64 (1990) 519–526.
[118] J.W. Shay, W.E. Wright, Quantitation of the frequency of immortalization of normal human diploid fibroblasts by SV40 large T-antigen, Exp. Cell Res. 184 (1989) 109–118.
[119] J.W. Shay, B.A. Van Der Haegen, Y. Ying, W.E. Wright, The frequency of immortalization of human fibroblasts and mammary epithelial cells transfected with SV40 large T-antigen, Exp. Cell Res. 209 (1993) 45–52.
[120] M. Meyerson, C.M. Counter, E.N. Eaton, L.W. Ellisen, P. Steiner, S.D. Caddle, et al., hEST2, the Putative Human Telomerase Catalytic Subunit Gene, Is Up-Regulated in Tumor Cells and during Immortalization, Cell. 90 (1997) 785–795.
[121] A.G. Bodnar, M. Ouellette, M. Frolkis, S.E. Holt, C.-P. Chiu, G.B. Morin, et al., Extension of Life-Span by Introduction of Telomerase into Normal Human Cells, Science. 279 (1998) 349–352.
[122] S. Franco, K.L. MacKenzie, S. Dias, S. Alvarez, S. Rafii, M.A.S. Moore, Clonal Variation in Phenotype and Life Span of Human Embryonic Fibroblasts (MRC-5) Transduced with the Catalytic Component of Telomerase (hTERT), Exp. Cell Res. 268 (2001) 14–25.
[123] R.J. O'Sullivan, J. Karlseder, Telomeres: protecting chromosomes against genome instability, Nat Rev Mol Cell Biol. 11 (2010) 171–181.

[124] C.P. Morales, S.E. Holt, M. Ouellette, K.J. Kaur, Y. Yan, K.S. Wilson, et al., Absence of cancer-associated changes in human fibroblasts immortalized with telomerase, Nat Genet. 21 (1999) 115–118.
[125] E. Lapi, S.D. Agostino, S. Donzelli, H. Gal, E. Domany, G. Rechavi, et al., PML, YAP, and p73 Are Components of a Proapoptotic Autoregulatory Feedback Loop, Mol. Cell. 32 (2008) 803–814.
[126] S. Buonamici, D. Li, F.M. Mikhail, A. Sassano, L.C. Platanias, O. Colamonici, et al., EVI1 Abrogates Interferon-{alpha} Response by Selectively Blocking PML Induction, J Biol Chem. 280 (2005) 428–436.
[127] K. Jensen, C. Shiels, P.S. Freemont, PML protein isoforms and the RBCC/TRIM motif, Oncogene. 20 (2001) 7223–4233.
[128] B.B. Quimby, V. Yong-Gonzalez, T. Anan, A.V. Strunnikov, M. Dasso, The promyelocytic leukemia protein stimulates SUMO conjugation in yeast, Oncogene. 25 (2006) 2999–3005.
[129] Y. Chu, X. Yang, SUMO E3 ligase activity of TRIM proteins, Oncogene. (2010).
[130] R. Bernardi, P.P. Pandolfi, Structure, dynamics and functions of promyelocytic leukaemia nuclear bodies, Nat Rev Mol Cell Biol. 8 (2007) 1006–1016.
[131] V. Lallemand-Breitenbach, H. de Thé, PML Nuclear Bodies, Cold Spring Harb. Perspect. Biol. 2 (2010).
[132] E. Van Damme, K. Laukens, T.H. Dang, X. Van Ostade, A manually curated network of the PML nuclear body interactome reveals an important role for PML-NBs in SUMOylation dynamics, Int. J. Biol. Sci. 6 (2010) 51–67.
[133] A. Janer, E. Martin, M.-P. Muriel, M. Latouche, H. Fujigasaki, M. Ruberg, et al., PML clastosomes prevent nuclear accumulation of mutant ataxin-7 and other polyglutamine proteins, J. Cell Biol. 174 (2006) 65–76.
[134] L. Fu, Y. Gao, A. Tousson, A. Shah, T.-L.L. Chen, B.M. Vertel, et al., Nuclear Aggresomes Form by Fusion of PML-associated Aggregates, Mol Biol Cell. 16 (2005) 4905–4917.
[135] T.G. Hofmann, H. Will, Body language: the function of PML nuclear bodies in apoptosis regulation, Cell Death Differ. 10 (2003) 1290–1299.
[136] M. Lang, T. Jegou, I. Chung, K. Richter, S. Munch, A. Udvarhelyi, et al., Three-dimensional organization of promyelocytic leukemia nuclear bodies, J Cell Sci. 123 (2010) 392–400.
[137] C.H. Eskiw, G. Dellaire, D.P. Bazett-Jones, Chromatin Contributes to Structural Integrity of Promyelocytic Leukemia Bodies through a SUMO-1-independent Mechanism, J. Biol. Chem. 279 (2004) 9577–9585.
[138] G. Meroni, Graciana Diez-Roux, TRIM/RBCC, a novel class of “single protein RING finger” E3 ubiquitin ligases, BioEssays. 27 (2005) 1147–1157.
[139] K. Ozato, D.-M. Shin, T.-H. Chang, H.C. Morse, TRIM family proteins and their emerging roles in innate immunity, Nat Rev Immunol. 8 (2008) 849–860.

[140] H. Tao, B.N. Simmons, S. Singireddy, M. Jakkidi, K.M. Short, T.C. Cox, et al., Structure of the MID1 Tandem B-Boxes Reveals an Interaction Reminiscent of Intermolecular Ring Heterodimers†,‡, Biochemistry (Mosc.). 47 (2008) 2450–2457.
[141] A. Rabellino, B. Carter, G. Konstantinidou, S.-Y. Wu, A. Rimessi, L.A. Byers, et al., The SUMO E3-ligase PIAS1 Regulates the Tumor Suppressor PML and Its Oncogenic Counterpart PML-RARA, Cancer Res. 72 (2012) 2275–2284.
[142] X. Wei, Z.K. Yu, A. Ramalingam, S.R. Grossman, J.H. Yu, D.B. Bloch, et al., Physical and Functional Interactions between PML and MDM2, J Biol Chem. 278 (2003) 29288–29297.
[143] T.H. Shen, H.-K. Lin, P.P. Scaglioni, T.M. Yung, P.P. Pandolfi, The Mechanisms of PML-Nuclear Body Formation, Mol. Cell. 24 (2006) 331–339.
[144] W. Condemine, Y. Takahashi, M. Le Bras, H. de Thé, A nucleolar targeting signal in PML-I addresses PML to nucleolar caps in stressed or senescent cells, J Cell Sci. 120 (2007) 3219–3227.
[145] Y. Geng, S. Monajembashi, A. Shao, D. Cui, W. He, Z. Chen, et al., Contribution of the C-terminal Regions of Promyelocytic Leukemia Protein (PML) Isoforms II and V to PML Nuclear Body Formation, J. Biol. Chem. 287 (2012) 30729–30742.
[146] M. Pampin, Y. Simonin, B. Blondel, Y. Percherancier, M.K. Chelbi-Alix, Cross Talk between PML and p53 during Poliovirus Infection: Implications for Antiviral Defense, J Virol. 80 (2006) 8582–8592.
[147] M.A. Maroui, M. Pampin, M.K. Chelbi-Alix, Promyelocytic Leukemia Isoform IV Confers Resistance to Encephalomyocarditis Virus via the Sequestration of 3D Polymerase in Nuclear Bodies ▿, J. Virol. 85 (2011) 13164–13173.
[148] R.D. Everett, J. Murray, A. Orr, C.M. Preston, Herpes Simplex Virus Type 1 Genomes Are Associated with ND10 Nuclear Substructures in Quiescently Infected Human Fibroblasts, J Virol. 81 (2007) 10991–11004.
[149] F. Catez, C. Picard, K. Held, S. Gross, A. Rousseau, D. Theil, et al., HSV-1 Genome Subnuclear Positioning and Associations with Host-Cell PML-NBs and Centromeres Regulate LAT Locus Transcription during Latency in Neurons, Plos Pathog. 8 (2012) e1002852.
[150] C.D. Meiering, M.L. Linial, The Promyelocytic Leukemia Protein Does Not Mediate Foamy Virus Latency In Vitro, J. Virol. 77 (2003) 2207–2213.
[151] M. Reichelt, L. Wang, M. Sommer, J. Perrino, A.M. Nour, N. Sen, et al., Entrapment of Viral Capsids in Nuclear PML Cages Is an Intrinsic Antiviral Host Defense against Varicella-Zoster Virus, Plos Pathog. 7 (2011) e1001266.
[152] T. Regad, A. Saib, V. Lallemand-Breitenbach, P.P. Pandolfi, H. de Thé, M.K. Chelbi-Alix, PML mediates the interferon-induced antiviral state against a complex retrovirus via its association with the viral transactivator, Embo J. 20 (2001) 3495–3505.

[153] B.E. Mchichi, T. Regad, M.-A. Maroui, M.S. Rodriguez, A. Aminev, S. Gerbaud, et al., SUMOylation Promotes PML Degradation during Encephalomyocarditis Virus Infection, J. Virol. 84 (2010) 11634–11645.
[154] G.G. Maul, H.H. Guldner, J.G. Spivack, Modification of discrete nuclear domains induced by herpes simplex virus type 1 immediate early gene 1 product (ICP0), J. Gen. Virol. 74 (1993) 2679–2690.
[155] C.-H. Nagel, N. Albrecht, K. Milovic-Holm, L. Mariyanna, B. Keyser, B. Abel, et al., Herpes Simplex Virus Immediate Early Protein ICP0 is Targeted by SIAH-1 for Proteasomal Degradation, J Virol. (2011) JVI.02207–10.
[156] E. Guccione, K.J. Lethbridge, N. Killick, K.N. Leppard, L. Banks, HPV E6 proteins interact with specific PML isoforms and allow distinctions to be made between different POD structures, Oncogene. 23 (2004) 4662–4672.
[157] J. Ahn, G. Hayward, The major immediate-early proteins IE1 and IE2 of human cytomegalovirus colocalize with and disrupt PML-associated nuclear bodies at very early times in infected permissive cells, J Virol. 71 (1997) 4599–4613.
[158] H.-R. Lee, D.-J. Kim, J.-M. Lee, C.Y. Choi, B.-Y. Ahn, G.S. Hayward, et al., Ability of the Human Cytomegalovirus IE1 Protein To Modulate Sumoylation of PML Correlates with Its Functional Activities in Transcriptional Regulation and Infectivity in Cultured Fibroblast Cells, J. Virol. 78 (2004) 6527–6542.
[159] A.L. Adamson, S. Kenney, Epstein-Barr Virus Immediate-Early Protein BZLF1 Is SUMO-1 Modified and Disrupts Promyelocytic Leukemia Bodies, J Virol. 75 (2001) 2388–2399.
[160] L. Marcos-Villar, F. Lopitz-Otsoa, P. Gallego, C. Munoz-Fontela, J. Gonzalez-Santamaria, M. Campagna, et al., Kaposi's Sarcoma-Associated Herpesvirus Protein LANA2 Disrupts PML Oncogenic Domains and Inhibits PML-Mediated Transcriptional Repression of the Survivin Gene, J Virol. 83 (2009) 8849–8858.
[161] K.L.B. Borden, RING fingers and B-boxes: Zinc-binding protein-protein interaction domains, Biochem. Cell Biol. 76 (1998) 351.
[162] F. Puvion-Dutilleul, M.K. Chelbi-Alix, M. Koken, F. Quignon, E. Puvion, H. De Thé, Adenovirus Infection Induces Rearrangements in the Intranuclear Distribution of the Nuclear Body-Associated PML Protein, Exp. Cell Res. 218 (1995) 9–16.
[163] X. Cheng, H.-Y. Kao, Post-translational modifications of PML: consequences and implications, Front. Oncol. 2 (2013).
[164] T. Sternsdorf, K. Jensen, H. Will, Evidence for Covalent Modification of the Nuclear Dot-associated Proteins PML and Sp100 by PIC1/SUMO-1, J Cell Biol. 139 (1997) 1621–1634.
[165] T. Kamitani, K. Kito, H.P. Nguyen, H. Wada, T. Fukuda-Kamitani, E.T.H. Yeh, Identification of Three Major Sentrinization Sites in PML, J. Biol. Chem. 273 (1998) 26675–26682.

[166] F. Galisson, L. Mahrouche, M. Courcelles, E. Bonneil, S. Meloche, M.K. Chelbi-Alix, et al., A novel proteomics approach to identify SUMOylated proteins and their modification sites in human cells, Mol. Cell. Proteomics. 10 (2011).
[167] A.C.O. Vertegaal, J.S. Andersen, S.C. Ogg, R.T. Hay, M. Mann, A.I. Lamond, Distinct and Overlapping Sets of SUMO-1 and SUMO-2 Target Proteins Revealed by Quantitative Proteomics, Mol. Cell. Proteomics. 5 (2006) 2298–2310.
[168] N. Saitoh, Y. Uchimura, T. Tachibana, S. Sugahara, H. Saitoh, M. Nakao, In situ SUMOylation analysis reveals a modulatory role of RanBP2 in the nuclear rim and PML bodies, Exp. Cell Res. 312 (2006) 1418–1430.
[169] M.H. Tatham, M.-C. Geoffroy, L. Shen, A. Plechanovova, N. Hattersley, E.G. Jaffray, et al., RNF4 is a poly-SUMO-specific E3 ubiquitin ligase required for arsenic-induced PML degradation, Nat Cell Biol. 10 (2008) 538–546.
[170] C. Gao, C.-C. Ho, E. Reineke, M. Lam, X. Cheng, K.J. Stanya, et al., Histone Deacetylase 7 Promotes PML Sumoylation and Is Essential for PML Nuclear Body Formation, Mol Cell Biol. 28 (2008) 5658–5667.
[171] M. Campagna, D. Herranz, M.A. Garcia, L. Marcos-Villar, J. Gonzalez-Santamaria, P. Gallego, et al., SIRT1 stabilizes PML promoting its sumoylation, Cell Death Differ. (2010).
[172] S. Weidtkamp-Peters, T. Lenser, D. Negorev, N. Gerstner, T.G. Hofmann, G. Schwanitz, et al., Dynamics of component exchange at PML nuclear bodies, J Cell Sci. 121 (2008) 2731–2743.
[173] D.-Y. Lin, Y.-S. Huang, J.-C. Jeng, H.-Y. Kuo, C.-C. Chang, T.-T. Chao, et al., Role of SUMO-Interacting Motif in Daxx SUMO Modification, Subnuclear Localization, and Repression of Sumoylated Transcription Factors, Mol. Cell. 24 (2006) 341–354.
[174] V. Lallemand-Breitenbach, M. Jeanne, S. Benhenda, R. Nasr, M. Lei, L. Peres, et al., Arsenic degrades PML or PML-RAR[alpha] through a SUMO-triggered RNF4/ubiquitin-mediated pathway, Nat Cell Biol. 10 (2008) 547–555.
[175] Y. Erker, H. Neyret-Kahn, J.-S. Seeler, A. Dejean, A. Atfi, L. Levy, Arkadia, a novel SUMO-targeted ubiquitin ligase involved in PML degradation, Mol. Cell. Biol. (2013).
[176] E.L. Reineke, M. Lam, Q. Liu, Y. Liu, K.J. Stanya, K.-S. Chang, et al., Degradation of the Tumor Suppressor PML by Pin1 Contributes to the Cancer Phenotype of Breast Cancer MDA-MB-231 Cells, Mol Cell Biol. 28 (2008) 997–1006.
[177] X.-W. Zhang, X.-J. Yan, Z.-R. Zhou, F.-F. Yang, Z.-Y. Wu, H.-B. Sun, et al., Arsenic Trioxide Controls the Fate of the PML-RARα Oncoprotein by Directly Binding PML, Science. 328 (2010) 240–243.
[178] E. Gresko, S. Ritterhoff, J. Sevilla-Perez, A. Roscic, K. Frobius, I. Kotevic, et al., PML tumor suppressor is regulated by HIPK2-mediated

phosphorylation in response to DNA damage, Oncogene. 28 (2008) 698–708.
[179] I. Nefkens, D.G. Negorev, A.M. Ishov, J.S. Michaelson, E.T.H. Yeh, R.M. Tanguay, et al., Heat shock and Cd2+ exposure regulate PML and Daxx release from ND10 by independent mechanisms that modify the induction of heat-shock proteins 70 and 25 differently, J Cell Sci. 116 (2003) 513–524.
[180] M. Fanelli, A. Fantozzi, P. De Luca, S. Caprodossi, S. Matsuzawa, M.A. Lazar, et al., The Coiled-coil Domain Is the Structural Determinant for Mammalian Homologues of Drosophila Sina-mediated Degradation of Promyelocytic Leukemia Protein and Other Tripartite Motif Proteins by the Proteasome, J Biol Chem. 279 (2004) 5374–5379.
[181] W.-C. Yuan, Y.-R. Lee, S.-F. Huang, Y.-M. Lin, T.-Y. Chen, H.-C. Chung, et al., A Cullin3-KLHL20 Ubiquitin Ligase-Dependent Pathway Targets PML to Potentiate HIF-1 Signaling and Prostate Cancer Progression, Cancer Cell. 20 (2011) 214–228.
[182] D. Guan, D. Factor, Y. Liu, Z. Wang, H.-Y. Kao, The epigenetic regulator UHRF1 promotes ubiquitination-mediated degradation of the tumor-suppressor protein promyelocytic leukemia protein, Oncogene. (2012).
[183] P.P. Scaglioni, T.M. Yung, L.F. Cai, H. Erdjument-Bromage, A.J. Kaufman, B. Singh, et al., A CK2-Dependent Mechanism for Degradation of the PML Tumor Suppressor, Cell. 126 (2006) 269–283.
[184] K.-S. Chang, Y.-H. Fan, M. Andreeff, J. Liu, Z.-M. Mu, The PML gene encodes a phosphoprotein associated with the nuclear matrix, Blood. 85 (1995) 3646–3653.
[185] T. Shiromizu, J. Adachi, S. Watanabe, T. Murakami, T. Kuga, S. Muraoka, et al., Identification of Missing Proteins in the neXtProt Database and Unregistered Phosphopeptides in the PhosphoSitePlus Database As Part of the Chromosome-Centric Human Proteome Project, J. Proteome Res. (2013).
[186] F. Hayakawa, M.L. Privalsky, Phosphorylation of PML by mitogen-activated protein kinases plays a key role in arsenic trioxide-mediated apoptosis, Cancer Cell. 5 (2004) 389–401.
[187] Q. Yang, X. Deng, B. Lu, M. Cameron, C. Fearns, M.P. Patricelli, et al., Pharmacological Inhibition of BMK1 Suppresses Tumor Growth through Promyelocytic Leukemia Protein, Cancer Cell. 18 (2010) 258–267.
[188] J.H. Lim, Y. Liu, E. Reineke, H.-Y. Kao, Mitogen-activated Protein Kinase Extracellular Signal-regulated Kinase 2 Phosphorylates and Promotes Pin1 Protein-dependent Promyelocytic Leukemia Protein Turnover, J. Biol. Chem. 286 (2011) 44403–44411.
[189] E.L. Reineke, Y. Liu, H.-Y. Kao, Promyelocytic Leukemia Protein Controls Cell Migration in Response to Hydrogen Peroxide and Insulin-like Growth Factor-1, J. Biol. Chem. 285 (2010) 9485–9492.

[190] Q. Yang, L. Liao, X. Deng, R. Chen, N.S. Gray, J.R. Yates, et al., BMK1 is involved in the regulation of p53 through disrupting the PML–MDM2 interaction, Oncogene. (2012).
[191] Y. Percherancier, D. Germain-Desprez, F. Galisson, X.H. Mascle, L. Dianoux, P. Estephan, et al., Role of SUMO in RNF4-mediated PML degradation: PML sumoylation and phospho-switch control of its SUMO binding domain dissected in living cells, J Biol Chem. 284 (2009) 16595–16608.
[192] P. Stehmeier, S. Muller, Phospho-Regulated SUMO Interaction Modules Connect the SUMO System to CK2 Signaling, Mol. Cell. 33 (2009) 400–409.
[193] S. Yang, C. Kuo, J.E. Bisi, M.K. Kim, PML-dependent apoptosis after DNA damage is regulated by the checkpoint kinase hCds1/Chk2, Nat Cell Biol. 4 (2002) 865–870.
[194] R. Bernardi, P.P. Scaglioni, S. Bergmann, H.F. Horn, K.H. Vousden, P.P. Pandolfi, PML regulates p53 stability by sequestering Mdm2 to the nucleolus, Nat Cell Biol. 6 (2004) 665–672.
[195] Y. Tagata, H. Yoshida, L.A. Nguyen, H. Kato, H. Ichikawa, F. Tashiro, et al., Phosphorylation of PML is essential for activation of C/EBPε and PU.1 to accelerate granulocytic differentiation, Leukemia. 22 (2008) 273–280.
[196] R.D. Everett, P. Lomonte, T. Sternsdorf, R. van Driel, A. Orr, Cell cycle regulation of PML modification and ND10 composition, J. Cell Sci. 112 (1999) 4581–4588.
[197] L.M. Schang, J. Phillips, P.A. Schaffer, Requirement for Cellular Cyclin-Dependent Kinases in Herpes Simplex Virus Replication and Transcription, J. Virol. 72 (1998) 5626–5637.
[198] G. Karaca, D. Hargett, T.I. McLean, J.S. Aguilar, P. Ghazal, E.K. Wagner, et al., Inhibition of the stress-activated kinase, p38, does not affect the virus transcriptional program of herpes simplex virus type 1, Virology. 329 (2004) 142–156.
[199] S. Wang, P.M. Fischer, Cyclin-dependent kinase 9: a key transcriptional regulator and potential drug target in oncology, virology and cardiology, Trends Pharmacol. Sci. 29 (2008) 302–313.
[200] L.A. Samaniego, N. Wu, N.A. DeLuca, The herpes simplex virus immediate-early protein ICP0 affects transcription from the viral genome and infected-cell survival in the absence of ICP4 and ICP27, J. Virol. 71 (1997) 4614–4625.
[201] K.O. Smith, Relationship Between the Envelope and the Infectivity of Herpes Simplex Virus, Proc. Soc. Exp. Biol. Med. Soc. Exp. Biol. Med. New York N. 115 (1964) 814–816.
[202] W.Z. Cai, P.A. Schaffer, Herpes simplex virus type 1 ICP0 plays a critical role in the de novo synthesis of infectious virus following transfection of viral DNA., J. Virol. 63 (1989) 4579–4589.

[203] P.A. Schaffer, G.M. Aron, N. Biswal, M. Benyesh-Melnick, Temperature-sensitive mutants of herpes simplex virus type 1: isolation, complementation and partial characterization, Virology. 52 (1973) 57–71.
[204] W.P. Halford, C.D. Kemp, J.A. Isler, D.J. Davido, P.A. Schaffer, ICP0, ICP4, or VP16 Expressed from Adenovirus Vectors Induces Reactivation of Latent Herpes Simplex Virus Type 1 in Primary Cultures of Latently Infected Trigeminal Ganglion Cells, J Virol. 75 (2001) 6143–6153.
[205] S.C. Das, D. Nayak, Y. Zhou, A.K. Pattnaik, Visualization of Intracellular Transport of Vesicular Stomatitis Virus Nucleocapsids in Living Cells, J. Virol. 80 (2006) 6368–6377.
[206] U.K. Laemmli, Cleavage of Structural Proteins during the Assembly of the Head of Bacteriophage T4, Nature. 227 (1970) 680–685.
[207] M.A. Pagano, J. Bain, Z. Kazimierczuk, S. Sarno, M. Ruzzene, G. Di Maira, et al., The selectivity of inhibitors of protein kinase CK2: an update, Biochem. J. 415 (2008) 353.
[208] K.L. Mossman, H.A. Saffran, J.R. Smiley, Herpes Simplex Virus ICP0 Mutants Are Hypersensitive to Interferon, J. Virol. 74 (2000) 2052–2056.
[209] K.M. Eidson, W.E. Hobbs, B.J. Manning, P. Carlson, N.A. DeLuca, Expression of Herpes Simplex Virus ICP0 Inhibits the Induction of Interferon-Stimulated Genes by Viral Infection, J. Virol. 76 (2002) 2180–2191.
[210] K.P. Anderson, E.H. Fennie, Adenovirus early region 1A modulation of interferon antiviral activity., J. Virol. 61 (1987) 787–795.
[211] Y. Zhi, R.M. Sandri-Goldin, Analysis of the Phosphorylation Sites of Herpes Simplex Virus Type 1 Regulatory Protein ICP27, J. Virol. 73 (1999) 3246–3257.
[212] W.R. Sacks, C.C. Greene, D.P. Aschman, P.A. Schaffer, Herpes simplex virus type 1 ICP27 is an essential regulatory protein., J. Virol. 55 (1985) 796–805.
[213] K. Xia, N.A. DeLuca, D.M. Knipe, Analysis of phosphorylation sites of herpes simplex virus type 1 ICP4, J. Virol. 70 (1996) 1061–1071.
[214] T. Wisner, C. Brunetti, K. Dingwell, D.C. Johnson, The Extracellular Domain of Herpes Simplex Virus gE Is Sufficient for Accumulation at Cell Junctions but Not for Cell-to-Cell Spread, J. Virol. 74 (2000) 2278–2287.
[215] C. Boutell, R.D. Everett, J. Hilliard, P.A. Schaffer, A. Orr, D.J. Davido, Herpes Simplex Virus Type 1 ICP0 Phosphorylation Mutants Impair the E3 Ubiquitin Ligase Activity of ICP0 in a Cell Type-Dependent Manner, J. Virol. 82 (2008) 10647–56.
[216] S.G. Whalen, R.C. Marcellus, D. Barbeau, P.E. Branton, Importance of the Ser-132 phosphorylation site in cell transformation and apoptosis induced by the adenovirus type 5 E1A protein, J. Virol. 70 (1996) 5373–5383.
[217] J.W. Critchfield, J.E. Coligan, T.M. Folks, S.T. Butera, Casein kinase II is a selective target of HIV-1 transcriptional inhibitors, Proc. Natl. Acad. Sci. U. S. A. 94 (1997) 6110–6115.

[218] J. Rowe, R.J. Greenblatt, D. Liu, J.F. Moffat, Compounds that target host cell proteins prevent varicella-zoster virus replication in culture, ex vivo, and in SCID-Hu mice, Antiviral Res. 86 (2010) 276–285.
[219] A.V. Ljubimov, S. Caballero, A.M. Aoki, L.A. Pinna, M.B. Grant, R. Castellon, Involvement of Protein Kinase CK2 in Angiogenesis and Retinal Neovascularization, Invest. Ophthalmol. Vis. Sci. 45 (2004) 4583 –4591.
[220] R.E. Randall, S. Goodbourn, Interferons and viruses: an interplay between induction, signalling, antiviral responses and virus countermeasures, J Gen Virol. 89 (2008) 1–47.
[221] G.R. Stark, I.M. Kerr, B.R.G. Williams, R.H. Silverman, R.D. Schreiber, How Cells Respond to Interferons, Annu. Rev. Biochem. 67 (1998) 227–264.
[222] C.D. Conrady, W.P. Halford, D.J.J. Carr, Loss of the Type I Interferon Pathway Increases Vulnerability of Mice to Genital Herpes Simplex Virus 2 Infection, J. Virol. 85 (2011) 1625–1633.
[223] M.F. Van den Broek, U. Müller, S. Huang, M. Aguet, R.M. Zinkernagel, Antiviral defense in mice lacking both alpha/beta and gamma interferon receptors., J. Virol. 69 (1995) 4792–4796.
[224] S.Y. Hwang, P.J. Hertzog, K.A. Holland, S.H. Sumarsono, M.J. Tymms, J.A. Hamilton, et al., A null mutation in the gene encoding a type I interferon receptor component eliminates antiproliferative and antiviral responses to interferons alpha and beta and alters macrophage responses, Proc. Natl. Acad. Sci. 92 (1995) 11284.
[225] U. Muller, U. Steinhoff, L.F. Reis, S. Hemmi, J. Pavlovic, R.M. Zinkernagel, et al., Functional Role of Type I and Type II Interferons in Antiviral Defense, Science. 264 (1994) 1918–1921.
[226] S. Bereczky, G. Lindegren, H. Karlberg, S. Åkerström, J. Klingström, A. Mirazimi, Crimean–Congo Hemorrhagic Fever Virus Infection Is Lethal for Adult Type I Interferon Receptor-Knockout Mice, J. Gen. Virol. 91 (2010) 1473–1477.
[227] C.N. Detje, T. Meyer, H. Schmidt, D. Kreuz, J.K. Rose, I. Bechmann, et al., Local Type I IFN Receptor Signaling Protects Against Virus Spread Within the Central Nervous System, J. Immunol. 182 (2009) 2297–2304.
[228] J.E. Durbin, R. Hackenmiller, M.C. Simon, D.E. Levy, Targeted Disruption of the Mouse Stat1 Gene Results in Compromised Innate Immunity to Viral Disease, Cell. 84 (1996) 443–450.
[229] M.C. Smith, C. Boutell, D.J. Davido, HSV-1 ICP0: paving the way for viral replication, Future Virol. 6 (2011) 421–429.
[230] P. Paladino, K.L. Mossman, Mechanisms employed by herpes simplex virus 1 to inhibit the interferon response, J. Interf. Cytokine Res. Off. J. Int. Soc. Interf. Cytokine Res. 29 (2009) 599–607.
[231] P. Paladino, S.E. Collins, K.L. Mossman, Cellular Localization of the Herpes Simplex Virus ICP0 Protein Dictates Its Ability to Block IRF3-Mediated Innate Immune Responses, Plos One. 5 (2010) e10428.

[232] K.L. Mossman, P.F. Macgregor, J.J. Rozmus, A.B. Goryachev, A.M. Edwards, J.R. Smiley, Herpes Simplex Virus Triggers and Then Disarms a Host Antiviral Response, J Virol. 75 (2001) 750–758.
[233] C.M. Counter, W.C. Hahn, W. Wei, S. Dickinson Caddle, R.L. Beijersbergen, P.M. Lansdorp, et al., Dissociation among in vitro telomerase activity, telomere maintenance, and cellular immortalization, Proc. Natl. Acad. Sci. U. S. A. 95 (1998) 14723–14728.
[234] K. Misawa, T. Nosaka, S. Morita, A. Kaneko, T. Nakahata, S. Asano, et al., A Method to Identify cDNAs Based on Localization of Green Fluorescent Protein Fusion Products, Proc. Natl. Acad. Sci. 97 (2000) 3062–3066.
[235] E.C. Dimmer, R.P. Huntley, Y. Alam-Faruque, T. Sawford, C. O'Donovan, M.J. Martin, et al., The UniProt-GO Annotation database in 2011, Nucleic Acids Res. 40 (2012) D565–D570.
[236] W.C. Hahn, S.K. Dessain, M.W. Brooks, J.E. King, B. Elenbaas, D.M. Sabatini, et al., Enumeration of the Simian Virus 40 Early Region Elements Necessary for Human Cell Transformation, Mol. Cell. Biol. 22 (2002) 2111–2123.
[237] B. van der Loo, M.J. Fenton, J.D. Erusalimsky, Cytochemical Detection of a Senescence-Associated β-Galactosidase in Endothelial and Smooth Muscle Cells from Human and Rabbit Blood Vessels, Exp. Cell Res. 241 (1998) 309–315.
[238] M. Hou, D. Xu, M. Björkholm, A. Gruber, Real-Time Quantitative Telomeric Repeat Amplification Protocol Assay for the Detection of Telomerase Activity, Clin. Chem. 47 (2001) 519–524.
[239] H. Zhu, C. Zheng, J. Xing, S. Wang, S. Li, R. Lin, et al., Varicella-Zoster Virus Immediate-Early Protein ORF61 Abrogates the IRF3-Mediated Innate Immune Response through Degradation of Activated IRF3, J. Virol. 85 (2011) 11079 –11089.
[240] G.A.D. Hardy, S.F. Sieg, B. Rodriguez, W. Jiang, R. Asaad, M.M. Lederman, et al., Desensitization to type I interferon in HIV-1 infection correlates with markers of immune activation and disease progression, Blood. 113 (2009) 5497 –5505.
[241] R.-L. Kuo, C. Zhao, M. Malur, R.M. Krug, Influenza A virus strains that circulate in humans differ in the ability of their NS1 proteins to block the activation of IRF3 and interferon-β transcription, Virology. 408 (2010) 146–158.
[242] ATCC: Catalog Search, (n.d.).
[243] N.W. Kim, M.A. Piatyszek, K.R. Prowse, C.B. Harley, M.D. West, P.L.C. Ho, et al., Specific Association of Human Telomerase Activity with Immortal Cells and Cancer, Science. 266 (1994) 2011–2015.
[244] A.J. Klingelhutz, S.A. Foster, J.K. McDougall, Telomerase activation by the E6 gene product of human papillomavirus type 16, Nature. 380 (1996) 79–82.
[245] K. Hiyama, Telomeres and Telomerase in Cancer, Springer, 2009.

[246] Q.M. Chen, V.C. Tu, J. Catania, M. Burton, O. Toussaint, T. Dilley, Involvement of Rb family proteins, focal adhesion proteins and protein synthesis in senescent morphogenesis induced by hydrogen peroxide, J. Cell Sci. 113 (2000) 4087–4097.
[247] G.P. Dimri, X. Lee, G. Basile, M. Acosta, G. Scott, C. Roskelley, et al., A biomarker that identifies senescent human cells in culture and in aging skin in vivo, Proc. Natl. Acad. Sci. U. S. A. 92 (1995) 9363–9367.
[248] C.A. Brailovsky, L.D. Berman, C. Chany, Decreased interferon sensitivity and production in cells transformed by SV40 and other oncogenic agents, Int. J. Cancer J. Int. Cancer. 4 (1969) 194–203.
[249] A.V. Rathi, P.G. Cantalupo, S.N. Sarkar, J.M. Pipas, Induction of interferon-stimulated genes by Simian virus 40 T antigens, Virology. 406 (2010) 202–211.
[250] Y. Ito, L. Montagnier, Heterogeneity of the sensitivity of vesicular stomatitis virus to interferons., Infect. Immun. 18 (1977) 23–27.
[251] W.E. Stewart, W.D. Scott, S.E. Sulkin, Relative Sensitivities of Viruses to Different Species of Interferon, J. Virol. 4 (1969) 147–153.
[252] R.T. Taylor, W.A. Bresnahan, Human Cytomegalovirus Immediate-Early 2 Gene Expression Blocks Virus-Induced Beta Interferon Production, J. Virol. 79 (2005) 3873–3877.
[253] M.P. Langford, D.A. Weigent, G.J. Stanton, S. Baron, Virus plaque-reduction assay for interferon: Microplaque and regular macroplaque reduction assays, in: Sidney Pestka (Ed.), Methods Enzymol., Academic Press, 1981: pp. 339–346.
[254] S.E. Collins, R.S. Noyce, K.L. Mossman, Innate Cellular Response to Virus Particle Entry Requires IRF3 but Not Virus Replication, J. Virol. 78 (2004) 1706–1717.
[255] K.L. Mossman, J.R. Smiley, Herpes Simplex Virus ICP0 and ICP34.5 Counteract Distinct Interferon-Induced Barriers to Virus Replication, J Virol. 76 (2002) 1995–1998.
[256] K.L. Norman, F. Farassati, P.W.K. Lee, Oncolytic viruses and cancer therapy, Cytokine Growth Factor Rev. 12 (2001) 271–282.
[257] G.N. Barber, VSV-tumor selective replication and protein translation, Oncogene. 24 (2005) 7710–7719.
[258] W.Z. Cai, P.A. Schaffer, A cellular function can enhance gene expression and plating efficiency of a mutant defective in the gene for ICP0, a transactivating protein of herpes simplex virus type 1., J Virol. 65 (1991) 4078–4090.
[259] J.L. Douglas, M.P. Quinlan, Efficient nuclear localization and immortalizing ability, two functions dependent on the adenovirus type 5 (Ad5) E1A second exon, are necessary for cotransformation with Ad5 E1B but not with T24ras., J. Virol. 69 (1995) 8061–8065.
[260] J. Bartek, J. Bartkova, N. Kyprianou, E.N. Lalani, Z. Staskova, M. Shearer, et al., Efficient immortalization of luminal epithelial cells from human

mammary gland by introduction of simian virus 40 large tumor antigen with a recombinant retrovirus, Proc. Natl. Acad. Sci. 88 (1991) 3520.
[261] D.E. Wazer, X.L. Liu, Q. Chu, Q. Gao, V. Band, Immortalization of Distinct Human Mammary Epithelial Cell Types by Human Papilloma Virus 16 E6 or E7, Proc. Natl. Acad. Sci. 92 (1995) 3687–3691.
[262] J.W. Shay, W.E. Wright, H. Werbin, Defining the molecular mechanisms of human cell immortalization, Biochim. Biophys. Acta Bba - Rev. Cancer. 1072 (1991) 1–7.
[263] D. Ahuja, M.T. S|[aacute]|enz-Robles, J.M. Pipas, SV40 large T antigen targets multiple cellular pathways to elicit cellular transformation, Oncogene. 24 (2005) 7729–7745.
[264] A. Brehm, S.J. Nielsen, E.A. Miska, D.J. McCance, J.L. Reid, A.J. Bannister, et al., The E7 oncoprotein associates with Mi2 and histone deacetylase activity to promote cell growth, Embo J. 18 (1999) 2449–2458.
[265] D. Patel, S.-M. Huang, L.A. Baglia, D.J. McCance, The E6 protein of human papillomavirus type 16 binds to and inhibits co-activation by CBP and p300, Embo J. 18 (1999) 5061–5072.
[266] S.H. Ali, J.A. DeCaprio, Cellular transformation by SV40 large T antigen: interaction with host proteins, Semin. Cancer Biol. 11 (2001) 15–23.
[267] E. Valls, X. de la Cruz, M.A. Martínez-Balbás, The SV40 T antigen modulates CBP histone acetyltransferase activity, Nucleic Acids Res. 31 (2003) 3114–3122.
[268] S.M. Frisch, J.S. Mymryk, Adenovirus-5 E1A: paradox and paradigm, Nat. Rev. Mol. Cell Biol. 3 (2002) 441–452.
[269] D. Brockmann, H. Esche, The multifunctional role of E1A in the transcriptional regulation of CREB/CBP-dependent target genes, Curr. Top. Microbiol. Immunol. 272 (2003) 97–129.
[270] P.L. Hyland, S.S. McDade, R. McCloskey, G.J. Dickson, K. Arthur, D.J. McCance, et al., Evidence for Alteration of EZH2, BMI1 and KDM6A and Epigenetic Reprogramming in Human Papillomavirus Type-16 E6/E7 Expressing Keratinocytes, J. Virol. (2011).
[271] H.P. Li, Y.W. Leu, Y.S. Chang, Epigenetic changes in virus-associated human cancers, Cell Res. 15 (2005) 262–271.
[272] P.G. Cantalupo, M.T. Sáenz-Robles, A.V. Rathi, R.W. Beerman, W.H. Patterson, R.H. Whitehead, et al., Cell-type specific regulation of gene expression by simian virus 40 T antigens, Virology. 386 (2009) 183–191.
[273] J.J. Zhang, U. Vinkemeier, W. Gu, D. Chakravarti, C.M. Horvath, J.E. Darnell, Two Contact Regions Between Stat1 and CBP/P300 in Interferon Γ Signaling, Proc. Natl. Acad. Sci. 93 (1996) 15092–15096.
[274] L.V. Ronco, A.Y. Karpova, M. Vidal, P.M. Howley, Human papillomavirus 16 E6 oncoprotein binds to interferon regulatory factor-3 and inhibits its transcriptionalactivity, Genes Dev. 12 (1998) 2061–2072.
[275] R. Sundararajan, E. White, E1B 19K Blocks Bax Oligomerization and Tumor Necrosis Factor Alpha-Mediated Apoptosis, J. Virol. 75 (2001) 7506–7516.

[276] J. Han, P. Sabbatini, D. Perez, L. Rao, D. Modha, E. White, The E1B 19K Protein Blocks Apoptosis by Interacting with and Inhibiting the P53-Inducible and Death-Promoting Bax Protein., Genes Dev. 10 (1996) 461–477.
[277] M. Debbas, E. White, Wild-Type P53 Mediates Apoptosis by E1A, Which Is Inhibited by E1B., Genes Dev. 7 (1993) 546–554.
[278] P. Rajan, S. Swaminathan, J. Zhu, C.N. Cole, G. Barber, M.J. Tevethia, et al., A novel translational regulation function for the simian virus 40 large-T antigen gene., J. Virol. 69 (1995) 785–795.
[279] C. Lindvall, M. Hou, T. Komurasaki, C. Zheng, M. Henriksson, J.M. Sedivy, et al., Molecular Characterization of Human Telomerase Reverse Transcriptase-immortalized Human Fibroblasts by Gene Expression Profiling: Activation of the Epiregulin Gene, Cancer Res. 63 (2003) 1743–1747.
[280] W.A. Bresnahan, G.E. Hultman, T. Shenk, Replication of Wild-Type and Mutant Human Cytomegalovirus in Life-Extended Human Diploid Fibroblasts, J Virol. 74 (2000) 10816–10818.
[281] B.P. McSharry, C.J. Jones, J.W. Skinner, D. Kipling, G.W.G. Wilkinson, Human telomerase reverse transcriptase-immortalized MRC-5 and HCA2 human fibroblasts are fully permissive for human cytomegalovirus, J Gen Virol. 82 (2001) 855–863.
[282] H. Xin, O.M. Pereira-Smith, D. Choubey, Role of IFI 16 in cellular senescence of human fibroblasts, Oncogene. 23 (2004) 6209–6217.
[283] M.L. Nguyen, R.M. Kraft, M. Aubert, E. Goodwin, D. DiMaio, J.A. Blaho, p53 and hTERT Determine Sensitivity to Viral Apoptosis, J Virol. 81 (2007) 12985–12995.
[284] C.E. Lilley, M.S. Chaurushiya, C. Boutell, R.D. Everett, M.D. Weitzman, The Intrinsic Antiviral Defense to Incoming HSV-1 Genomes Includes Specific DNA Repair Proteins and Is Counteracted by the Viral Protein ICP0, Plos Pathog. 7 (2011) e1002084.
[285] M. Kalamvoki, B. Roizman, ICP0 enables and monitors the function of D cyclins in herpes simplex virus 1 infected cells, Proc. Natl. Acad. Sci. 106 (2009) 14576–14580.
[286] D. Cuchet, A. Sykes, A. Nicolas, A. Orr, J. Murray, H. Sirma, et al., PML isoforms I and II participate in PML-dependent restriction of HSV-1 replication, J Cell Sci. (2010) jcs.075390.
[287] R.D. Everett, C. Parada, P. Gripon, H. Sirma, A. Orr, Replication of ICP0-Null Mutant Herpes Simplex Virus Type 1 Is Restricted by both PML and Sp100, J Virol. 82 (2008) 2661–2672.
[288] N.M. Sawtell, The role of PML in HSV pathogenesis and latency, (2008).
[289] R.D. Everett, G. Sourvinos, C. Leiper, J.B. Clements, A. Orr, Formation of Nuclear Foci of the Herpes Simplex Virus Type 1 Regulatory Protein ICP4 at Early Times of Infection: Localization, Dynamics, Recruitment of ICP27, and Evidence for the De Novo Induction of ND10-Like Complexes, J Virol. 78 (2004) 1903–1917.

[290] D. Cuchet-Lourenço, C. Boutell, V. Lukashchuk, K. Grant, A. Sykes, J. Murray, et al., SUMO Pathway Dependent Recruitment of Cellular Repressors to Herpes Simplex Virus Type 1 Genomes, Plos Pathog. 7 (2011) e1002123.
[291] M.K. Chelbi-Alix, H. de Thé, Herpes virus induced proteasome-dependent degradation of the nuclear bodies-associated PML and Sp100 proteins, Oncogene. 18 (1999) 935–941.
[292] D. Cuchet-Lourenço, E. Vanni, M. Glass, A. Orr, R.D. Everett, Herpes Simplex Virus 1 Ubiquitin Ligase ICP0 Interacts with PML Isoform I and Induces Its SUMO-Independent Degradation, J. Virol. 86 (2012) 11209–11222.
[293] C. Boutell, A. Orr, R.D. Everett, PML Residue Lysine 160 Is Required for the Degradation of PML Induced by Herpes Simplex Virus Type 1 Regulatory Protein ICP0, J Virol. 77 (2003) 8686–8694.
[294] P. Gripon, S. Rumin, S. Urban, J. Le Seyec, D. Glaise, I. Cannie, et al., Infection of a human hepatoma cell line by hepatitis B virus, Proc. Natl. Acad. Sci. U. S. A. 99 (2002) 15655–15660.
[295] M. Glass, R.D. Everett, Components of Promyelocytic Leukemia Nuclear Bodies (ND10) Act Cooperatively To Repress Herpesvirus Infection, J. Virol. 87 (2013) 2174–2185.
[296] D.J. McGeoch, M.A. Dalrymple, A.J. Davison, A. Dolan, M.C. Frame, D. McNab, et al., The complete DNA sequence of the long unique region in the genome of herpes simplex virus type 1, J Gen Virol. 69 (1988) 1531–1574.
[297] B.L. Strang, N.D. Stow, Blocks to herpes simplex virus type 1 replication in a cell line, tsBN2, encoding a temperature-sensitive RCC1 protein, J. Gen. Virol. 88 (2007) 376–383.
[298] L. Naldini, U. Blömer, P. Gallay, D. Ory, R. Mulligan, F.H. Gage, et al., In vivo gene delivery and stable transduction of nondividing cells by a lentiviral vector, Science. 272 (1996) 263–267.
[299] S. Kane, H. Sano, S.C.H. Liu, J.M. Asara, W.S. Lane, C.C. Garner, et al., A Method to Identify Serine Kinase Substrates. Akt PHOSPHORYLATES A NOVEL ADIPOCYTE PROTEIN WITH A Rab GTPASE-ACTIVATING PROTEIN (GAP) DOMAIN, J Biol Chem. 277 (2002) 22115–22118.
[300] A.G. Sotnikov, D. Negorev, A.M. Ishov, G.G. Maul, [Monoclonal antibodies against protein Daxx and its localization in nuclear domains 10], Tsitologiia. 43 (2001) 1123–1129.
[301] W. Condemine, Y. Takahashi, J. Zhu, F. Puvion-Dutilleul, S. Guegan, A. Janin, et al., Characterization of Endogenous Human Promyelocytic Leukemia Isoforms, Cancer Res. 66 (2006) 6192–6198.
[302] J.V. Olsen, B. Blagoev, F. Gnad, B. Macek, C. Kumar, P. Mortensen, et al., Global, In Vivo, and Site-Specific Phosphorylation Dynamics in Signaling Networks, Cell. 127 (2006) 635–648.

[303] S.-T. Kim, D.-S. Lim, C.E. Canman, M.B. Kastan, Substrate Specificities and Identification of Putative Substrates of ATM Kinase Family Members, J. Biol. Chem. 274 (1999) 37538–37543.
[304] G.L. Christensen, C.D. Kelstrup, C. Lyngsø, U. Sarwar, R. Bøgebo, S.P. Sheikh, et al., Quantitative Phosphoproteomics Dissection of Seven-transmembrane Receptor Signaling Using Full and Biased Agonists, Mol. Cell. Proteomics. 9 (2010) 1540–1553.
[305] D.G. Negorev, O.V. Vladimirova, A.V. Kossenkov, E.V. Nikonova, R.M. Demarest, A.J. Capobianco, et al., Sp100 as a Potent Tumor Suppressor: Accelerated Senescence and Rapid Malignant Transformation of Human Fibroblasts through Modulation of an Embryonic Stem Cell Program, Cancer Res. 70 (2010) 9991 –10001.
[306] M.A. Maroui, S. Kheddache-Atmane, F. El Asmi, L. Dianoux, M. Aubry, M.K. Chelbi-Alix, Requirement of PML SUMO Interacting Motif for RNF4- or Arsenic Trioxide-Induced Degradation of Nuclear PML Isoforms, Plos One. 7 (2012) e44949.
[307] R.D. Everett, M.-L. Parsy, A. Orr, Analysis of the Functions of Herpes Simplex Virus Type 1 Regulatory Protein ICP0 That Are Critical for Lytic Infection and Derepression of Quiescent Viral Genomes, J Virol. 83 (2009) 4963–4977.
[308] D.J. Davido, W.F. Zagorski, G.G. Maul, P.A. Schaffer, The Differential Requirement for Cyclin-Dependent Kinase Activities Distinguishes Two Functions of Herpes Simplex Virus Type 1 ICP0, J. Virol. 77 (2003) 12603–12616.
[309] T.I. McLean, S.L. Bachenheimer, Activation of cJUN N-Terminal Kinase by Herpes Simplex Virus Type 1 Enhances Viral Replication, J Virol. 73 (1999) 8415–8426.
[310] Z. Li, Y. Yamauchi, M. Kamakura, T. Murayama, F. Goshima, H. Kimura, et al., Herpes Simplex Virus Requires Poly(ADP-Ribose) Polymerase Activity for Efficient Replication and Induces Extracellular Signal-Related Kinase-Dependent Phosphorylation and ICP0-Dependent Nuclear Localization of Tankyrase 1, J. Virol. 86 (2012) 492–503.
[311] Y. Galanty, R. Belotserkovskaya, J. Coates, S. Polo, K.M. Miller, S.P. Jackson, Mammalian SUMO E3-ligases PIAS1 and PIAS4 promote responses to DNA double-strand breaks, Nature. 462 (2009) 935–939.
[312] G. Dellaire, R.W. Ching, K. Ahmed, F. Jalali, K.C.K. Tse, R.G. Bristow, et al., Promyelocytic leukemia nuclear bodies behave as DNA damage sensors whose response to DNA double-strand breaks is regulated by NBS1 and the kinases ATM, Chk2, and ATR, J Cell Biol. 175 (2006) 55–66.
[313] C.-C. Chang, M.T. Naik, Y.-S. Huang, J.-C. Jeng, P.-H. Liao, H.-Y. Kuo, et al., Structural and Functional Roles of Daxx SIM Phosphorylation in SUMO Paralog-Selective Binding and Apoptosis Modulation, Mol. Cell. 42 (2011) 62–74.

[314] L. Wu, K. Luo, Z. Lou, J. Chen, MDC1 regulates intra-S-phase checkpoint by targeting NBS1 to DNA double-strand breaks, Proc. Natl. Acad. Sci. 105 (2008) 11200–11205.
[315] I. Torrecilla, E.J. Spragg, B. Poulin, P.J. McWilliams, S.C. Mistry, A. Blaukat, et al., Phosphorylation and regulation of a G protein–coupled receptor by protein kinase CK2, J. Cell Biol. 177 (2007) 127–137.
[316] N. Blom, S. Gammeltoft, S. Brunak, Sequence and structure-based prediction of eukaryotic protein phosphorylation sites, J. Mol. Biol. 294 (1999) 1351–1362.
[317] C.J.A. Sigrist, E. de Castro, L. Cerutti, B.A. Cuche, N. Hulo, A. Bridge, et al., New and continuing developments at PROSITE, Nucleic Acids Res. 41 (2012) D344–D347.
[318] C.J.A. Sigrist, L. Cerutti, N. Hulo, A. Gattiker, L. Falquet, M. Pagni, et al., PROSITE: A documented database using patterns and profiles as motif descriptors, Brief. Bioinform. 3 (2002) 265–274.
[319] R.D. Everett, Construction and Characterization of Herpes Simplex Virus Type 1 Mutants with Defined Lesions in Immediate Early Gene 1, J Gen Virol. 70 (1989) 1185–1202.
[320] J.R. Morris, C. Boutell, M. Keppler, R. Densham, D. Weekes, A. Alamshah, et al., The SUMO modification pathway is involved in the BRCA1 response to genotoxic stress, Nature. 462 (2009) 886–890.
[321] K. Luo, H. Zhang, L. Wang, J. Yuan, Z. Lou, Sumoylation of MDC1 is important for proper DNA damage response, Embo J. 31 (2012) 3008–3019.
[322] J.R. Danielsen, L.K. Povlsen, B.H. Villumsen, W. Streicher, J. Nilsson, M. Wikström, et al., DNA damage–inducible SUMOylation of HERC2 promotes RNF8 binding via a novel SUMO-binding Zinc finger, J. Cell Biol. 197 (2012) 179–187.
[323] F.T.M. Chang, J.D. McGhie, F.L. Chan, M.C. Tang, M.A. Anderson, J.R. Mann, et al., PML bodies provide an important platform for the maintenance of telomeric chromatin integrity in embryonic stem cells, Nucleic Acids Res. 41 (2013) 4447–4458.
[324] C. Doil, N. Mailand, S. Bekker-Jensen, P. Menard, D.H. Larsen, R. Pepperkok, et al., RNF168 Binds and Amplifies Ubiquitin Conjugates on Damaged Chromosomes to Allow Accumulation of Repair Proteins, Cell. 136 (2009) 435–446.
[325] G.S. Stewart, Solving the RIDDLE of 53BP1 recruitment to sites of damage, Cell Cycle. 8 (2009) 1532–1538.
[326] Z.-X. Xu, A. Timanova-Atanasova, R.-X. Zhao, K.-S. Chang, PML Colocalizes with and Stabilizes the DNA Damage Response Protein TopBP1, Mol Cell Biol. 23 (2003) 4247–4256.